LOYOLA UNIVERSITY CHICAGO 1870 AD · MAJOREM · DEI · GLORIAM
eCOMMONS

Loyola University Chicago
Loyola eCommons

Dissertations
Theses and Dissertations

2021

Cardioprotective Extracellular Vesicles Derived-Micrornas: Sorting Mechanisms and Functions

Anh P. Phan

Follow this and additional works at: https://ecommons.luc.edu/luc_diss

 Part of the Pharmacology, Toxicology and Environmental Health Commons

Recommended Citation

Phan, Anh P., "Cardioprotective Extracellular Vesicles Derived-Micrornas: Sorting Mechanisms and Functions" (2021). *Dissertations*. 3898.
https://ecommons.luc.edu/luc_diss/3898

This Dissertation is brought to you for free and open access by the Theses and Dissertations at Loyola eCommons. It has been accepted for inclusion in Dissertations by an authorized administrator of Loyola eCommons. For more information, please contact ecommons@luc.edu.

This work is licensed under a Creative Commons Attribution-Noncommercial-No Derivative Works 3.0 License.
Copyright Â© 2021 Anh P Phan

LOYOLA UNIVERSITY CHICAGO

CARDIOPROTECTIVE EXTRACELLULAR VESICLES DERIVED-MICRORNAS: SORTING MECHANISMS AND FUNCTIONS

A DISSERTATION SUBMITTED TO

THE FACULTY OF THE GRADUATE SCHOOL

IN CANDIDACY FOR THE DEGREE OF

DOCTOR OF PHILOSOPHY

PROGRAM IN MOLECULAR PHARMACOLOGY AND NEUROSCIENCE

BY

ANH P. PHAN

CHICAGO, IL

DECEMBER 2021

Copyright by Anh P. Phan, 2021
All rights reserved.

ACKNOWLEDGMENTS

First of all, I would like to express my deepest appreciation to my advisor, Dr. W Keith Jones for his immense knowledge, relentless support, and patience. During my PhD study, he has encouraged and at the same time challenged me to think outside of the box and to grow as an independent scientist. Further, I would also like to extend my sincere gratitude to the other members of my dissertation committee, Dr. Simon Kaja, Dr. Wendy Karje, Dr. Joana Bakowska and Dr. Susmita Sahoo, for their time, thoughtful input and valuable guidance throughout my studies. Finally, I would like to thank my family and friends for their contribution to my studies through their unconditional love and support.

TABLE OF CONTENTS

LIST OF TABLES

LIST OF FIGURES

LIST OF ABBREVIATIONS

AA	arachidonic acid
AD	Alzheimer's disease
Ago2	Argonaute 2
AHA	American Heart Association
Akt	Ak mouse strain
Bcl-2	B-Cell CLL/Lymphoma 2
btn	biotinylated
CDC	cardiosphere derived cell
CDC	cardiosphere-derived stem cells
COX	cyclooxygenase
CPC	cardiac progenitor cells
CVD	cardiovascular diseases
DAVID	database for annotation, visualization and integrated discovery
DMEM	Dulbecco's modified Eagle medium
EMMPRIN	extracellular matrix metalloprotease inducer
EMSA	electrophoretic gel shift assay
EPO	erythropoietin
ESCRT	endosomal-sorting complex required for transport

EV	extracellular vesicles
FABP	fatty acid binding proteins
FGF-β	fibroblast growth factor-β
FOXO1	Forkhead Box O1
GAPDH	glyceraldehyde 3-phosphate dehydrogenase
GO	gene ontology
GSK-3β	glycogen synthase kinase-3β
GVHD	graft-versus-host disease
HCC	hepatocellular cancer cell
hESC	human-derived embryonic stem cells
HF	heart failure
HGF	hepatocyte growth factor
hnRNP	heterogeneous nuclear ribonucleoprotein
HSC	haematopoietic stem cells
I/R	ischemia/reperfusion
ICAM	intercellular adhesion molecules
IGF-1	insulin-like growth factor
ILV	intraluminal vesicles
iPSC	inducible pluripotent stem cells
ISEV	International Society of Extracellular Vesicles
LAD	left anterior descending
LBPA	lipid lysobisphosphatidic acid

LDH	lactate dehydrogenase
lncRNAs	long non-coding RNAs
LPS	lipopolysaccharides
LVEF	left ventricular ejection fraction
MEME	multiple Em for motif elicitation
MI	myocardial infarction
miRNAs	micro RNAs
mPTP	mitochondrial permeability transition pore
mRNAs	messenger RNAs
MSC	messenchymal stem cells
MVB	multivesicular bodies
NF-κB	nuclear factor-kappaB
NSF	N-ethylmaleimide sensitive factor
nSMase2	neutral sphingomyelinase type II
ORF	open reading frame
PCA	principal component analysis
PDCD4	programed cell death 4
PDGF	platelet-derived growth factor
PD-L1	programed death ligand-1
PGE2	prostaglandin E2
piRNAs	PIWI-interacting RNAs
PPARs	peroxisome proliferator-activated receptors

pre-miRNA	precursor miRNA
pri-miRNA	primary miRNA
Pten	phosphatase and tensin homologue
RBPs	RNA binding proteins
RIPA	radioimmunoprecipitation assay
RISC	RNA induced silencing complex
ROS	reactive oxygen species
rRNAs	ribosomal RNAs
SDS-PAGE	sodium dodecyl sulfate polyacrylamide gel
SERCA	sarco/endoplasmic reticulum Ca2+-ATPase
Sfrp2	frizzled related protein 2
sim I/R	simulated ischemia/reperfusion
SM proteins	Sec1/Munc-18 related proteins
SNARES	soluble N-ethylmaleimide-sensitive-factor attachment protein receptors
snoRNAs	small nuclear RNAs
TCR	T cell receptor
TGF-β	transforming growth factor-β
tRNAs	transfer RNAs
TSG101	tumor susceptibility gene 101 protein
TTC	triphenyl tetrazolium chloride
TUNEL	terminal deoxynucleotidyl transferase dUTP nick end labeling
UTR	untranslated region

VEGF	vascular endothelial growth factor
Vps4	vacuolar protein sorting associated protein 4
vtRNAs	vault RNAs

ABSTRACT

Extracellular vesicles (EVs) are nano-size membrane bound vesicles that are derived from the fusion of multivesicular endosomes with the plasma membranes. EVs have important roles in intercellular communication through the transfer of their unique cargoes including RNA, DNA and protein molecules to recipient cells. Mesenchymal stem cell (MSC)-derived EVs have been shown to reduce infarct size and reduce the progress of heart failure after cardiac ischemia/reperfusion (I/R) injury in animal models. Small non-coding RNAs such as microRNA (miRNA) have been indicated as one of the active components that mediate the beneficial effects of MSC-derived EVs. However, the selective packaging mechanisms of these EV-enriched miRNAs as well as their specific functions in recipient cardiomyocytes are still incompletely understood.

Regarding the sorting mechanisms of miRNAs into MSC-derived EVs, we characterized the role of heterogeneous nuclear ribonucleoprotein A2B1 (hnRNPA2B1) in controlling the distribution of the miRNA population to EVs. We showed that disruption of the gene encoding hnRNPA2B1 prevented much of the loading of miR-486-5p into MSC-derived EVs. Based on RNA immunoprecipitation, gel-shift and biotinylated RNA pull-down assays, we confirmed the interaction of miR-486-5p and hnRNPA2B1. Because miR-486-5p was the predominant miRNA in EVs and almost absent in producer cells, we focused on the function of miR-486-5p in cardioprotection against I/R injury. Using different in vitro and in vivo functional assays, we demonstrated that miR-486-5p is protective against I/R injury

by inhibition of PDCD4-induced apoptosis in cardiomyocytes. The findings represented here indicated that hnRNPA2B1 interacts with miRNAs and mediates packing of miRNAs into MSC-derived EVs via a specific nucleotide motif in the miRNAs. One of the most highly EV-packaged miRNAs, miR-486-5p is cardioprotective in cardiomyocytes and in the heart.

CHAPTER I

INTRODUCTION

Epidemiology and Burden of Cardiovascular Diseases

Cardiovascular diseases (CVD) remain the most common devastating health problem for men and women worldwide, accounting for 18.6 million deaths in 2019 globally[1]. Myocardial infarction (MI), a common endpoint for ischemic heart disease/coronary artery diseases, is a leading cause of CVD deaths worldwide. Thanks to measures to reduce risk factors as well as advances in therapies for coronary revascularization, the incidence of MI and associated fatalities rates have been steadily decreasing overtime[2], though the American Heart Association (AHA) projects a new MI case is diagnosed every 40 seconds in the United States (US)[1]. An average of 600,000 American will suffer new heart attacks and 200,000 will have recurrent attacks in 2021[1]. While the current standard of care is to open the occluded vessel and reduce the time to reperfusion, patients who survive remain at a high risk for recurrent MI and heart failure (HF). Heart failure developing after MI hospitalization is very prevalent and is approximately 20-30% at the first year after discharge for MI[3]. The economic burden of CVD (direct and indirect cost) for the US healthcare system is enormous, amounting to $300 billion per year and is expected to increase rapidly to $1.1 trillion in 2035[1].

Ischemia/Reperfusion Injury

One of the primary conditions of CVD is myocardial infarction (MI), caused by ischemia/reperfusion (I/R) injury leading to irreversible cardiomyocyte loss. Myocardial infarction is defined as insufficient blood flow to the heart, resulting in the formation of infarct injury[4]. During ischemia, the anaerobic glycolysis prevails in cardiomyocytes, leading to accumulation of hydrogen ion and decrease in cell pH. Cardiac acidosis causes the Na^+/H^+ exchanger remove excess H^+ ion, overloading the cell with Na^+ ion, which in turn produces calcium overload due to the reverse operation of sodium-calcium exchanger. Ischemia also depletes ATP because of reduction in oxidative phosphorylation, deactivating Na^+/K^+ ATPase which is responsible Ca^{2+} efflux. Likewise, the reuptake of calcium back to the endoplasmic reticulum by the sarco/endoplasmic reticulum Ca^{2+}-ATPase (SERCA) pump is decreased, leading to further accumulation of cytosolic Ca^{2+}. Excessive cytosolic Ca^{2+} causes osmotic swelling and induces necrosis via action of Ca^{2+}-dependent proteases and cellular structure disruption.

During reperfusion, oxygen is re-introduced by restoration of blood flow, resuming oxidative phosphorylation. ATP-dependent hypercontracture in Ca^{2+} overloaded myocytes and pH normalization induce the opening of a non-selective channel, the mitochondrial permeability transition pore (mPTP). In addition, the restoration of oxidative phosphorylation causes a burst of reactive oxygen species (ROS). ROS damage proteins, lipids, nucleic acids, which further disrupt cellular structure. Furthermore, mPTP opening activates inflammatory and pro-thrombogenic cascades, inducing release of cytokine and apoptosis.

Because the heart has limited ability to regenerate, the infarcted region becomes scarred; the remodeling process ensues, leading to heart failure. The 5-year survival rate of HF patients remains at 50% in spite of advances in therapeutic intervention[5]. Therefore the introduction of novel treatments to salvage damaged and vulnerable cardiomyocytes after MI injury, thus preventing the loss of cardiac function is urgently necessary[6; 7].

In acute MI (AMI), an infarct kills 25% of the ventricle can cause a loss of as many as one billion cardiomyocytes[8]. Because the heart is often considered as a post mitotic organ with limited capacity for self-renewal, the infarcted region becomes fibrotic and scarred and remodeling occurs. The damaged and remodeled heart has lost contractile capacity due to the loss of cardiomyocytes and the increased stiffness of the ventricle, leading to the development of heart failure as a result. Prognosis for HF remains poor as the 5-year survival rate of HF failure is 50% with an increase in the risk of sudden cardiac arrest[9]. Several studies have shown a strong correlation between infarct size and mortality[10; 11]. Overall, larger infarct size is associated with worse clinical outcomes, including the likelihood that patients will experience heart failure, stroke, and death[11]. Therefore the introduction of novel treatments to salvage damaged and vulnerable cardiomyocytes after MI injury is urgently necessary.

Over the past decades, extensive studies on MI pathophysiological mechanisms have resulted in the development of various experimental interventions, including pharmacologic and nonpharmacologic protective strategies. Numerous therapeutic treatments have been proposed to protect the ischemic myocardium with potential cardioprotective effects in experimental animal models. However, only a few have been

translated into positive results in clinical practice[12]. Ischemic pre-, per-, post-, remote-conditioning (a series of controlled brief ischemia and reperfusion cycles), and pharmacological intervention have been shown to mitigate the I/R injury and limit myocardial infarct size in preclinical situations[13]. Unfortunately, most of the clinical trials yield conflicting or underpowered results[14; 15]. For instance, reperfusion therapy combined with agents such as ATP-sensitive potassium channel openers, Na^+/H^+ exchange inhibitors, glycogen synthase kinase-3β (GSK-3β) inhibitor, adenosine receptor agonist, cyclosporin A and erythropoietin showed infarct size-limiting effects and improved cardiac function in experimental animals[16]. However, most protective agents failed to reproduce meaningful impact in human AMI patients due to notable discrepancies between preclinical experiments and clinical setting including species differences in cardiomyocytes, age, treatment for concomitant diseases, and practical considerations in patients[16].

In recent years, potential uses of extracellular vesicles (EV) in the cardiovascular field as sources for therapeutic applications and diagnostic biomarkers have gained immense interest. EV from stem cells can activate beneficial signaling pathways in CVD, leading to improvement in cardiac function and smaller infarct size[17; 18; 19]. These processes are controlled by a variety of protein, nucleic acids, small molecules and paracrine factors released from stem cells in the damaged myocardium. As administration of EV has been shown to mediate cardioprotective properties, they represent a new frontier for novel approaches toward cardioprotection.

Extracellular Membranous Vesicles Released from Cells

EVs are a broad, heterogeneous group of membrane-enclosed structures used by all prokaryotic and eukaryotic cells to carry bioactive molecules including proteins, lipids, and nucleic acids. EVs serve as a means for intercellular communication, by triggering receptor-based signaling, and by delivery of their contents or cargo. Based on cellular origin and classification of the International Society of Extracellular Vesicles (ISEV), EVs can be subdivided into three subclasses roughly on the basis of size and their release mechanisms, including exosomes (40-100 nm), released by multivesicular body, microvesicles (100-1,000 nm), and apoptotic bodies (100-5,000 nm), released from direct budding from the cytoplasmic membrane [20; 21]. However, there is a lack of consensus on specific markers for EV subpopulations such as exosomes, microvesicles/microparticles[20]. Furthermore, common EV isolation methods (differential centrifugation or commercial kits) do not achieve fully separation of EV from non-vesicular entities. Therefore, we will use the term "EV" in the place of "exosomes" as encouraged by ISEV in this document[20; 22]. Please note that our preparations and characterizations are not different from those commonly used in "exosome" studies.

Initially, EV were viewed as by-products of cell homeostasis or cell damage, perhaps containing cellular "garbage" for disposal. The first report about the presence of EV in extracellular space came from a study of intracellular compartments that mediate transferrin endocytosis and recycling of the transferrin receptor[23]. In recent decades, the interest in EV has exploded, with an exponential increase in scientific publication over the years[24]. EV are thought to play a crucial role in cell-to-cell communication and a means of

transferring molecules between cells. For example, one of the earliest EV studies reported that EV from dendritic cells carry functional major histocompatibility complex class I, II that can prime T lymphocytes to induce antitumor immune response[25]. Moreover, EV facilitate the transfer of proteins, lipids, nucleic acids (mRNA, miRNA, DNA), organelles (mitochondria) from cell to cell and are attributed to the development of several diseases, including cancer, neurodegenerative disease, heart failure and liver disease[26]. These features have prompted researchers to explore EV as useful biomarkers in cancer and other ailments, as they carry cell content as cargo, and that content contains information about the cell that produced the EV. Furthermore, EV have been proposed to be potential carriers for drug delivery due to their cell membrane composition and immune privileged status. For example, EV-encapsulated paclitaxel produces stronger antineoplastic efficacy than conventional treatments, including small molecular entities, proteins, miRNA and mRNA. Importantly, exosomes do not invoke an immune response and thus are not cleared from the circulation by the immune system, nor cause rejection[27]. Despite intensive research and a growing body of literature, EV biology is in its infancy and we are just beginning to understand the involvement of EVs in cellular physiology and pathophysiology.

Extracellular Vesicle Biogenesis, Release and Uptake

The biogenesis and cargo composition of EV vary between different parental cell types, and in the same cell type in different physiological/pathological states[21]. Exosomes are considered a particular fraction of the EV population defined by size and by origin from the endosomal cellular compartment, though exosomes can also be derived from outward

budding of the plasma membrane in T cells[28]. Exosomal biogenesis starts by inward budding of the early endosome to form intraluminal vesicles (ILV), leading to the formation of multivesicular bodies (MVB). During the formation of ILV, certain cytoplasmic and membrane proteins are integrated into them. The accumulated ILV in the MVB lumen then have two possible destinies. One, they may deliver their payload with lysosome for degradation of vesicular content. Two, they may fuse with cytoplasmic membrane to release vesicles to the extracellular milieu by endocytic pathway. Cargo loading into ILV is mediated by two general mechanisms: endosomal-sorting complex required for transport (ESCRT)-dependent and ESCRT-independent pathways. The ESCRT complex -0, -I, -II, -III. are recruited to endosomal membrane's cytosol for the sorting of selected proteins to ILV which requires ubiquitination of cytosolic domains of exosomal cargoes[29]. In addition to its role in sequestration of ubiquitinated cargos, the ESCRT machinery also facilitates generation of membrane curvature on endosomes. Combination of ESCRT-I and II is reported to induce formation of inward budding structures by stabilizing the bud neck on the biogenesis of MVB using giant unilamellar vesicles and purified ESCRT complexes[30]. After the budding process to form ILV is completed, vacuolar protein sorting associated protein 4 (Vps4) provides energy for the ESCRT complex to separate from the MVB membrane and recycle complex for additional rounds of function. On the other hand, ILV can be generated at the endosomal membrane in the absence of ESCRT. The ESCRT-independent pathway depends on lipid raft microdomains and requires lipid ceramide and neutral sphingomyelinase type II (nSMase2), an enzyme that converts sphingomyelin located in the MVB membrane to ceramide. Inhibition of nSMase2 with GW4869 blocks

production and release of exosomes[31]. Other proteins involved in cargo loading in both ESCRT-dependent/independent sorting pathways are transmembrane proteins belonging to the tetraspanin family, including CD63, CD9, CD81 and CD82. CD63 is particularly abundant in MVB and exosomes and are useful markers for exosome characterization[32].

After the MVB matures, it is transported toward the cell membrane by actin and microtubules. Membrane fusion between the MVB and the plasma membrane then results in EV being secreted into the extracellular space[21]. This process relies on small GTPases such as Rab-27a/b, -7, -11, -31, -35 and soluble N-ethylmaleimide-sensitive-factor attachment protein receptors (SNARES) family proteins like YKTS6, VAMP7. Rab-27a/b are in charge of the tethering of MVBs to plasma membrane[33], while the other v-SNAREs including VAMP3 and VAMP7, in concert with the ATPase N-ethylmaleimide sensitive factor (NSF), are responsible for the docking and fusion of MVBs with cellular membrane, releasing exosomes into the extracellular space[34]. In addition, one study reported that calcium influx can enhance exosome release in hematopoietic K562 cell lines[35]. An increase in formation of large MVB and release of exosomes are observed with treatment using monensin, a sodium ionophore that increases intracellular Ca^{2+} by reversing the Na^{+}/Ca^{2+} exchanger. Treatment with Ca^{2+} chelator abrogates the intracellular calcium-induced EV release, whereas EV secretion increases by Ca^{2+} ionophore. Intraluminal calcium levels are regulated by thapsigargin-sensitive Ca^{2+} pump and inositol 1,4,5-inositoltriphosphate IP3 receptor[35].

The binding of EV to their target cells is likely dependent on proteins expressed on the EV surface and receptors on the plasma membrane of recipient cells. EV bind to their

recipient cells by using integrin, tetraspanin, heparan sulfate proteoglycan, lipid and extracellular matrix components. For instance, integrin on EV has been shown to interact with intercellular adhesion molecules (ICAM) of target cells to promote docking and uptake of EV. Treatment with antibodies against integrin or its ligand ICAM decreases EV uptake by dendritic cells[36]. Other molecules such as tetraspanin also can contribute to the docking of EV to the target cell membrane[37]. Blocking the binding site of tetraspanin CD81 or CD9 with antibodies reduces EV uptake by dendritic cells[36]. Once bound to recipient cells, EV can commit to various fates. EV can attach to membrane receptors of target cell to modulate signaling pathways[25; 38]. For example, follicular dendritic cells-derived microvesicles carrying MHC class II molecules and other proteins not expressed by recipient cells bind and stimulate B cells[39]. Alternatively, in order to elicit a response at recipient cells, EV can be engulfed by caveolin- and clathrin-mediated endocytosis, macropinocytosis, or phagocytosis, depending on vesicle size[32]. There are also findings that highlight the role of lipid raft domains within the plasma membrane in EV internalization. These rafts can be found in both caveolin-and clathrin-dependent endocytosis. Depletion of cholesterol disrupts these rafts and reduces EVs uptake[40].

After binding with membrane of recipient cells and uptaken by different mechanisms, EVs follow the endocytic pathway to reach MVB, leading to degradation of EV contents at lysosome. In order to avoid being targeted by lysosome, EV can fuse with the endosome limiting membrane. This process is not entirely understood, although protein Alix, phosphatidylinositol-3-phosphate, and lipid lysobisphosphatidic acid (LBPA) appear to control this event[41]. The back-fusion is thought to be important for delivery of

intraluminal nucleic acid payloads such as miRNA. On the other hand, EV can dock and merge directly with plasma membranes to release their material into the cytoplasm of recipient cells by membrane fusion[42; 43; 44]. The process of direct fusion is associated with GTPase Rab proteins, Lamp-1, SNAREs and Sec1/Munc-18 related proteins (SM proteins)[42]. There is evidence that direct fusion of EV from metastatic melanoma cells with the membrane of normal cell is determined by lipid composition of tumor cell membrane and the low acidity condition of malignant tumor[43]. Additionally, some studies indicated the presence of endogenous retrovirus class I proteins syncytin-1 and syncytin-2 on the surface of placenta-derived EV promotes the fusion of EV with recipient cell membranes. Attenuation of proper maturation of syncytin with furin inhibitors significantly reduces EV uptake, suggesting the important role of both syncytin-1 and syncytin-2 in EV fusion events[44].

Extracellular Vesicles Composition

The complexity of EV-derived components has been constantly updated with data from many proteomic and genomic studies. ExoCarta, a public resource database of datasets from eukaryotic-derived EV, contains information on 41,860 protein entries, 4,946 mRNA entries, 2,838 miRNA entries and 1,116 lipid entries, thus illustrating the complex composition of EV with various potential functions[45].

Protein Components

Generally, EV are enriched with proteins required for their biogenesis, including component proteins of ESCRT machinery, and of the tetraspanin family (CD63, CD81, CD82, and CD9). Other proteins include cytoskeleton components (actin, myosin, cofilin-1, tubulins), heat shock proteins (HSP70, HSP90), antigen presentation class I/II, metabolic enzymes, signaling proteins (GTPase, transforming protein RhoA), and ribosomal proteins. Certain protein components are consistently abundant in EVs (CD63, CD81, HSP70, and TSG101). In fact, they are widely accepted as EV marker proteins and can be used to demonstrate the purity of EV preparations[20; 46]. However, there are some reports about their presence in apoptotic bodies[47]. Additionally, different producer cells and cell culture conditions influence the types of specific proteins expressed in EVs. EV-derived proteins have been shown to produce measurable changes in behavior of receiving cells. For example, EVs isolated from dendritic cells can transfer TLR4, a cell membrane receptor to TLR4 deficient cells and trigger inflammatory responses to lipopolysaccharides (LPS) stimulation in those recipient cells[48]. In another study, EVs were shown to shuttle a specific set of synaptic proteins including AMPA receptor to the presynaptic terminal[49]. These findings support the role of EVs as important mediators for transferring receptors and other protein cargo from cell to cell, inducing functional changes in recipient cells.

Lipid Components

Aside from proteins and nucleic acids components, EV are also enriched in arachidonic acid (AA), and its prostaglandin derivatives (e.g., prostaglandin E2 (PGE2), 15-deoxy-Δ-12,14-prostaglandin J2 (15d-PGJ2)), cholesterol, phosphatidylserine, phosphatidic acid, sphingomyelin, and other fatty acids that are involved in MBV/ILV/EV formation and

cargo sorting into MVB. In one study, fatty acids and prostaglandin brought by EV were accumulated in recipient RBL-2H3 cells allowing micromolar concentrations of prostaglandin to trigger further biological responses[50]. Therefore, endosomal PGE2 and/or 15d-PGJ2 may serve to provide intracellular PGE2 for signaling. The EV-derived AA transferred by EVs also can be utilized by cyclooxygenase (COX) and PGE synthase in endoplasmic reticulum of recipient cells, resulting in additional PGE2 synthesis. EV-derived lipids can bind with lipid binding proteins, including fatty acid binding proteins (FABP) or nuclear receptors such as peroxisome proliferator-activated receptors (PPARs) in cells that uptake EV. This interaction forms AA/FABP/PPARs cytosolic complex and enables PPARs to exert biological functions in the nucleus[51]. EV isolated from activated T lymphocytes are internalized via endogenous phosphatidylserine receptors, increase cholesterol accumulation and proinflammatory cytokine production in monocytes and macrophages, thus promoting atherogenesis[52]. These findings further support EV as efficient mediator for cell-to-cell communication via lipid-induced signaling and gene expression.

Nucleic Acids Components

EV carry within them a heterogeneous population of RNA molecules which have also been found to be involved in intercellular communication. Initial report showed that EV RNA content consisted of mature miRNAs and mRNAs with size ranging from 200 nucleotides to 5kb[53]. Further comprehensive RNA sequencing studies have found the presence of most known non-coding RNA species, including ribosomal RNAs (rRNAs), long non-coding RNAs (lncRNAs), PIWI-interacting RNAs (piRNAs), transfer RNAs (tRNAs), small nuclear RNAs (snoRNAs), YRNAs and vault RNAs (vtRNAs) [54; 55]. In human plasma-

derived EV RNA species, microRNA is the most abundant, accounting for over 42.32% of raw counts and 76.20% of all mappable counts[54]. Once RNAs such as miRNAs and intact mRNAs are loaded into EV, they can be functional when transferred by EV between cells.

Messenger RNA

Many studies have reported mRNA as EV cargo and EV-derived mRNA function in recipient cells. Among EV-derived RNA species, mRNA is one of the least abundant EV RNAs, consisting of about 2.1% of all mapped RNAs in human plasma-derived EV[54]. The average length of EV mRNAs is smaller than 1000nt. In recipient cells, mRNA can function as a template for protein production. This event was reported by the presence of reporter proteins translated from mRNA transported from glioblastoma to endothelial cells[56] or between mast cells[53]. In the co-culture model of HEK293T cells and glioblastoma, translation of transferred mRNA was started within one hour after EV uptake by recipient cells[57]. The cell-to-cell transfer and active translation of EV mRNA were also reported in studies using Cre-loxP technology[58; 59]. The transfer of functional Cre-recombinase mRNA in red blood cell (RBC)-derived EV induces recombination in Purkinje neurons of floxed reporter mice[58]. Furthermore, to distinguish protein cargo and newly synthesized proteins in target cells, Maugeri *et al.* used lipid nanoparticles to deliver mRNA encoding human erythropoietin (EPO) to epithelial cells which was packaged into epithelial cells EV. These mRNAs were protected in EV and able to produce human EPO in recipient mouse cells[59]. Additionally, RBC-derived EV electroporated with mRNA for Cas9 have been used to deliver RNAs for CRISPR-Cas9 genome editing system which mediated functional gene

editing in recipient cells[60]. These studies support that EV are able to deliver functional mRNA to recipient cells effectively.

Long non-coding RNA

EV also contain long non-coding RNA (lncRNA) and circular RNA (circRNA). The lncRNA are defined as transcripts exceeding 200 nucleotides, which are not translated into protein. While the circRNAs are circular closed loop single stranded RNAs derived from protein encoding genes, primarily the introns, which may encode proteins but also have aspects of non-coding RNAs. LncRNA and circ RNA are known to function to mediate cell signaling, especially in the development of cancer. In human hepatocellular cancer cell (HCC)-derived EV, several lncRNAs are significantly expressed in EV relative to donor cells. Of these lncRNAs, lncRNA TUC339 is the most highly enriched. TUC339 function is implicated in tumor cell proliferation and cell adhesion to extracellular matrix[61]. In another study, lncRNA H19 in EV released from $CD90^+$ liver cancer cells can alter the phenotype of endothelial cells, promoting angiogenesis and cell adhesion[62]. Other lncRNAs that are enriched and released through EV include lncRNA ARSR (renal cancer)[63] and lncRNA CRNDE-h (colorectal cancer)[64]. The cited studies demonstrate that lncRNA can be transferred between cells via EV and subsequently modulate cellular function of recipient cells.

On the other hand, circRNAs act as miRNA sponges by competitive binding of miRNAs, preventing the binding of miRNA with their target mRNAs. For instance, EV-enriched circRNA-100284 isolated from arsenide-transformed cells has been shown to promote cell proliferation and induce malignant transformation. circRNA-100284 exerts its

inhibitory effect as a sponge of miR-217, thus increasing levels of EZH2, a transcriptional activator, in recipient cells[65]. Additionally, circular RNA is highly stable and is resistant to exonuclease-mediated degradation, and thus can be used as markers for tumor diagnosis. For example, specific circRNAs were detected in hepatic cancer cell-derived EVs. CircRNA expression in colorectal cancer patients was different from healthy subjects. Specifically, 67 circRNAs were absent, while 257 new circRNAs species were discovered in cancer patients[66].

MicroRNA

MicroRNAs (miRNAs) are single-stranded small non-coding RNAs (20-25 nucleotides in length) [67]. miRNAs are among important post-transcriptional regulators for protein-coding genes. Since their discovery in C. elegans in 1993 [68], fully one-third of human mRNAs have been predicted to be targets of miRNAs [69]. The biogenesis of miRNAs begins with the transcription by RNA polymerase II to generate the primary miRNA (pri-miRNA) from its gene. pri-miRNA is double-stranded long RNA (1000 nt) with hairpin structures. Because miRNA is embedded in the stem region of pri-miRNA, miRNA needs to be released by endoribonucleases. First, Dorsha, a class 2 ribonuclease III, cleaves pri-miRNA near the end of the stem. This new short hairpin structure is called precursor miRNA (pre-miRNA) and transported from the nucleus to the cytoplasm by the Exportin-5 complex. After being released from Exportin-5 in the cytoplasm, the stem-loop of pre-miRNA is cleaved by the Dicer complex, generating a double-stranded RNA of 22 nt. This RNA duplex is then loaded into the RNA-induced silencing complex (RISC) where it is unwound and a single strand (guide strand) is used to help RISC bind to the conserved

recognition site on the target mRNAs. It is known that miRNA acts through base-pairing of their seed sequence, nucleotides 2-7, with sequences in the 3'-untranslated region (3'-UTR) of the target mRNA[70; 71]. If the binding of RISC to the target mRNA is a nearly perfect match, it will lead to mRNA degradation, whereas a partial match will lead to a translational inhibition[67; 70]. In addition, miRNAs and their cognate binding sites in target mRNAs are well conserved evolutionarily, supporting the regulatory importance of these interactions[70].

Prevailing data suggest the transfer of functional EV-derived miRs from EV producer cells to recipient cells, with a variety of downstream effects on different molecular and physiological functions and disease models. Liu *et al.* showed that miR-193b is released in the central nervous system via EV and reduces the accumulation of amyloid precursor protein in neuronal cells, thus functioning in the development of Alzheimer's disease (AD)[72]. miR-193b can be used as a novel, non-invasive biomarker for AD[72]. In another study, neuron-derived EVs were loaded with miR-124a and shown to modulate synaptic transmission by miR-124a-specific targeting of the glutamate transporter GLT1 in astrocytes[73]. As another example, miR-19 content in astrocyte-derived EV induces downregulation of tumor Pten, promoting brain metastasis[74]. In the context of inflammatory response, miR-155 and miR-146a are released from dendritic cells via EVs and shuttled between immune cells to regulate cellular response to endotoxin. MiR-155 enhances while miR-146a reduces endotoxin-induced inflammation[75]. Examples of functional transfer of miRNAs by EV in mammalian cells are summarized in Table 1.

Sorting Mechanisms of MicroRNAs into EV

Multiple mechanisms for selective sorting miRNA into EV have been discovered, including different affinity for membrane lipids, interaction with RNA binding proteins (RBPs) with specific RNA sequence motifs, and RNA post-transcriptional modifications. The neutral sphingomyelinase 2 (nSMase2)-dependent pathway is the first reported mechanism for RNA sorting[76]. Blocking or overexpressing nSMase2, a hydrolase that regulates the biosynthesis of ceramide, leads to altered levels of EV-derived miRNAs including miR-16 and miR-146a[76]. miRNAs can be loaded into EVs by RNA-RBP interaction. One of these RBPs is Argonaute 2 (Ago2), a component of RNA induced silencing complex (RISC). Ago2 has been implicated in controlling secretion into EV of certain miRNAs including let-7a miRNA, miR-100 and miR320a into EV through the KRAS-MeRK-ERK signaling pathway[77]. Similarly, Y-Box binding protein 1 (YBX-1)[78] and La protein[79] are other RBPs that can interact with miR-223/miR-133 for the former and miR-122 for the latter through specific RNA binding protein-RNA interactions. Other studies have reported that sequence motif-dependent RNA-RBP interaction is involved. The SUMOylated form of heterogeneous nuclear ribonucleoprotein A2B1 (hnRNPA2B1) has been shown to direct the sorting of a group of miRNAs that has a specific short motif GGAG (EXO motif) into primary T lymphoblast-derived EVs. Removing the EXO motif from EV-enriched miRNAs or adding the EXO motif into cell- retained miRNAs significantly changed the ratio of the miR levels in EV to producer cells.

Table 1. Functional Transfer of miRNAs by EV in Mammalian Cells

Disease condition	Model	Donor cells	miRNA	Acceptor cells	Biological effects	Ref.
Rhabdomyosarcoma	*In vitro, in vivo*, mice	Myoblast	miR-486-5p	Fibroblast, myoblast	Cell migration, invasion, colony formation	80
Breast cancer	*In vitro, in vivo*, mice	Breast cancer cells	miR-9, miR-195, miR-203	Endothelial cells, epithelial cells, breast cancer cells	Tumorigenesis, angiogenesis, cell invasion, cell proliferation, drug resistance	81
Glioblastoma	*In vitro, in vivo*, mice	Glioma cells	miR-9, miR-21	Microglia, brain endothelial cells	Angiogenesis, immunosuppression	82
Cardiovascular diseases	*In vitro, in vivo*, mice	Cardiac stem cells	miR-21, miR-132, miR-210, miR-451, miR-146a	Various cell types	Apoptosis inhibition, angiogenesis, myocardial fibrosis	83
Myocardial infarction	*In vitro, in vivo*, mice	Bone marrow MSC	miR-21, miR-22, miR-let7, miR-29, miR-24, miR-34, miR-130, miR-378	Various cell types	Apoptosis and autophagy inhibition, angiogenesis, immunosuppression	17; 84; 85
Muscle injury	*In vitro, in vivo*, rat	Bone marrow MSC	miR-494	Myoblast	Skeletal muscle regeneration, angiogenesis	86
Middle cerebral artery occlusion	*In vitro, in vivo*, rat	Bone marrow MSC	miR-133b	Neural cells	Neurite outgrowth	87
Hepatocellular carcinoma	*In vitro, in vivo*, mice	Adipose MSC	miR-122	Hepatocellular carcinoma	Cell cycle and growth	88
Liver fibrosis	*In vitro, in vivo*, mice	Adipose MSC	miR-181-5p	Liver cells	Apoptosis autophagy	89
Skull defect	*In vitro, in vivo*, rat	Adipose MSC	miR-375	Bone marrow MSC	Osteogenic differentiation, bone regeneration	90
Neurodegenerative disorder	*In vitro*	Neural precursor cells	miR-21	Neural progenitor cells	Neurogenesis	91
Insulin resistance	*In vitro, in vivo*, mice	Adipose macrophage	miR-155	Liver and muscle cells	Insulin sensitivity	92
Lipodystrophy and obesity	*In vitro, in vivo*, mice	Adipocytes from brown adipose tissue	miR-99b	Liver cells	Glucose tolerance	93

Altering hnRNPA2B1 expression or its sumoylation resulted in changes of EXO miRNAs levels[94]. Using a similar approach, Santangelo et al. found that hnRNPQ (SYNCRIP) was found to bind miRNAs harboring a GCUG common sequence (hEXO motif) that are selectively sorted into hepatocyte-derived EVs. Silencing hnRNPQ with shRNA led to a significant reduction of several EV-enriched miRNAs, while insertion of an hEXO motif into an intracellular miRNA increased its sorting into EVs[95]. Finally, the 3' end post-transcriptional modification of miRNA sequences mediates their relative abundance in parent cells *vs*. EV[96]. The uridylation of the 3'-ends of miRNA enhances the selective sorting of miRNA isoforms into EVs, whereas 3'-end adenylated miRNA isoforms are highly retained in producer B-cells. In summary, specific enzymes or proteins can direct miRNA sorting into EVs, and certain miRNAs with specific sequences can be selectively sorted to EVs in certain producer cell types.

Significance of Extracellular Vesicles

Canonically, cells often communicate directly with adjacent cells through gap junctions and cell surface receptor/ligand interactions. Communication with distant cells occurs through molecules including proteins, lipids or nucleotides that are released by cells and bind to receptors on the target cells. Such paracrine signalings are important for cell-cell communications in normal/pathological conditions. Emerging data has proven that EVs can deliver functional molecules, including proteins, transmembrane receptors, lipids, messenger RNA (mRNA) and non-coding RNA (ncRNA) and so modulate phenotypic features and responses of recipient cells. The bioactive cargoes in EVs can impact recipient cells via direct interaction with surface-bound ligands, by transfer of activated receptors or

by release/delivery of functional proteins, lipids, and/or nucleic acids to recipient cells. In fact, multiple studies have demonstrated that EVs play important roles in dissemination metastasis of cancer cells and tumor progression. Specifically, EVs from cancer cells can change cell motility by targeting extracellular matrix[97], and can promote drug resistance[63], tumor angiogenesis [98], and metastasis of tumor cells[99]. Tumor-secreted EVs can promote cancer progression by targeting immune cells. In one study, EVs derived from epithelial ovarian cancer induced macrophage M2 polarization[100]. This phenotype is mediated by miR-940 content in the EVs, leading to metastasis and low survival rates[100]. Several cancer cells can transform local fibroblasts into cancer-associated fibroblasts through the transmission of hTERT mRNA via EVs[101]. These transformed fibroblasts in turn can modify cellular metabolism, enhance glycolysis, and reduce oxidative phosphorylation[102]. On the other hand, immune cells release EVs that target cancer cells. Natural killer (NK) cell-derived EV shows antitumor effects against melanoma cells with minimal side effects on normal human kidney cells. The cytotoxicity is modulated by Fas ligand and perforin expressed in NK-derived EVs[103].

Beside cancer, EV can serve as a mediator in the spread of disease. The presence of neurodegenerative disease-related EV cargo proteins such as Aβ/tau in Alzheimer's disease[104; 105], alpha-synuclein in Parkinson's disease[106] or prion in infectious prion disease[107] supports that EVs represent an important means of intercellular cross-talk in physiologic and pathologic conditions.

Stem Cells and -based Extracellular Vesicles Therapy for Myocardial Infarction

Stem cell biology is one of the newest and fastest growing areas in life science. Based on their proliferation capacity, stem cells can be divided into pluripotent cells (including embryonic stem cell (ESC), inducible pluripotent stem cells (iPSC)), and multipotent cells with limited potential (such as cardiac progenitor cells (CPC), cardiosphere-derived stem cells (CDC), and bone marrow stem cells (MSC))[108].

The heart is one of the most attractive solid organs for regenerative medicine as loss of cardiac cells underlies much of the morbidity and mortality of heart disease. The rationale of these early studies is based on the regenerative capacity of stem cells to differentiate into different types of cells and tissues. Indeed, stem cell-based therapy has been studied to support the reparative process of cardiac tissue and to improve the function of damaged myocardium in cardiovascular diseases for several decades[109].

Human-derived Embryonic Stem Cells (hESC) or allogeneic iPSC are promising sources for direct cell replacement of damaged myocardium due to their unlimited self-renewable capacity and indisputable ability to differentiate into cardiomyocytes[108]. Cardiomyocytes derived from hESC- and iPSC have similar cardiac gene expression patterns, as well as cardiac specific sarcomeric proteins and ion channels. These cells display functional properties of cardiomyocytes in regard to electric activity, excitation-contraction coupling and neurohormonal signaling[108]. Importantly, they have been demonstrated to survive in the long term post-transplantation, grow and regenerate infarcted myocardium in primate models[72; 110]. Improvement in cardiac function (ejection fraction, fractional shortening) is associated with partial remuscularization of the scar by

grafted cardiomyocytes. However, concerns over the post-transplant arrhythmias and teratomas formation remain and require more effort to control these unwanted side effects before clinical application of pluripotent stem cells[72]. More recently, new evidence suggested that iPSC-derived EV can recapitulate beneficial effects of their parent cells for heart repair[111]. ESC (iPSC)-EV represents a potentially therapeutic alternative in treating CVD while circumvent some ethical concerns related to pluripotent stem cells research.

With other multipotent stem cells, the idea that some of these stem cells can transdifferentiate into new cardiomyocytes and blood vessels, thereby replacing dead myocardium is one of the biggest controversies in the field. The trans-differentiation hypothesis was first proposed in 2001 with c-kit^{+}, lineage negative (Lin^{-}) bone marrow cells[112]. Newly formed myocardium was reported to occupy 68% of the infarcted ventricle after transplanting the bone marrow cells[112]. Based on these results, a variety of clinical studies were run with various bone marrow-derived stem cell types, but there was no significant benefits found[113; 114]. The improvements found in preclinical and studies were judged to be due to paracrine effects and transdifferentiation did not occur[115; 116]. For example, study using reporter transgenes to monitor transdifferentiation events showed no transdifferentiation of haematopoietic stem cells (HSC) into cardiomyocytes in both normal and injured adult mouse hearts[115]. Later murine studies using CPC and CDC also claimed evidence of transdifferentiation and repair[117], but it was later found that these cells do not contribute to differentiation of cardiomyocytes[118]. In one study, cardiosphere CDC-derived EV can reproduce the functional effects of CDC transplantation in suppressing apoptosis, enhancing angiogenesis while inhibition of EV production by CDC attenuated

those benefits[19]. Further investigation suggested that miR-146a may contribute to some of the therapeutic benefits of CDC-derived EV[19]. Besides EV, CDC released several growth factors including vascular endothelial growth factor (VEGF), hepatocyte growth factor (HGF), and insulin-like growth factor (IGF-1) that are able to exert cardioprotective properties.

Overall, the consensus today is that there are no cardiac-resident stem cells and that circulating stem cells, including MSC do not regenerate myocardium. Beneficial effects, though small, are reparative and are thought to be due to paracrine mechanisms[119]. We now believe that some of the results reported for stem cell repair are due to these paracrine protective and reparative effects combined with difficulties distinguishing cell fusion from division, and salvage from regeneration.

Bone marrow-derived Stromal Cells

Mesenchymal stem cells (MSC) are multipotent stem cells obtained from bone marrow, adipose tissues and umbilical cord tissue[120]. To address inconsistencies in tissue sources and cell preparation methods, the Mesenchymal and Tissue Stem Cell Committee of the International Society for Cellular Therapy proposes three criteria defining MSC based on their characteristics, consisting of (1) being adherent to plastic in standard culture conditions (2) expressing positive surface markers including CD105, CD73 and Cd90 while not expressing negative surface markers including CD45, CD34, CD14, CD11b, CD79α and HLA class II (3) being able to differentiate to osteoblasts, adipocytes, chondroblasts under standard in vitro differentiating conditions[121].

Among different types of stem cells employed in stem cell based therapy for the treatment of I/R injury, MSC were seen as promising candidates due to ease of isolation, low immune response and safety profile[109; 122]. MSC can escape immune rejection due to low expression of HLA and co-stimulatory molecules, making them somewhat immune privileged[120]. Furthermore, several early-phase I clinical trials such as Transendocardial Autologous Cells in Ischemic Heart Failure Trial (TAC-HFT) [123] and Percutaneous Stem Cell Injection Delivery Effects On Neomyogenesis in Dilated Cardiomyopathy (POSEIDON)[124] have demonstrated good safety profiles for MSC based cell therapies, which are still being investigated to this day for a variety of diseases and injuries. MSC have been demonstrated to facilitate tissue repair of ischemic tissue. This effect is associated with reduction in apoptosis in the border zone and improvement of cardiac function measured by left ventricular ejection fraction (LVEF) in animal model[125; 126]. In human clinical trials, MSC injection shows a modest improvement in ejection fraction of recipient hearts[124; 127; 128]. Report of adult human bone marrow-derived cells transdifferentiating into cardiomyocytes prompted considerable interest in MSC[129]. However, as mentioned above, subsequent studies has shown definitively that MSC do not transdifferentiate into cardiomyocytes. Less than 1% of transplanted MSC were able to home and engraft in target tissues[130]. Therefore, MSC probably exert their effects via paracrine mechanisms through the release of extracellular vesicles and cytokines.

MSC-derived EV in Cardiac Repair

Many of the studies that attributed to stem cells, including MSC, the ability to regenerate new cardiomyocytes by trans-differentiation, failed to delineate effects upon

salvage of myocardium from growth of new muscle. In fact, implantation of MSC has been shown to elicit cardioprotective effects against cell death after acute ischemia/reperfusion. The possibility of using MSC-EV to reduce damage after myocardial infarction has been widely evaluated. Indeed, numerous studies have reported that MSC-derived EVs recapitulates many of the tissue-healing effects of MSC in *in vitro* assays and *in vivo* models. The first evidence for the beneficial effect of ***paracrine effects*** on the heart was reported by Gnecchi *et al*[131]. They discovered that injection of conditioned medium from mesenchymal stem cell (MSC) cultures overexpressing anti-apoptotic protein Akt1 showed cardioprotection in both cell culture and murine models of MI. The cardioprotective effect of the conditioned medium of the overexpression Akt1-MSC induces secretion of frizzled related protein 2 (Sfrp2), a modulator of Wnt signaling, to upregulate β-catenin and other antiapoptotic genes. Silencing Sfrp2 in Akt-overexpressed MSC abrogates the protective effect of the condition medium[132]. In 2010, Lai *et al.* was the first group to isolate and report cytoprotection of MSC-EV in reducing the infarct size in an animal model for myocardial I/R injury[18]. EVs derived from conditioned culture media of MSC have similar size, morphological features and common surface markers as other cell types, including CD81 and CD9. They also harbor adhesion molecules expressed on the MSC membrane, including CD44, CD29 and CD73[133]. EV contain the metabolic enzyme glyceraldehyde 3-phosphate dehydrogenase (GAPDH) which can supply depleted ATP-producing glycolytic enzymes after ischemic injury. Furthermore, heat shock protein HSP70 and antioxidant enzymes such as glutathione S-transferase in the EV cargo can reduce damage induced by protein aggregation and oxidative stress[134].

MSC-derived EV Suppresses Apoptosis

Apoptosis is defined as energy-dependent programmed cell death when the cellular damage is beyond the repair process. Apoptosis is characterized by blebbed membrane, shrinked organelles, and fragmented, condensed DNA, resulting in release of apoptotic bodies to be internalized by phagocytes. In addition to necrosis, apoptosis plays an important role in I/R injury-induced cell death of cardiomyocytes, which eventually leads to heart failure[135]. Therefore, many strategies have been developed to block apoptosis in I/R injury, including MSC-derived EV. This approach has been shown to successfully reduce reperfusion-mediated apoptosis and improve cardiac function in animal studies. Evidence suggests that MSC-EV-mediated anti-apoptotic effects are exerted by miRNAs cargo content. Among anti-apoptotic miRNAs in MSC-derived EV, miR-21-5p is highly enriched in both parental cells and EV. Transfer of miR-21-5p from EV secreted by human endometrium-derived MSC promotes myocardial salvage and enhances cardiac function after MI in a rat model. MiR-21-5p mediates these paracrine actions by modulating the Pten/PI3K/Akt pathway[136]. One study also found higher levels of miR-21-5p in EV released from MSC under oxidative stress than EV collected from MSC under normal conditions. Exosomal miR-21-5p inhibits Pten expression in C-kit+ cardiac stem cells, leading to cytoprotection against apoptosis triggered by oxidative stress[137]. In agreement with these results, our group reported the cardioprotective activity of MSC-derived EV using cell culture and mouse model for I/R injury through miR-21-5p delivery. In this case, these EV reduce cardiomyocyte necrosis, apoptosis and autophagy by inhibiting FasL, Pten, Beclin1, PDCD4[17]. Likewise, Wang *et al.* demonstrated that EV secrets from bone marrow-derived

MSC (BMSC) reduce apoptosis and production of ROS in cardiac stem cells (CSC). Under hypoxic condition EV collected from BMSC have higher protective effects than those cultured under normoxic condition. Hypoxia also increases miR-214 expression in BMSC-derived EV, which is transferred into CSC and suppresses CaMKII involved in oxidative stress-induced apoptosis and Ca^{2+} homeostasis[138]. The effect of hypoxic preconditioning on MSC-derived EV is confirmed in other studies, which miR-210[139] and miR-125b[140] in hypoxia conditioned MSC-EV increase cell survival and reduce infarct size post-MI. Interestingly, EV derived from senescent MSC have weak activities in inhibiting apoptosis, promoting angiogenesis and reducing fibrosis. RNA sequencing revealed that miR-221-3p level is decreased in aged MSC-derived EV, compared to young ones. Overexpressed miR-221-3p enhanced pro-survival Akt pathway, increased proangiogenic VEGF, while down-regulated Pten and pro-apoptotic protein cleaved-caspase-3[141].

Furthermore, long non-coding RNA (lncRNA) in the cargo of MSC-EV also regulates apoptosis. EV isolated from macrophage migration inhibitory factor is enriched with lncRNA-NEAT1, which inhibits expression of miR-142-3p and activates Forkhead Box O1 (FOXO1) signaling pathway[142]. MiR-142-3p has been reported to inhibit survival and growth pathways whereas loss of miR-142-3p preserves cardiac function during adaptive hypertrophy. Therefore, lncRNA-NEAT-1/miR-142-3p/FOXO1 represents a novel cellular RNA signaling pathway in cardioprotection[143].

MSC-derived EV Reduces Inflammation

After initial cardiac injury, cardiac macrophages are recruited and accumulate to promote repair through crosstalk with other cardiac cells, including fibroblasts and

endothelial cells. This can lead to myocardial salvage after reperfusion, but it can also trigger a hyper-inflammatory reperfusion injury-associated response, which is mediated by immune cells such as neutrophils and macrophages. Striking a balance between optimizing pro-reparative macrophages and suppressing maladaptive immune cells is the key to promoting optimal healing[144]. Evidence for immunomodulatory properties of MSC-derived EVs as a treatment in acute MI has recently emerged. It has been documented that MSC-EVs have anti-inflammatory effects by limiting the infiltration and proliferation of CD3+ T cells and enhancing them to secret anti-inflammatory cytokines such as IL-10 and TGF-β into the infarcted myocardium[145]. MSC-EVs also suppress B-cell proliferation and differentiation[146]. Several studies support that miRNAs in MSC-EVs contribute to their anti-inflammatory effects. In one study, administration of MSC-EVs alleviated inflammation and reduced infarct size after myocardial I/R in a mouse model. The efficacy of MSC-EV was dependent on the interaction of its transfer of miR-182 from MSC-EVs with to macrophages. MiR-182 mediates the capacity to switch between M1 and M2 macrophages through targeting toll-like receptor 4 (TLR4)/NF-κB/PI3K/AKT signaling pathway[147]. Similar results showed that EVs derived from adipose MSCs (AMSCs) induces an anti-inflammatory M2 macrophages phenotype. This effect is mediated via transferring of a group of upregulated miRNAs in AMSC-EVs, including miR-21, mir-34a-5p, and miR-146a-5p[148].

In addition to miRNAs, protein cargo of MSC-EVs can regulate the immune response. A significant amount of regulatory factors for inducing immune tolerance are detected in MSC-EVs, including programmed death ligand-1 (PD-L1), galectin-1 and TGF-β[149]. PD-L1 is an essential component of the PD-1/PD-L1 pathway in T cell receptor (TCR) signaling, thus

reducing glucose metabolism and cytokine synthesis, and blocking proliferation and survival of T-cell[150]. Galectin-1 is a negative regulator for both innate and adaptive immune response, inhibiting cell growth, and promoting apoptosis of activated immune cells[151]. On the other hand, TGF-β function in immune response is context-dependent to stimulate either pro- or anti-inflammatory pathways[152]. These findings shed a new light on using MSC-derived EV as novel therapies for myocardial injury.

MSC-derived EV Enhances Angiogenesis

Angiogenesis is the formation of new blood vessels from pre-existing vasculature. After the onset of MI, adequate angiogenesis salvages infarcted myocardium through necessary perfusion of oxygen, and nutrients, preventing cell death, expansion of infarct and dilation of the left ventricular. In contrast, poor angiogenesis causes hypoperfusion of viable myocardium, promotes apoptosis and dysfunction of cardiomyocytes, leading to decreased contractile function and heart failure[153]. Therefore developing efficient pro-angiogenic therapeutics represents a promising strategy for treatment of acute MI. Indeed, several studies have shown MSC-derived EV stimulate angiogenesis in target cells. Treatment with MSC-EV upregulates expression of a number of pro-angiogenic and angiogenesis-associated factors, such as vascular endothelial growth factor (VEGF), pro-angiogenic fibroblast growth factor-β (FGF-β) in cardiac cells[154].

Evidence suggests that MSC-EV elicit pro-angiogenic effects via vesicle-bound vesicle- protein cargo. In one study, MSC-derived EVs have abundant levels of VEGF, matrix metalloprotease-9 (MMP-9), and extracellular matrix metalloprotease inducer (EMMPRIN), whose role in stimulating angiogenesis has been reported[155]. Knocking down EMMPRIN

causes loss of EMMPRIn in EVs and reduces the ability of MSC-EVs to stimulate angiogenesis both *in vitro* and *in vivo*. Proteomic analysis of MSC-EVs from another study revealed the presence of pro-angiogenic factors including transforming growth factor-β (TGF-β), VEGF, platelet-derived growth factor (PDGF), interleukin-8 (IL-8)[156], adhesion proteins associated with endothelial cell proliferation and angiogenesis including ezrin, galectin-1, p195[157], and nuclear factor-kappaB (NF-κB) signaling pathway proteins[158].

In addition to protein cargo, MSC-EVs mediate pro-angiogenic effects through direct transfer of their miRNA contents. Mayourian *et al.* demonstrated that treatment with miR-21-5p contained in human MSC-EVs increased expression of proangiogenic factors VEGF-α, TGF-β, angiopoietin-1 via the PI3K signaling cascade in cardiomyocytes[159]. In another study, Ferguson et al. profiled the miRNA content of MSC-derived EV and identified biological processes modulated by exosomal miRNAs. They found the top EV enriched miRNAs (miR-21-5p, miR-23a-3p, and miR-1246) are predicted to target angiogenesis and tissue remodeling pathways including TGF-β signaling, PDGF signaling, and Wnt signaling. This network analysis was confirmed by the upregulation of mRNA for mediator of angiogenesis genes (ephrin type-B receptor 2 (EPHB2), and neuropilin 2 (NRP2)) and pro-angiogenesis genes (angiopoietin-1 (ANGPT1), ANGPT4, and ANGPTL4) in HUVEC treated with MSC-EV. Furthermore MSC-EV loaded miR-130a-3p showed angiogenic effects through targeting the antiangiogenic protein HOXA5[160]. Taken together, these studies suggest involvement of MSC-derived EV in angiogenesis post MI.

Clinical Trials Involving MSC-derived EV

Currently, the lack of standards for cell culture conditions, as well as optimal protocols for production, isolation, storage underlies much batch-to-batch variation of EV products. Additional criteria to determine therapeutic dose, administration regime and reliable assays to assess miRNA transfer and efficacy are needed to facilitate the use of MSC-derived EVs in the clinical setting[161]. However there are several ongoing trials to evaluate the safety and therapeutic efficacy of MSC-derived EVs in patients. Some published clinical studies show encouraging results. In one study, treatment with MSC-EVs reduced the production of pro-inflammatory cytokines IL1β, TNFα, and IFNγ from peripheral blood mononuclear cells in patients with severe forms of graft-versus-host disease (GVHD)[162]. In another study, the administration of umbilical cord MSC-derived EVs improved the kidney function in chronic kidney diseases as assessed by improvement of glomerular filtration rate, serum creatinine levels and reduction of inflammation[163].

In conclusion, numerous studies have shown the therapeutic efficacy of MSC-derived EVs and their potential for human clinical trials. The purpose of this study is to elucidate the mechanisms by which MSC EVs exert therapeutic effects and to improve these effects in models of IR injury.

Summary of Goals and Hypothesis

Myocardial infarction is the one of the leading causes of CVD death worldwide[164]. In MI, occlusion of coronary arteries results in insufficient blood supply to myocardial cells. Subsequently, there is an imbalance between oxygen supply and demand, reduced ATP levels, increased influx of calcium. Together, these adverse events trigger cell death.

Reperfusion is necessary to reestablish blood flow return to the ischemic area, and yet, reperfusion can do further damage causing irreversible cardiomyocyte loss, namely ischemia-reperfusion injury[4]. I/R injury, if untreated, can lead to heart failure and death. Therefore, finding new therapeutics to reduce damage after MI is desperately needed[4; 7; 164]. EV-associated miRNA cargoes have been shown to be preferentially enriched in EV and to be functional in the target cells[165; 166; 167]. However, the sorting mechanism and the cellular functions of specific MSC-derived EV associated miRNA have yet to be resolved, particularly in their relationship to CVD therapy. We propose that EV and specific miRNAs are critical mediators of the beneficial effects of transplanted MSC in the heart. Our lab finding that some of the protective effect of MSC-derived EV may still persist after removal of miR-21-5p[17], suggests there must be other protective exosomal miRNAs whose functions in I/R injury have not previously been studied. Our discovery that a specific group of miRNAs are selectively sorted into MSC-EV provides a jumping off point to investigate the contribution of these miRs to cardioprotection in the heart. Therefore the central hypothesis for this dissertation is that RNA-binding proteins are involved in the selective transport of miRNAs containing specific RNA-sorting sequences into extracellular vesicles to exert protective effects against ischemia/reperfusion injury. This hypothesis was tested by pursuing the following two aims.

Aim 1. Determine the Mechanism of Selective Sorting of miRNAs into MSC-derived EV

The microRNA content of EV is important for intercellular communication[168]. During EV biogenesis, mRNA/ncRNA can be loaded via passive transport or via active sorting mechanisms[169]. Passive loading of miRNA such as miR-21-5p relies on mass action effect,

whereas active EV sorting involves the recognition of specific sequences[94; 95] or post-translational modifications of ncRNA[170]. Our preliminary data indicates the relative abundance of specific miRNAs is not the same in parent cells and EV. Several miRNAs such as miR-486-5p, miR-122-5p and miR-451a were detected at relative high levels in EV relative to producer cells, suggesting the loading of exosomally enriched MSC miRNAs is an active and selective process. The objective of Aim 1 is to identify key components of the miRNA selective sorting apparatus which control the sorting of enriched exosomal nucleic acids.

Aim 2. Examine the Protective Effects of Selectively Sorted EV miRNA against myocardial I/R injury**.**

MSC-derived EV have demonstrated the ability to ameliorate tissue injury via their miRNA and protein cargoes[18; 171; 172]. Our lab recent study indicated that miR-21-5p is a key factor behind the protective effect of MSC derived EV due to the suppression of PDCD4, Pten, Peli1 and FasL[17]. We observed a significant protection after injection of wild-type EV, compared to saline group. Pre-treatment with miR-21-5p-depleted EV produced a small but not significant reduction of infarct size, suggesting other EV cargo may also contribute into the cardioprotection. Our preliminary study shows that miR-486-5p, the top enriched EV miRNA targets pro-apoptotic protein PDCD4 *in vitro*. Therefore, the objective of Aim 2 is to identify cytoprotective effects of EV-selectively sorted miRNAs, with a focus on miR-486-5p.

Innovation and Significance

These studies are novel and innovative in that their findings shed light on MSC EV-associated non-coding RNA secretome. A mechanistic understanding of exosomal miRNA-sorting as well as the function of specific miRNAs will allow possible selective modification of exosomal miRNA cargo which, in turn, opens the way for development of cell-free molecular therapeutic approaches for damage-associated with ischemia reperfusion injury.

CHAPTER II

MATERIALS AND METHODS

Animal

B6.129 mice (8-10 weeks) were purchased from Jackson labs (#002609) and were maintained per NIH guidelines in the Guide for the Care and Use of Laboratory Animals [173] and animal protocol approved by Institutional Animal Care and Use Committee at Loyola University Chicago (LU permit number 206610). Upon arrival, mice were acclimated for seven days prior to any procedures. Mice were housed in a group of two and had accessed to food and water *ad libitum*. Animals were kept on a standard 12:12 light/dark cycle. All procedures and techniques using animals were performed by qualified researchers. All efforts were made to minimize animal suffering.

Ischemia/Reperfusion Injury

We used an *in vivo* model for occlusion of left anterior descending (LAD) coronary artery to induce I/R injury as described[174]. Mice were anesthetized with sodium pentobarbital (90 mg/kg, intraperitoneal injection). Respiratory rate was maintained at 100±5/min. using a mini-ventilator (Harvard Apparatus). The heart was accessed by lateral thoracotomy between the 2nd and 3rd ribs. LAD artery was tighten with a 8-0 nylon suture at the position 2-4 mm from the tip of the left atrial appendage, and was occluded for 45 min., followed by reperfusion overnight. Successful myocardial ischemia and reperfusion were monitored by widening of the QRS complex, T wave inversion, and ST segment and

reversal of those changes[174]. Animal temperature was monitored with rectal probe thermometer and was maintained at 33.5-36.5^{o}C by a heating pad throughout the procedure. We excluded mice from the experiment if we observed no change in ST interval, or inconsistent change during ischemia phase, or no reversal of the ST-elevation throughout reperfusion phase.

Infarct Size Assessment

Mice were sacrificed 24 hours after *in vivo* I/R injury by sodium pentobarbital overdose as described previously[174]. The heart was perfused with 1% triphenyltetrazolium chloride (TTC) in PBS via the aorta. Then the areas of the heart not at risk was stained by perfusing with a 5% phthalo blue dye in PBS (Heucotech, # 515303) while the suture around the LAD was still secured. TTC is a redox indicator that turns from colorless to red by living cells, whereas dead cells remain white. Then the hearts were partially frozen at -20^{o}C and sliced into 4-5 1mm pieces, weighted and imaged with a Nikon camera. The viable, dead, and area not at risk regions were quantified with NIH Image J. The percent area at risk was calculated as described previously [175].

Cell Culture and Extracellular Vesicles Isolation

MSC were isolated from bone marrow and bone chips of femur and tibia of female B6.129 mice (8-10 weeks). The isolation and expansion of MSC were performed as previously described[17]. Briefly, muscle and connective tissue were cleansed from the bone. After the tip of the bones were clipped, the marrow was flushed from the bone with a 21-gauge needle into isolation medium consisting of RPMI-1640 (Fisher, # 11875093) with 10% Fetal Bovine Serum (FBS) (Gibco, #10082147), 10% horse serum (HS) (Gibco, #

16050122), 100U/ml penicillin, 100 µg/ml streptomycin (ThermoFisher, #15140122) and 12 µM L-glutamine (ThermoFisher, #25030149). After all bones had been flushed, suspension was filtered through a 70 µm cell strainer, and plated into T-75 flask. After 24 hour, cells were rinsed with PBS to remove non-adherent cells and new isolation medium was added. This process was repeated for two weeks until cells reached 80% confluent. Cells were lifted with 0.25% Trypsin-EDTA (ThermoFisher, #25200056) and plated into a new T-75 flask (passage 1). Cells that did not lift were discarded. After isolation 2-4 weeks, MSC were expanded with Iscove modified Dulbecco medium (IMDM) (ThermoFisher, #31980030) containing 10% exosome-free FBS, 10% exosome-free HS, 100 U/ml penicillin, 100 µg/ml streptomycin and 12 µM L-glutamine. At passage 5^{th}, expression of surface marker of MSCs such as D44, CD29 and Sca1 was confirmed with flow cytometry (**Table 2 and Fig. 1**). H9c2 cells (ATCC) were maintained in Dulbecco's Modified Eagle Medium (DMEM) (ThermoFisher, # 12430054) supplemented with 10% FBS.

Table 1. Antibodies Used in Flow Cytometry Experiment

Cell types	Antibody-fluorophore	Amount/10^6 cells
MSC	CD29 - Phycoerythrin	1µl
	CD44 - Allophycocyanin	1µl
	Sca-1 - Pacific Blue™	5µl
Hematopoietic stem cell	CD45 - Phycoerythrin-Cy7	1µl
Leucocyte	CD11b - Brilliant Violet™	5µl

EVs were then isolated by ultracentrifugation at 100,000xg for 70 min. EV pellet was resuspended in 500µl PBS and subjected to clean up step at 100,000xg for 70 min. one additional time. 200 µl PBS was used to re-suspend the final EV pellets. EV samples were stored at -80oC for subsequent analysis.

CD29

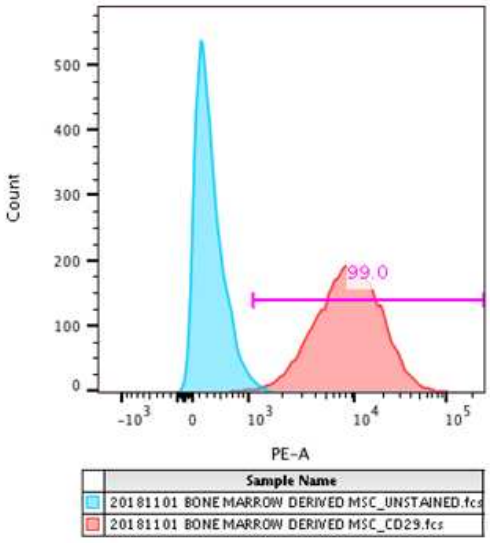

CD45

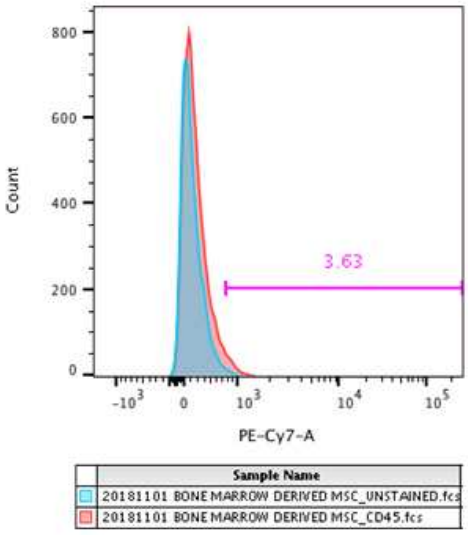

CD44

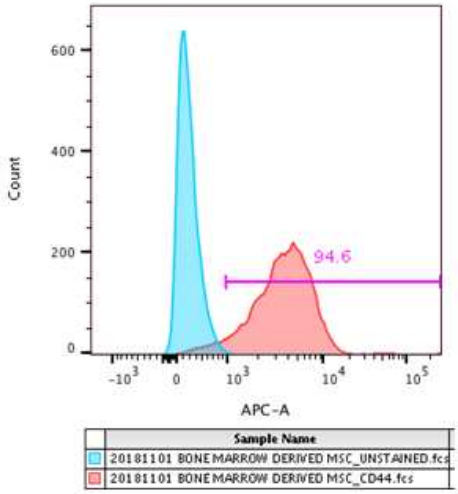

CD11b

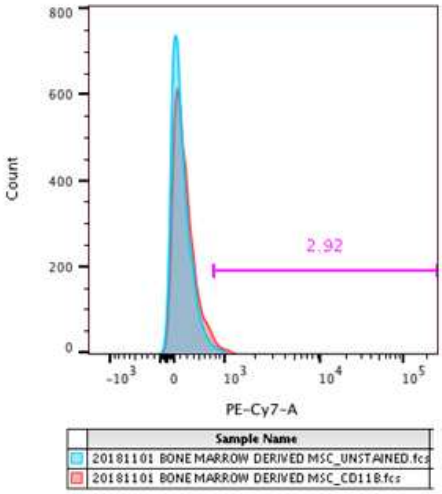

Sca-1

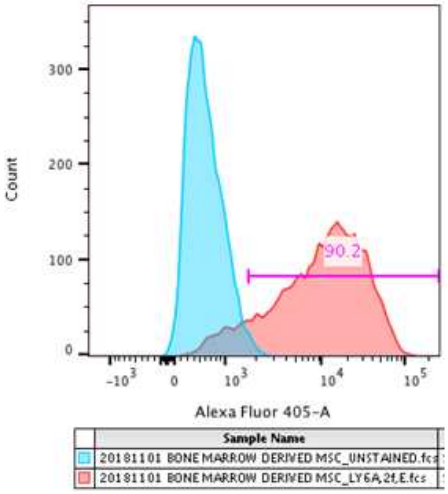

Figure 1. Surface Markers of MSCs. Wild-type MSC of passage 5 were detached with Accutase (Stemcell, # AT104) and stained with fluorescently conjugated primary antibodies for CD29, CD44, Sca-1, CD45 and CD11b (red line). Negative controls were unlabeled cells (cyan line). A shift to the right indicates the present of the antigen in the cells.

Small RNA Sequencing of miRNAs

Small RNA sequencing was carried on: miRNA from MSCs (N=4), MSC EV (N=3), hnRNPA2B1 KO EV (N=3), Cas9 EV (N=3). Illumina library prep and sequencing were completed by the Loyola Genomic Facility for MSC and EV and by Northwestern University Genomic Facility for hnRNPA2B1 KO EV and Cas9 EV. Analysis on differential expression of MSC and EVs were performed by Dr. Yutao Liu at Augusta University, Georgia. The RNA concentrations were measured using the Qubit 2.0 Fluorometer (Invitrogen) while quality was evaluated using the RNA6000 Nano chip on the Agilent 2100 Bioanalyzer (Agilent Technologies).

Small RNA Libraries Generation and Sequencing.

NEBNext Multiplex Small RNA Library Prep Kit for Illumina was used to prepare template libraries cDNA from total RNA of MSCs (N=4) and EV (N=3, one failed quality control) and TruSeq Small RNA library prep kit (Illumina) for total RNA of EV from hnRNPA2B1 KO and Cas9 as described previously[17]. The libraries (N=3-4) were then analyzed using Illumina Hiseq 2000 instruments to yield 50 base pair single end reads . The sequencing reads, after removing adapters and low quality reads, were aligned to the mouse genome (GRCm38) using BowTie (v.0.12.8) and analyzed by DESeq. 1.5-fold cutoff and Benjamini-Hochburg adjusted $P \leq 0.05$ were used to analyze miRNAs that expressed differently between conditions.

DAVID and miRNA Targets Prediction

For the Gene Ontology (GO) enrichment analysis, the gene functional classification tool DAVID (Database for Annotation, Visualization and Integrated Discovery) was utilized to characterize by GO annotation into two categories: the cellular compartment, and functional clustering of the mass-spectrometry dataset to annotate biological meaning for the data[176]. A corrected $P \leq 0.05$ was considered significant.

The targets of miRNA of interest were identified using the DIANA-microT-CDS and MiRanda targeting algorithm on Targetscan.org(mmu_71)[177] and microRNA.org[178]. We used PathwayStudio to collect biological pathways that were relevant to cell death (annotated with the terms 'apoptosis' or 'cell survival' or 'death'). Weighted context +++ score from Targetscan was used to rank miRNA and target protein. Only targets with the highest negative score were considered for further analysis.

RNA-motif Identification

To identify over-represented sequence motif on EV-enriched miRNA, we employed a web-based tool Multiple Em for Motif Elicitation (MEME) at https://meme-suite.org/meme/[179]. Eight EV-enriched miRNAs from small RNA-sequencing that have *P*-adjusted ≤ 0.05 and more than 1000 reads in EV, were used as input sequence. The same criteria were applied for six cell-retained miRNAs. The zero-or-one occurrences per sequence (ZOOPS) model was selected to find motifs width of 4-8 bases.

Proteomic Analyses

In-solution digestion was used for protein identification with samples isolated from MSC and EVs as described previously[180]. In brief, samples were diluted to 100 mM ammonium

bicarbonate solution, pH8. DTT was added to the samples to at final concentration of 10mM and incubated at 55^{o}C for 30 min. Samples were then alkylated with 200mM iodoacetamide. Samples were digested by incubation at 37^{o}C overnight with trypsin MS grade (ThermoFisher, #PI90057) 1:25 trypsin to protein (w/w). Digestion was stopped by adding trifluoroacetic acid to a final concentration of 1%. Samples were desalted using a C18 Omix Zip Tip for Orbitrap analysis. LC-MS measurements were performed at Proteomic core facility of Northwestern University.

Transmission Electron Microscope

Negative staining was used to image and assess the morphology of EVs with transmission electron microscope[181]. In brief, 50µl of EV were fixed with 1ml of 2% paraformaldehyde for 5 min. 10 µl of the EV suspension was loaded onto a carbon film coated 200 mesh copper EM grid , incubated for 1 min, and stained with 1% uranyl acetate for 1 min. The excess staining solution was removed with filter paper. The images of EV were captured under a transmission electron microscope (Philips CM120 120kV) after the grids were dried.

EV Nanosight Experiment

EVs isolated from conditioned medium of wild type MSCs, hnRNPA2B1 KO MSC, Cas9 MSC control, were diluted in PBS (1:1000 ratios), drawn into a 1 ml syringe,
and loaded into sample chamber of Nanosight NS3000 instrument (Malvern). The particles were visualized with 20x magnification. The Nanoparticle Tracking Analysis software was used to quantify the size distribution and concentration of particles in the samples. Each

sample was measured three times and the counts were averaged. PBS was used as a baseline for measurement.

HnRNPA2B1 Protection Assay

To confirm the presence of hnRNPA2B1 inside of EV, EV were isolated from 250 ml conditioned medium, as described above. The pellet after ultracentrifugation steps was resuspended in 10 µL HBSS or 1% Triton X-100, vortexed, and incubated at room temperature for 5 min as described previously[182]. Half of the HBSS-resuspended samples and Triton X-treated sample were incubated with 5 µl proteinase K solution (20 mg/ml) (Promega, #S46897). Additionally, 10 µg of WT-MSC cell lysate was treated with 5 µl proteinase K solution (20 mg/ml) or HBSS. All samples were incubated for 30 min. at 65°C with proteinase K, followed by 15 min. at 95°C to deactivate the proteinase K. Subsequently, 15 µl RIPA buffer supplemented with 1:25 100X proteinase inhibitor (ThermoFisher, #PI88669) was added to the samples. Samples were then prepared for the Western blot procedure, resolved on a 10% polyacrylamide gel, transferred and immunoblotted against hnRNPA2B1 and HSP-70.

CRISPR-Cas9 Genome Editing of hnRNPA2B1

Three different guide RNAs (gRNAs) targeting the second exon of hnRNPA2B1 open reading frame, were designed using Benchling tool (https://www.benchling.com/crispr/). The design was to remove the second exon and introduce a premature stop codon to truncate the mRNA and produce a loss-of-function allele. The gRNAs were phosphorylated, annealed and cloned into lenti-CRISPR v2 backbone vector as described[182]. To produce viral particles, gRNA/Cas9 plasmid, viral packaging plasmid ΔNRF,

and viral envelope plasmid VsV-g (5µg each) were co-transfected into packaging 293T cells with Lipofectamine™ 3000 (Thermo Scientific, #L3000015) according to manufacturer's instructions. In brief, 5µg of each construct (15 µg total DNA) was diluted in 500µl of OptiMEM, while 40µl of P3000 reagent was added into diluted DNA and mixed gently. In another tube, 15µl of Lipofectamine3000 was diluted in 500µl of OptiMEM. Then the diluted DNA was mixed with diluted Lipofectamine in a volume of 1000 µl, and incubated for 5 min. at room temperature. Transfection complex was added into designated plates with 10ml of regular medium and placed back in incubator for 6 hours. The transfection was stopped by removing the medium containing the transfection complex and adding 10ml of regular medium (see **Cell Culture and Extracellular Vesicles Isolation**).

Table 2. List of gRNAs used to target the second exon of hnRNPA2B1 gene

Hnrnpa2b1_Assembly_1_FWD	CAC CGT TCC GAA AGC TCT TTA TTG G
Hnrnpa2b1_Assembly_1_REV	AAA CCC AAT AAA GAG CTT TCG GAA C
Hnrnpa2b1_Assembly_2_FWD	CAC CGA GAA ACT ACT ATG AGC AAT
Hnrnpa2b1_Assembly_2_REV	AAA CAT TGC TCA TAG TAG TTT CTC
Hnrnpa2b1_Assembly_3_FWD	CAC CGA GAA ACT ACT ATG AGC AAT G
Hnrnpa2b1_Assembly_3_REV	AAA CCA TTG CTC ATA GTA GTT TCT C

Plates were left in a 37°C incubator overnight. After 48 hours, supernatant containing viral particles was collected by centrifugation at 1,000xg for 20 min., and filtered through 0.45 µm low protein binding filter. The stable MSC lines expressing gRNAs against hnRNPA2B1 were generated by transduction of WT-

MSC with 500 µl lentiviral aliquot per well (24 well plates; 10,000 cells/well). Selection with puromycin (4 µg/ml) in complete medium was started 48 hours post transduction and ended after all untransduced MSC (control plate) died. The polyclonal populations were expanded and tested for the deletion of hnRNPA2B1 by immunoblot for hnRNPA2B1 (SCBT, # sc-374053).

Nuclear extracts for EMSA and RIP

Nuclear extracts of WT-MSC or hnRNPA2B1 KO-MSC for gel-shift assay were prepared using NE-PER™ Nuclear and Cytoplasmic Extraction Reagent (ThermoFisher, #78835). 5 x 10^6 cells were harvested by trypsinization, and then centrifuged at 500xg for 5 min., washed with PBS before being resuspended in 500 µl of cold Cytoplasmic Extraction Reagent (CER) I supplemented with 100X protease inhibitor. The suspension was incubated on ice for 10 min. before 27.5 µl of cold CER II was added and incubated on ice for 1 min. The cytoplasmic fraction (supernatant) was collected by centrifugation at 16,000xg for 5 min. The pellet (nuclear fraction) was suspended in 100 µl ice-cold NER supplemented with 100X protease inhibitor (ThermoFisher, #PI88669). The suspension was incubated on ice, and vortexed for 15 sec. on highest setting every 10 min. for a total of 40 min. The nuclear extract (supernatant) was isolated by centrifugation at 16,000xg for 10 min. The protein concentration was measured with BCA Protein Assay (ThermoFisher, # 23225).

To prepare nuclear extract for the immunoprecipitation and biotinylated RNA pull-down assays, WT-MSCs were cultured to reach 80-90% confluent for subcellular fractionation. Cells were rinsed twice with PBS, trypsinized and collected by centrifugation

at 1,000 xg for 5 minutes at 4°C. The cell pellet was rinsed twice with cold PBS, resuspended in 1 ml of ice-cold cell lysis buffer supplemented with 1 mM DTT, 4U/ml RNAse inhibitor (ThermoFisher, #AM2682), and 1X protease inhibitor cocktail (ThermoFisher, #23225), incubated on ice for 10 minutes. The nuclei were collected by centrifugation at 1,000xg for 5 minutes at 4°C. The nuclei pellet was resuspended with 600 µl of ice-cold TSE buffer (0.02 M Tris-HCI, pH 7.8; 0.1 M NaCl; 1 mM EDTA) supplemented with 1mM DTT, 4U/ml RNAse inhibitor, and 1X protease inhibitor cocktail. The nuclei lysate was sonicated five times on ice (9 seconds at 0.5 outputs), passed through a 27-gauge syringe five times, then incubated on ice for 20 minutes with occasional vortexing every 10 minutes, followed by a 10 minutes spin at 16,000xg at 4°C. The supernatant was collected for further experiments. Protein concentration was measured by standard Bradford assay (ThermoFisher, #23225). 25µl (10%) of the nuclei lysate was put in a new tube labeled as "Input".

RNA Immunoprecipitation (RIP) Assay

750µg of nuclear lysate was premixed with 10µg anti-hnRNPA2B1-B7 (SCBT, # sc-374053) or IgG antibody (Vector, #58421) in RIP buffer and incubated overnight at 4°C. 10µl (10%) of the lysate was used as an "input" sample. Then 50µl of washed Dynabead (ThermoFisher, #14112-89) was mixed with antibody-antigen complex, and incubated for 2 hours at 4°C. Beads were captured using a magnetic stand (ThermoFisher, #65002, and washed three times with 500µl cold PBS containing 0.1% Tween-20 detergent. After the last wash, the beads was incubated at 55°C for 30min with 100µl of PBS supplemented with 0.5% NP40, 40U/µl RNase inhibitor and 50µg proteinase K. The elutant

was purified using Qiazol reagent (Qiagen, #79306) and concentration of RNA was quantified using Nanodrop spectrophotometer. Mature miRNA expression levels were quantified using miScript SYBR Green PCR Kit (Qiagen, #218073) on AriaMX instrument.

EMSA and Super-shift Assay

The *in vitro* interaction between miRNA and the proteins in nuclear lysate were evaluated by electrophoretic gel shift assay (EMSA). The assay was carried out with LightShift™ Chemiluminescent RNA EMSA Kit (ThermoFisher, # 20158) according to the manufacturer's instructions. In brief, 100 µg of nuclear lysate was mixed with 1 pmol of 3'-biotinylated miRs (mmu-miR-486-5p: UCCUGUACUGAGCUGCCCCGAG-[Btn], mmu-miR-122a: UGGAGUGUGACAAUGGUGUUUG-[Btn], mmu-miR-451a: AAACCGUUACCAUUACUGAGUU-[Btn], mmu-miR-1291a: UGGCCCUGACUGAAGACCAGCAGU-[Btn]) (Sigma-Aldrich), in a volume of 20µl 10X REMSA binding buffer supplemented with 2µg tRNA and 5% glycerol, and incubated for 30 min. at room temperature. The RNA-protein complex was loaded on a 5% native polyacrylamide gel, and electrophoresed until the bromophenol blue dye had migrated to halfway down through the gel. The RNA-protein complex was then transferred to a positively charged 0.45 µm nylon membrane (ThermoFisher, # 77016) in 0.5X TBE buffer (0.13 M Tris-HCl (pH 7.6), 45 mM boric acid, 2.5 mM EDTA) at 300 mA for 45 min. After biotinylated RNA-protein complex was cross-linked using a UV-crosslinker (Boekel Scientific) for 2 min., the membrane was blocked, washed, equilibrated, and stained with luminol/peroxide- as described in the manufacturer's protocol (ThermoFisher, # 20158). Chemiluminescent signal was visualized using a Chemidoc Imager (Biorad). The super-shift assay was

conducted as described above, with the addition of 1 µg antibody against hnRNPA2B1 (SCBT, # sc-374053).

Biotinylated-RNA Pull-down Assay

1 µg of biotinylated RNA (Sigma-Aldrich, TX) was mixed with 500µl of 500 µg of nuclear lysate, 100X protease inhibitor (ThermoFisher, # 23225), 40U/µL RNase inhibitor (ThermoFisher, #AM2682), and 2X TENT buffer (20mM Tris-HCl, 2mM EDTA, 500mM NaCl, 1% Triton X-100), and incubated for 30 min. at room temperature. The RNA-protein complexes were fixed using a UV-crosslinker (Boekel Scientific) for 10 min, and then mixed with 50 µl of streptavidin magnetic beads (NEB, #S1420S). The mixture was incubated for another 30 min. at room temperature. The beads were captured by a magnetic stand (ThermoFisher, #65002) and washed three times with 1X cold TENT buffer. After the last wash, the RNA-protein complex was eluted with 40 µl of 1X Laemmli buffer (Bio-Rad, #161-0474) and incubated at 95^{o}C for 5 min. The elutant were loaded on a 10% SDS-PAGE gel, separated at 120 mV for 60min., and transferred at 250 mA for 2 hours at 4^{o}C, followed by Western blot to detect target proteins. The competition assay was carried out as described above with the addition of 20X excess amount of unlabeled-miRNAs into the reaction before adding labeled miRNAs.

Simulated Ischemia-Reperfusion

10^4 H9c2 cells per well were seeded in a 96-well plate and the sim I/R injury model was established as described before[17]. Cells were incubated in ischemia mimetic solution (in mM: 125 NaCl, 8 KCl, 1.2 KH_2PO_4, 1.25 $MgSO_4$,1.2 $CaCl_2$, 6.25 $NaHCO_3$, 5 sodium lactate, 20 HEPES, pH 6.6 at 37ºC) in a hypoxic chamber (Biospherix) for 12 hours. The oxygen

level was kept below 0.5% by replacement with nitrogen, while CO_2 was kept at 5%. After 12 hours of ischemia, cells were returned to a normoxic incubator for 2 hours and the ischemia mimetic solution was replaced with complete growth medium. Cell viability was assessed by incubating cells for 30 min. with Hoechst 33342 solution (0.2 µg/ml) (ThermoFisher, #H3570) and propidium iodide (PPI) (2µ/ml) (ThermoFisher, #p3566). The images were captured and analyzed with Cytation™ 5 Cell Imaging Multi-Mode Reader (BioTek) using DAPI filter for $Hoechst^+$ to detect all cell, and the Texas Red filter for PPI^+ to detect necrotic cells. The percentage of cell survival was calculated by dividing the number of viable cells after sim I/R challenge by the number of viable cells before sim I/R.

RNA Isolation

For RNA extracted from cell and extracellular vesicles, Qiazol lysis reagent (Qiagen, #79306) was added at 1:3 parts sample to Qiazol, incubated for 5 min. at room temperature. Then 0.2ml of chloroform was added for each 0.25ml Qiazol in the sample. The samples were vortexed for 15 sec., incubated for 3 min. at room temperature, and spun at 12,000xg for 15 min. at 4°C. The upper aqueous phase containing RNA was transfer to a new tube for RNA precipitation with 0.5ml of 100% cold isopropanol per 0.75ml Qiazol lysis reagent. Samples were incubated at room temperature for 10 min., and then centrifuged at 12,000xg for 10 min. at 4°C.The supernatants were discarded completely while RNA pellets were washed with 1ml of 75% ethanol per 0.75ml Qiazol used for initial homogenization. Samples were vortexed 10-15 sec., centrifuged at 7,500xg for 5 min. at 4°C, and air dried. The RNA precipitates were resuspended in 15-20µl of RNAse free water and mixed until the precipitate was no longer visible. to deactivate glycogen. Concentration and

quality of RNA samples were evaluated with the Nanodrop spectrophotometer. Samples with 260/280 ratio above 1.8 were used for downstream analyses. RNA samples used for RNA-sequencing experiments were assessed with the Aligent 2100 Bioanalyzer system.

Reverse Transcription (RT)

For RT of mRNA, 200ng of isolated total RNA was mixed with 10µl 2X RT buffer, 2µl 20X Applied Biosystems RT enzyme mix (ThermoFisher, # 4368813), and RNAse free water in a volume of 20µl. The thermal profile was set as: 1 hour at 37^{o}C, 5 min. at 95^{o}C, and held at 4^{o}C. The cDNA product was diluted 10 fold with RNAse free water for quantitative PCR.

For RT of miRNA, 100ng of total RNA was mixed with 2µl 10X nucleic mix, 4µl 5X HiFlex buffer, 2µl miScript reverse transcriptase enzyme (Qiagen, #218160) and RNAse-free water in a volume of 20µl and placed in a thermal cycler under the following condition: 1 hour at 37^{o}C, 5 min. at 95^{o}C, and held at 4^{o}C. The cDNA was diluted in 200µl RNAse free water.

Quantitative Real Time PCR (qPCR) Analysis

For quantitative analysis of mRNA expression, qPCR was conducted with Applied Biosystems® SYBR® Green (ThermoFisher, #4309155). A 20µl of reaction mix contained 10µl 2X SYBR Green master mix, 0.25µl forward and reverse primers, 4.5µl RNAse free water and 5µl template cDNA. ROX dye in 2X SYBR Green master mix was used as passive reference. PCR was run on an AriaMX instrument with the thermal profile: 15 min. at 95^{o}C for hot start, denaturing for 15 sec. at 95^{o}C, annealing for 30 sec. between 55^{o}C-60^{o}C depend on primers, and extending for 30 sec. at 70^{o}C, followed by a melt cure. All reactions

were performed in triplicate and normalized to 18S using the $2^{(-\Delta\Delta CT)}$ method[183]. Primers for the mRNA of interest were designed using NIH Primer Blast software and ordered from IDT (Coralville, IA). For real time quantitative PCR of cDNA synthesized from miRNAs, a reaction of 20µl was consisted of: 2µl 10X miScript primer assay specific to the miRNA of interest (Qiagen, miR-486-5p #MS00029246, miR-122a #MS00001526, miR-451a # MS00002408, miR-22a-3p # MSY0000531, miR-1291a # MS00077048, miR-5121a # MS00043071), 2µl 10X miScript universal primer, 10µl 2X SYBR Green (Qiagen, # 218073), cDNA product and RNAse-free water. qPCR was carried out for 40 cycles with thermal cycling: 15 min. at 95°C, denaturing for 15 sec. at 94°C, annealing for 30 sec. at 55°C, and extending for 30 sec. at 72°C with data collection.

Table 3. List of Primers Used in qPCR for mRNA Expression Levels

PDCD4 total	*Pten*
(F) 5'-TACCGCATTTCCACCACGAG-3'	(F) 5'-GGCCAACCGATACTTCTCTCC-3'
(R) 5'-GCACAGAGTATGAGTGTGGGAC-3'	(R) 5'-CTGGATCAGAGTCAGTGGTGT-3'
PDCD4 sliced	*18S*
(F) 5'-GAAGGAGATGGAGGTCGTCTTAAACC-3'	(F) 5'-AGTCCCTGCCCTTTGTACACA-3'
R) 5'-AGGTGGTTACTCTTCGGTCCCT-3'	(R) 5'-CCGAGGGCCTCACTAAACC-3'

All reactions were performed in triplicate and U6 RNA (Qiagen, # MS00033740) was used as internal control. The relative expression of RNA to internal control was calculated using the $2^{(-\Delta\Delta CT)}$ method.

For absolute quantification of miRNA, a standard curve of cDNA synthesized with miScript mimetic miR-486a-5p (Qiagen, #MSY0003130) was used for determination of

copy number of the miRNA under study. In brief, 5µl of 20µM miScript miRNA mimetic was used to synthesize cDNA with miScript II RT kit (Qiagen, #218160). The cDNA was diluted in RNAse-free water to yield 10^{10}copies cDNA/µl. Serial dilution was prepared from the diluted cDNA and RNAse-free water. 2µl from each dilution (with template copy numbers in the PCR ranging from $10^{9}$to 10^{4}) was used to set up separate real-time PCR reactions. Results from the PCR were used to plot a standard curve of CT value against log copy number of miRNA of interest.

Transfection

H9c2 cells were seeded in 6-well plate to 70-80% confluent and transfected with either miR-486a-5p mimetic (Qiagen, #MSY0003130) or scrambled non-targeting miRNA (scramble) served as negative control (Qiagen, #1027280) using Lipofectamine™ 2000 (ThermoFisher, #11668019), according to the manufacturer's protocol (ThermoFisher, #11668019). In brief, Lipofectamine™ 2000 or mimetic of miR-486-5p or scramble was gently mixed with 250µl of Opti-MEM (Invitrogen, # 11058021) and incubated for 5 min. at room temperature. The diluted miRNA was combined with the diluted Lipofectamine in a volume of 500µl, mixed and incubated for another 20 min. at room temperature. Then RNA-Lipofectamine complex was added to each well and mixed gently. The complete growth medium was replaced 6 hours after transfection. Cells were collected for mRNA and protein analysis 24-48 hours post-transfection.

Dual-luciferase Reporter Assay for 3′-Untranslated Region (UTR) miR-486-5p Targets

The whole 3′- UTR from genes of interest (PDCD4 and Pten) were amplified from murine genomic DNA and inserted into pGL4 expressing luc2 sequence of firefly luciferase luc2 vector (Promega, #E6651). Constitutively active cytomegalovirus (CMV) promoter was used to drive the pGL4 plasmid. *Renilla* luciferase (Promega, # E2231) was used as internal control to normalize firefly luciferase activity. Co-transfection of firefly:*Renilla* co-reporter at 50:1 had minimal effect on the firefly luciferase signal (**Fig. 2**).

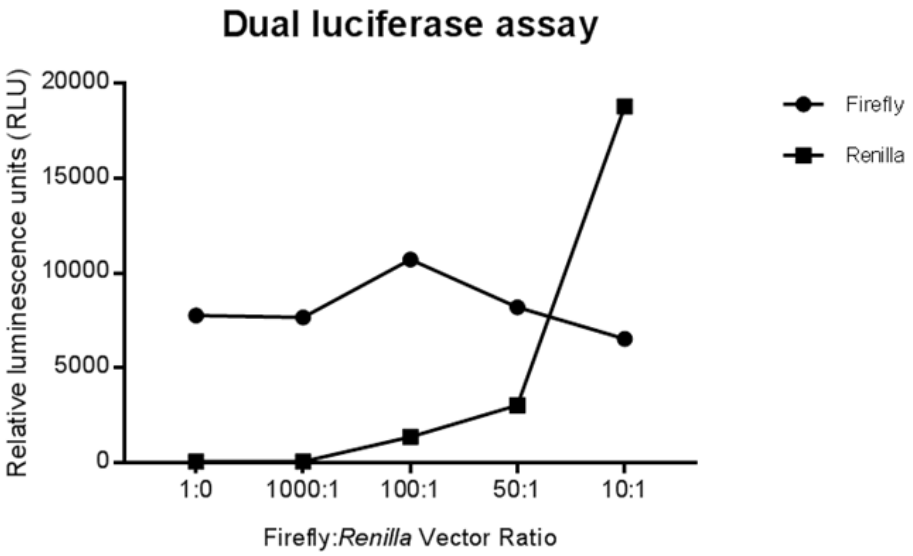

Figure 2. Raw relative luminescence units for firefly and co-reporter (Renilla) luciferase with Dual-luciferase Reporter Assay. Firefly luciferase vector was maintained at 500 ng, while co-reporter Renilla varied from 500 pg-50 ng. N = 6 for each condition.

H9c2 cells were grown in 96-well plates and transfected with the luciferase constructs (firefly luciferase:*Renilla* luciferase construct, 50:1) and a dose curve of miR-486-5p mimics (5'- UCCUGUACUGAGCUGCCCCGAG-3') or siRNA against *luc2* gene as positive control (5′-GGACGAGGACGAGCACUUCUU-3′, 3′-UUCCUGCUCCUGCUCGUGAAG-5′). using Lipofectamine™ 2000. The luciferase activity in the samples was quantified with Dual-

luciferase reporter assay system (Promega, # E1910). After 24 hours of transfection, H9c2 cells were washed with PBS, and lysed by adding 20 µl of 1X passive lysis buffer to each well and gently shaken at room temperature for 15 min. Firefly fluorescence (F) was detected by adding 100 µl of Luciferase assay reagent II (Promega, # E1910) to cell lysate; while Renilla fluorescence (R) was detected by subsequently adding 100 µl of Stop&Glo reagent (Promega, # E1910). Fluorescence signals were measured with Cytation 5 Multiple-reader (BioTek). Relative luciferase activity = F/R.

Western Blot

10^5-10^6 cells were washed twice with 500µl cold PBS and lysed by 100µl cold RIPA lysis buffer (Sigma, # R0278) supplemented with 10% protease inhibitor, 10% $NaVO_4$ and 10% phosphatase inhibitors PMSF (Sigma, # PPC1010). Lysates were kept on ice for 30 min., and then centrifuged at 10,000xg for 15 min to collect the supernatant for further analysis. Total protein was measured using BCA Protein Assay Kit (ThermoFisher, #23225). Cell lysates were diluted 1:5 and standard BSA (ThermoFisher, # 23209) was diluted 125-2000µg/ml in RIPA in total volumes of 25µl. Samples were mixed with 200µl BCA working reagent, incubated at 37^{o}C for 30 min. Absorbance was read at 562 nm by Cytation5 reader (BioTek). All measurements were triplicated.

For Western blot, 10- 20µg protein was loaded in each well of 10% or 12% sodium dodecyl sulfate polyacrylamide gel (SDS-PAGE). Electrophoresis was carried out at 75V for 15 min., then 120V for 60 min. Following gel electrophoresis, proteins were blotted onto 0.2 µm pore nitrocellulose membrane at 250 mA for 2 hour at 4^{o}C. After blocking with 5% non-fat milk in 1X TBS solution at room temperature for 1 hour, the membrane was probed

with antibodies specific for the protein of interest (**Table 5**) overnight with constant agitation at 4°C. Membranes were then incubated with anti-mouse IgG peroxidase secondary antibody or rabbit IgG for 2 hours at room temperature. Blots were detected using SuperSignal West Dura Extended Duration Substrate (ThermoFisher, #34075). Chemiluminescent signal was visualized with the Chemidoc (Biorad). Density of Western blot bands was quantified with ImageJ and normalized to β-actin or GAPDH. For some blots, membranes were stripped and re-probed to study multiple proteins of interest.

Measurement of LDH Release

The LDH release was measured with the LDH Cytotoxicity Detection Kit (Clontech, # MK401). Cell-free supernatant from different testing treatments were diluted 10 folds in a volume of 100 µl, then transferred to a flat-bottom clear 96-well plate. Samples were then mixed with 100 µl of Reaction Mixture (Clontech, # MK401). After 30 min. of incubation at 37°C while protected from light, 50µl of 1N HCl was added to stop the reaction. Then absorbance was measured at 490 nm using Cytation 5 reader (BioTek). A standard curve of LDH (0-90U/ml) LDH (Sigma-Aldrich, #L3888-500UN) and dilution factor were used to calculate the unit of LDH activity.

TUNEL Staining

Apoptosis post-sim I/R was detected by terminal deoxynucleotidyl transferase-mediated dUTP nick-end labeling (TUNEL) using DeadEnd™ Fluorometric TUNEL kit (Promega, # G3250). H9c2 cells were cultured in 8-well chamber slide (Nunc™ Lab-Tek™ II, ThermoFisher). After sim I/R, cells were fixed with 4% paraformaldehyde for 25 min. at 4°C. After two rinses with PBS, slides were immersed in permeation solution (0.2% Triton

X-100 in PBS) for 5 min. Samples were washed twice with PBS, and then were incubated with TdT reaction mix for 60 min. at 37°C. The cells were counterstained for nuclei using 4', 6-diamidino-2-phenylindole (DAPI) (Vector Laboratories, # H-1200-10). Images were acquired and analyzed using Cytation™ 5 Cell Imaging Multi-Mode Reader (BioTek). The percent of apoptotic cells were calculated the number of TUNEL-positive nuclei to the total number of DAPI staining nuclei in the same field.

Table 4. List of antibodies used in immunoblotting experiments

Target	**Company**	**Catalogue number**	**Dilution**
PDCD4	Cell Signaling	9535	1:1000
Pten	Cell Signaling	9188	1:1000
total Akt	Cell Signaling	4691	1:1000
phospho Akt (Ser473)	Cell Signaling	4060	1:1000
phospho Akt (Thr308)	Cell Signaling	9275	1:1000
Caspase-3	Cell Signaling	9662	1:1000
cleaved Caspase-3 (Asp175)	Cell Signaling	9664	1:1000
Bax	Cell Signaling	2772	1:1000
Bcl-2	Cell Signaling	4223	1:1000
HSP-70	Santa Cruz	sc-24	1:1000
Alix (3A9)	Cell Signaling	2171	1:1000
TSG-101 (C2)	Santa Cruz	sc-7964	1:1000
hnRNPA2B1 (B7)	Santa Cruz	sc-374053	1:1000
hnRNPA2B1 (EF67)	Santa Cruz	sc-53531	1:1000

hnRNPA1 (4B10)	Santa Cruz	sc-32301	1:1000
hnRNPA1 (9H10)	Santa Cruz	sc-56700	1:1000
hnRNPQ (I8E4)	Santa Cruz	sc-56703	1:1000
GAPDH (D16H11)	Cell Signaling	5174	1:1000
β-actin	Cell Signaling	4970	1:1000
Anti-rabbit	Cell Signaling	7074	1:5000
Anti-mouse	Cell Signaling	7076	1:2000

Four non-overlapped images of similar total cell numbers were randomly selected from each coverslip for counting and averaging.

In vivo Administration of miR-486-5p Mimetic

Modified oligonucleotides (miRNA mimetic) have been used to increase microRNA expression *in vivo*[184; 185]. Mimetic of miR-486a-5p (MIMAT0003130, UCCUGUACUGAGCUGCCCCGAG) was synthesized by Dharmacon (cat. # JLA.061818.A) was modified to increase resistance against endonucleases as well as cellular uptake, specifically: 2'-O-methyl modified residues, phosphorothioate linkage, and 3'-cholesterol modifiers, as described in previous study[185]. B6.129 male and female mice between 10 to 12 weeks old was injected via pericardial sac of either miR-486-5p mimetic or scrambled non-target miRNA at a dose of 40 μg of oligonucleotides that was complexed in a volume of 25 μl of nanoparticle-based *in vivo* transfection reagent (Altogen Biosystems, #5030). Myocardial infarction *in vivo* was performed 24h after treatment and infarcts assessed as described above.

Statistical Analysis

Statistical analyses were conducted with GraphPad Prism 7.0 software. Values were expressed as mean plus or minus standard deviation (SD). Data was analyzed by using one-way Anova for three or more independent groups or Student's unpaired t-test for two groups. Statistical significance between groups was set at $P \leq 0.05$. Both *a priori* and *post-hoc* power analysis was used to ensure that sample size is sufficient to achieve statistical significance. Specific assessment for RNA Seq analyses are described in the appropriate sections.

CHAPTER III

RESULTS

The overall hypothesis for this dissertation is that RNA-binding proteins are involved in the selective transport of miRNAs containing specific RNA-sorting sequences into EVs to exert protective effects against I/R injury. In this section, we describe experiments to address the hypothesis that RNA-binding proteins mediate the sorting of specific miRNAs into EVs. To address this this hypothesis, we had to investigate the repertoire of miRNAs in both producer cells and in their EVs, determine if sets of miRNAs selectively concentrated in EVs share common sequence motifs, identify the RNA-binding proteins that interact with these specific miRNAs, and demonstrate functional involvement of these RNA-binding proteins in active EV sorting events. The results of these experiments are described and shown below.

Purified MSC-derived EVs Contain RNA

We first sought to isolate EV in conditioned medium from other contaminating particle populations by differential centrifugation according to the previous study[187] (**Fig. 3A**). Cellular debris and large vesicles were removed during low and medium speed centrifugation, whereas EV were concentrated by high-speed centrifugation. Nanosight nanoparticle tracking analysis (NTA) demonstrated that MSC-derived EVs were 30 to 200 nm diameter vesicles, with a mean diameter of 100 nm (**Fig. 3B)**, while immunoblotting indicated that EVs expressed the surface markers Alix and TSG101 (**Fig. 3D**).

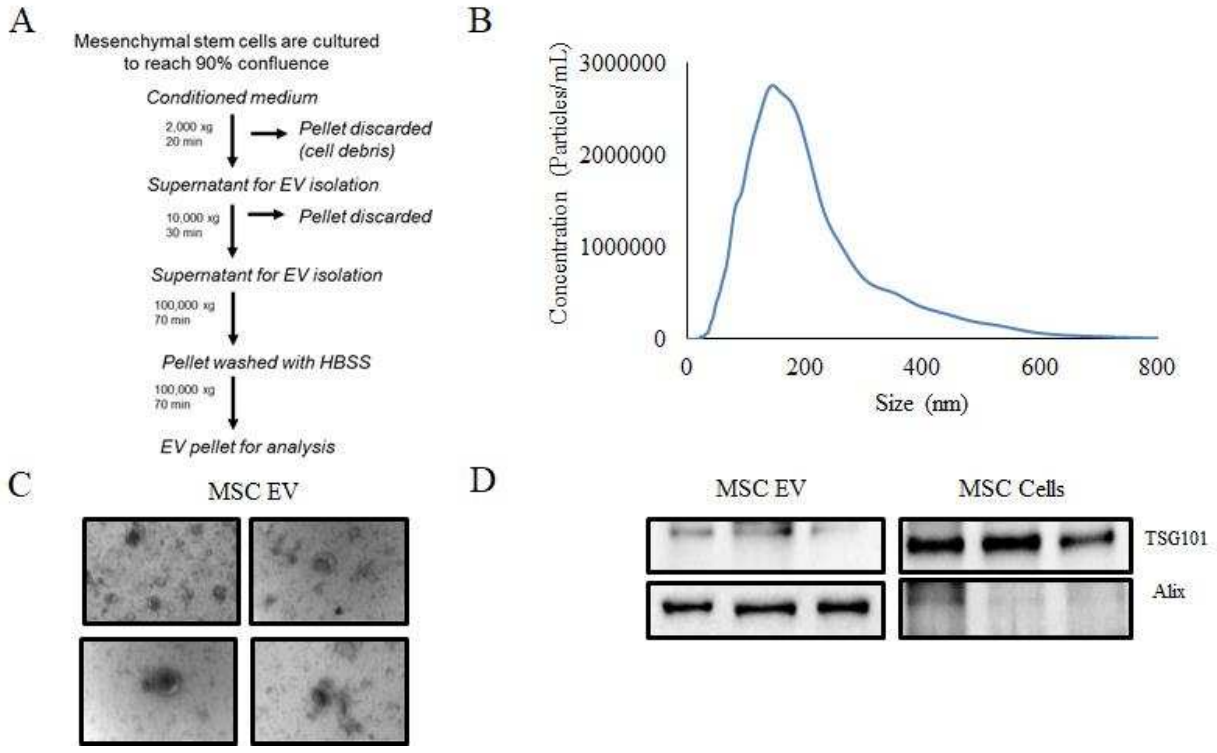

Figure 1. Purification and characterization of wild-type MSC-derived EV. (A) Schematic of the MSC-derived EV isolation process. (B) Size distribution and concentration of particles in EVs using nanoparticle analysis (size ~150 nm, concentration~5.8 x 10^{10} particles/mL). Plotted data is from one independent experiment (C) Representative electron microscopic image of EVs. (D) Immunoblotting of EV markers TSG101 (48 kDa), Alix (96 kDa).

MSC-derived EVs Contain Selectively Packaged miRNAs

Previous studies have indicated the presence of miRNAs in EV fractions[53]. To study miRNAs that are selectively loaded into EVs, we performed an Illumina-based small-RNA deep sequencing analysis of miRNA profiles in three and four independent biological replicates of MSC-derived EV and MSC cells respectively. The relative enrichment for each miRNA was calculated by normalizing to the total number of mapped-miRNA reads. We found miR-21-5p was the most abundant miRNA in both parent cells and their EV, which is

in agreement with our previous study[17]. Of these miRNAs in the EV fraction, 155 miRNAs were found to be upregulated, while 109 miRNAs were down-regulated (p-values adjusted ≤ *0.05*) in EV relative to cellular fractions. These results demonstrate that specific miRNAs are selectively sorted such that higher levels are in EVs relative to producer MSCs (*e.g.,* miR-486-5p, miR-122a and miR-451a). For example, miR-486-5p was found at levels ~5853-fold higher in EVs than in MSCs. The next highest differentially expressed EV-miRNA, miR-122a was ~3938-fold higher than in MSC parent cells. In contrast, specific repertoires of miRNAs were more highly represented in MSCs than in EVs (*e.g*. miR-1291, miR-30b-3p, and miR-5121) (**Fig. 4**). Importantly, the difference between the miRNA profiles of MSCs and EVs suggests the existence of active processes directing the sorting of a specific subsets of miRNAs into EVs.

A Subset of EV-enriched miRNAs Harbor a Specific Predicted Sequence Motif

As the sorting of miRNAs into EVs is known to sequence-dependent[94; 95], we performed a bioinformatics comparative analysis using Multiple Em for Motif Elicitation (MEME) algorithm with Zero-or-one occurrences per sequence (ZOOPS) sequence mixture model to identify over-represented sequence motifs among miRNAs that are highly represented in EVs rather than in MSCs as well as miRNAs that are highly retained in the producer cells[188]. On the one hand, sequence comparison of top EV-enriched miRNAs including miR-486-5p, miR-122a, miR-451a, and miR-150a (RPM in EV library >1000, and p-values adjusted ≤ 0.05) revealed that they shared a common short sequence motif ugGAGUu (**Fig. 5A**). To date, the specific ugGAGUu sequence we found in subset of miRNAs in MSC-derived EV has not been implicated in binding with RBPs. On the other hand, we did

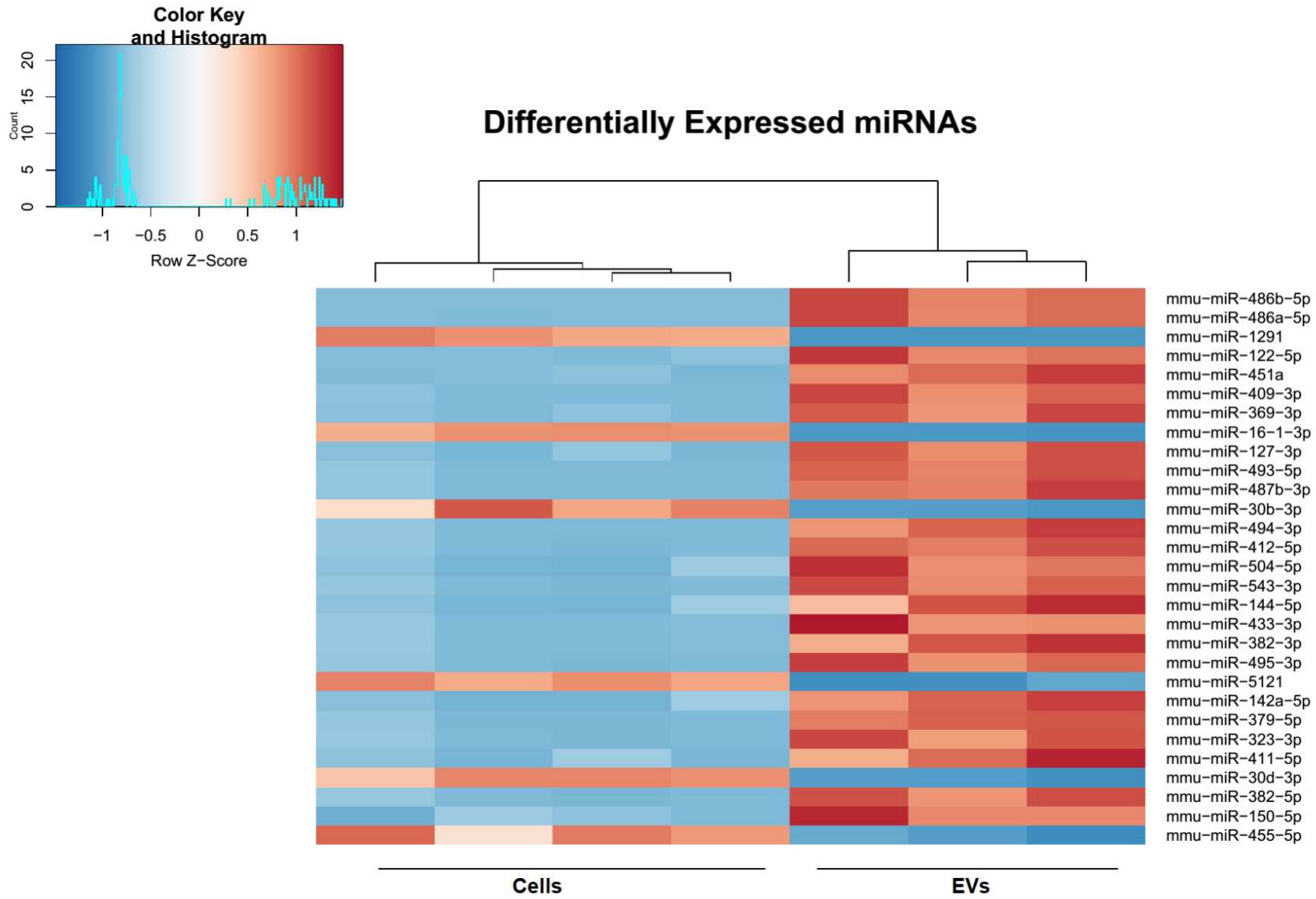
Color Key
and Histogram
Count
0
5
10
15
20
−1
−0.5
0
0.5
1
Row Z−Score
Differentially Expressed miRNAs
mmu−miR−486b−5p
mmu−miR−486a−5p
mmu−miR−1291
mmu−miR−122−5p
mmu−miR−451a
mmu−miR−409−3p
mmu−miR−369−3p
mmu−miR−16−1−3p
mmu−miR−127−3p
mmu−miR−493−5p
mmu−miR−487b−3p
mmu−miR−30b−3p
mmu−miR−494−3p
mmu−miR−412−5p
mmu−miR−504−5p
mmu−miR−543−3p
mmu−miR−144−5p
mmu−miR−433−3p
mmu−miR−382−3p
mmu−miR−495−3p
mmu−miR−5121
mmu−miR−142a−5p
mmu−miR−379−5p
mmu−miR−323−3p
mmu−miR−411−5p
mmu−miR−30d−3p
mmu−miR−382−5p
mmu−miR−150−5p
mmu−miR−455−5p
Cells
EVs

Figure 2. Overview of cellular and vesicular miRNA distribution in MSCs. Small RNA-sequencing analysis (Methods) of cellular and vesicular mature miRNAs from MSCs. The heat map shows expression values, expressed as fold enrichment (FE, red-blue) of mature miRNAs in cells (CL) versus extracellular vesicles (EVs).

not find this motif in miRNAs that are highly represented in cells relative to EVs such as miR-1291a, miR-5121a, and miR-16-1-3p. We also identified this group of cell-retained miRNAs shares a motif of AGAC (**Fig. 5B**).

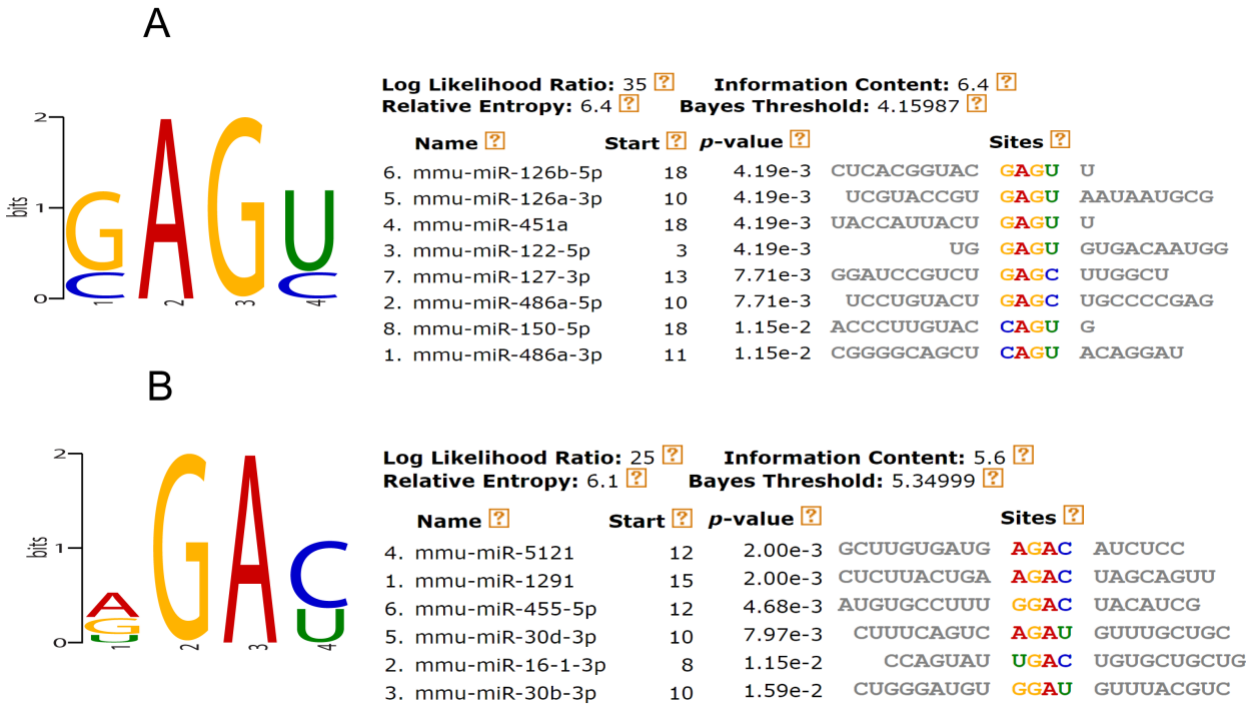

Figure 3. Identification of common sequence motifs among top EV-enriched and cell-retained miRNAs. Overrepresented motifs in miRNA populations from MSC-derived EVs (A) (RPM in EV library>1000, and *padj* ≤ *0.05 vs.* cells) or MSCs (B) were identified using the ZOOPs model[188].

RNA-binding Proteins are Expressed in MSC-derived EV

In order to investigate the hypothesis that RBPs mediate the sorting of miRNAs into EVs, we isolated EVs by differential centrifugation (**Methods**). EVs were characterized according to the current recommendations of ISEV20. To study which proteins were

expressed in MSC-derived EVs, we used mass-spectrometry for proteomic analysis (Methods). We detected 197 different proteins within the EV fraction. Cellular compartment clustering with DAVID showed that exosomal proteins were enriched in the EV lysate (**Fig. 6A-C**). Among the identified proteins, 30 of them were annotated as RNA-binding proteins, according to functional clustering (**Fig. 6D**). We found several types of heterogeneous nuclear ribonucleoproteins (hnRNP) expressed in the MSC-derived EVs, including hnRNPA2B1, hnRNPA1, and hnRNPQ.

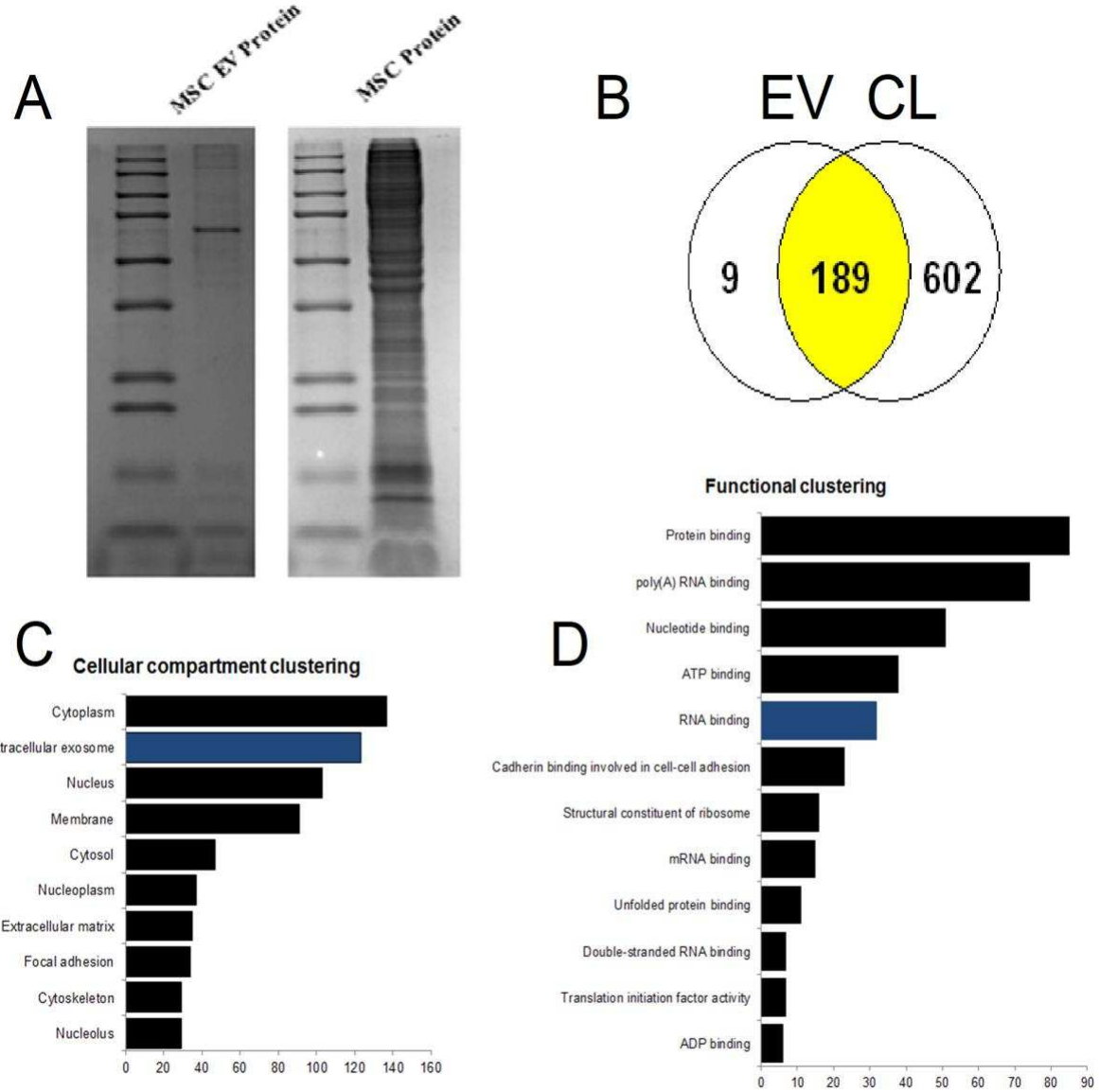

Figure 4. Identification of hnRNPA2B1 as a candidate for EV miRNA sorting protein. (A) Coomassie stain of MSC EV protein and MSC protein run on SDS-PAGE. (B) Venn diagram depicts results proteomic analysis of EV and producer cell lysates using mass spectrometry. A total of 602 MSC and 198 MSC EV proteins were identified by mass spectrometry with 189 common proteins identified. Gene ontology analysis for cellular compartment (C) and functional annotations of EV-related proteins (D) using DAVID Functional Annotation Bioinformatics Analysis[176].

Because hnRNPA2B1 is a known RNA binding protein in RNA processing/trafficking, is known to bind miRNAs, and is secreted by cells into EVs, we focused first on this RBP for studying the regulation of miRNAs loading into EVs. We confirmed the presence of hnRNPA2B1 in the EVs by Western blot (**Fig. 7A**). Furthermore, to identify whether hnRNPA2B1 is located inside or on the EV surface, purified EVs were treated with proteinase K with or without pretreatment with 1% Triton X-100 (to break membranes). The hnRNPA2B1 protein was resistant to proteinase K degradation but was degraded after treatment with detergent (**Fig. 7B**). These data showed that hnRNPA2B1 is abundant and localized primarily in the lumen of EVs.

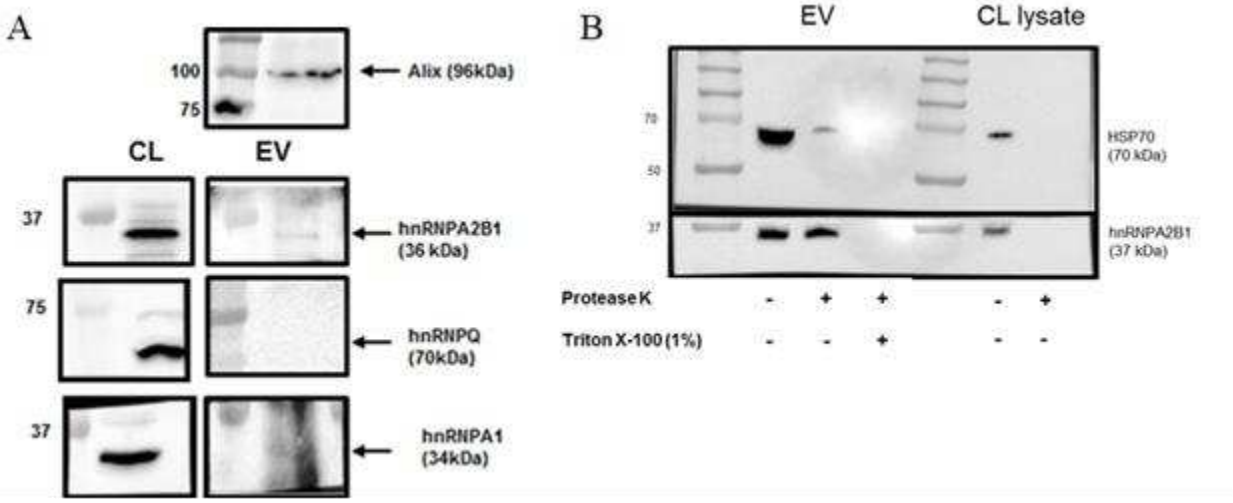

Figure 5. Identification of hnRNPA2B1 as a candidate for EV miRNA sorting protein. (A) Immunoblotting for hnRNPA2B1, hnRNPQ, hnRNPA1 and Alix in cells (CL) and extracellular vesicles (EV) protein lysate. (B) The presence of hnRNPA2B1 in EVs is validated by immunoblot of hnRNPA2B1 and HSP-70 in MSC-derived EVs isolated from 250

ml conditioned medium and MSC cellular lysate with or without prior treatment with 1% Triton X-1000 and degradation with proteinase K (**Methods**).

Downregulation of hnRNPA2B1 Alters Sorting of miRNA into EVs

In order to study the function of hnRNPA2B1 on miRNA sorting into EVs, we performed gene editing with CRISPR-Cas9 to knock-down hnRNPA2B1 levels. Because MSCs have been shown to be resistant to many non-viral transfection methods[189], we employed a lentiviral system. CRISPR guide RNAs (gRNAs) targeting the second exon of the hnRNPA2B1 open reading frame (ORF) (Methods) were selected using the CRISPR design tool from Benchling (https://www.benchling.com/crispr/). A non-targeting gRNA sequence that did not recognize any sequence in the mouse genome was used as negative control.

We recovered a clone 1.3 A2B1$^{-/-}$ and demonstrated it does not express hnRNPA2B1 by immunoblot analysis (**Fig. 8A**). The knocking-out of hnRNPA2B1 did not alter expression of other related RBPs, including hnRNPA1, and hnRNPQ (**Fig. 8B**). The A2B1$^{-/-}$ and Cas9 control cells grew normally under conditions for propagating MSCs.

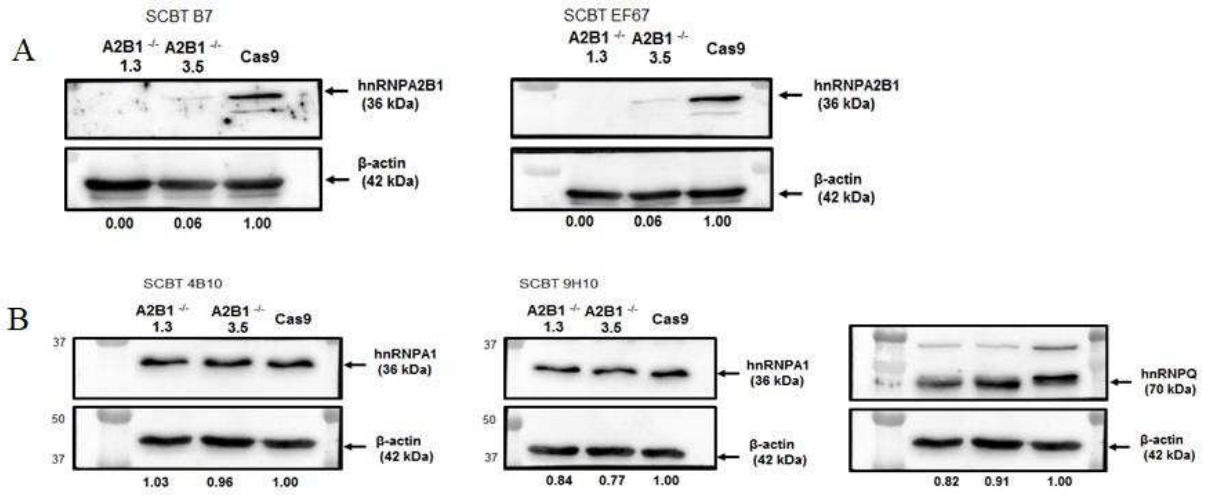

Figure 6. Knocking out hnRNPA2B1 with gene-editing CRISPR-Cas9. Representative example of immunoblotting for hnRNPA2B1 (36 kDa) with two different monoclonal antibodies against hnRNPA2B1 (SCBT B7 and SCBT EF67) (A), hnRNPA1 (36 kDa) with two different antibodies against hnRNPA1 (SCBT 4B10 and SCBT 9H10) and hnRNPQ (70 kDa) (B). Number below the Western blot lane represents ratio of target proteins (hnRNPA2B1, hnRNPA1, hnRNPQ)/β-actin.

We determined the effect of knocking out hnRNPA2B1 on miRNA biogenesis or processing proteins, which could alter the downstream of mature miRNA levels. Western blot analysis revealed that protein levels of Drosha and Dicer were unchanged after hnRNPA2B1 was knocked out (**Fig. 9**). This result supported minimal side effects of CRISPR-Cas-mediated genome editing.

We found A2B1$^{-/-}$ and Cas9 cell-released particles had a diameter of ~50 to 200 nm (average ~100nm) with approximately equal number of particles released into the medium when they reached 100% confluence (5.91 x $10^{11}$and 3.39 x 10^{11} particles/ml for A2B1$^{-/-}$ and Cas9) (**Fig. 10A**) with Nanosight nanoparticle tracking analysis. Immunoblotting revealed these EVs expressed typical surface markers for EVs including Alix, HSP-70, TSG101, and β-actin (**Fig. 10B**). These data confirmed that knocking out hnRNPA2B1 did not cause alteration in size distribution or concentration of particles.

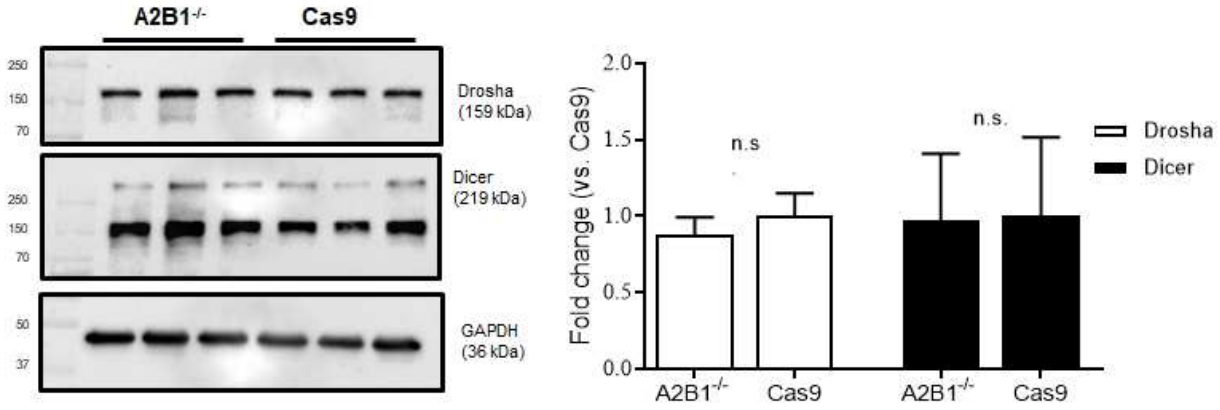

Figure 7. Knock out of hnRNPA2B1 did not alter protein levels of miRNA processing machinery in MSCs. (A) Immunoblotting results depicted fold change of Drosha and Dicer in A2B1$^{-/-}$ and Cas9 MSC cell line. (B) Protein band signal intensities were normalized to GAPDH intensities. Results are represented as mean ± SD (N=3/group) and analyzed using two-tailed, unpaired t-test. n.s. indicated non-significant, $P > 0.05$ *vs.* Cas9 MSC.

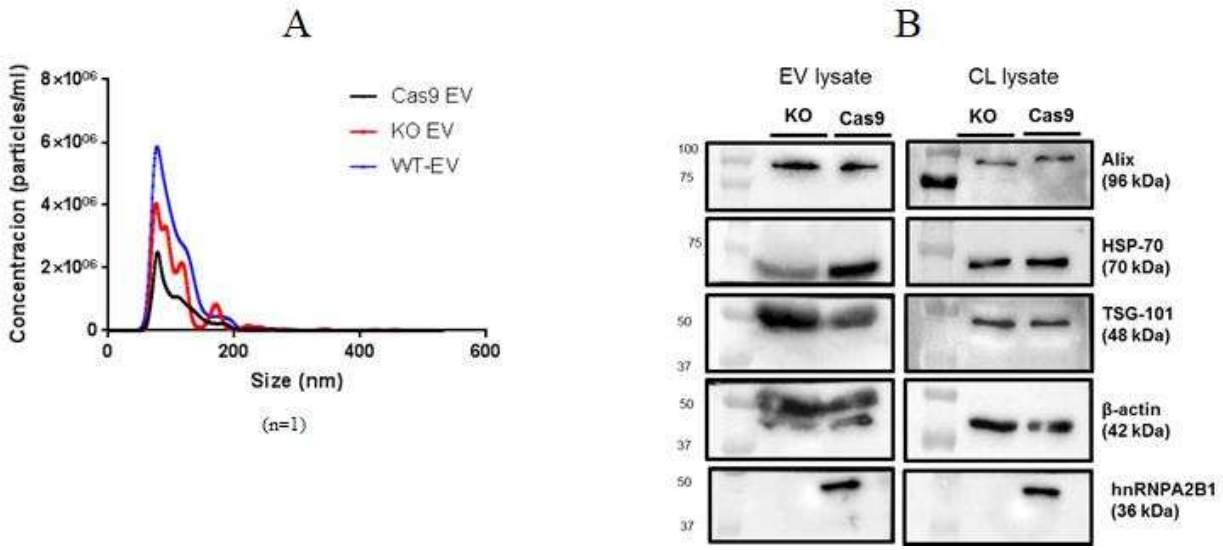

Figure 8. Characterization of hnRNPA2B1 knockout (KO) and Cas9 control-derived EVs. (A) Analysis of WT, CRISPR-Cas9 hnRNPA2B1 KO and CRISPR-Cas9 Control EVs by nanoparticle tracking analysis showing size distribution and concentration of particles in EVs (average size ~100 nm, concentration~5.91 x $10^{11}$and 3.39 x 10^{11} particles/ml for A2B1$^{-/-}$ and Cas9, respectively). Plotted data is from one experiment (N=1) (B) Immunoblotting of EV markers TSG101 (48 kDa), Alix (96 kDa), HSP-70 (70 kDa), β-actin (42 kDa) and hnRNPA2B1 (36 kDa) in extracellular vesicles (EVs) and cells (CLs).

In order to study the role of hnRNPA2B1 in regulation of miRNA sorting to MSC-derived EVs, small RNA sequencing and quantitative real time RT-PCR (qRT-PCR) were performed in cellular and vesicular fraction of A2B1$^{-/-}$ and Cas9 cell line. Our qRT-PCR analysis demonstrated significant alterations in cellular and vesicular distribution of several EV-associated miRNAs when hnRNPA2B1 was knocked out. Removal of hnRNPA2B1 significantly increased the accumulation in the cellular fraction of EV-sorted miR-122a and miR-486-5p, but did not alter the levels of cell-retained miRNAs including

miR-1291, miR-5121 (**Fig. 11**). In contrast, hnRNPA2B1 silencing significantly reduced the levels of miR-122a and miR-486-5p in EVs (**Fig. 12**). We did not observe any significant difference in the vesicular levels of the negative control, miR-22-3p. We also had non-significant results with miR-451 (**Figs. 11-12**).

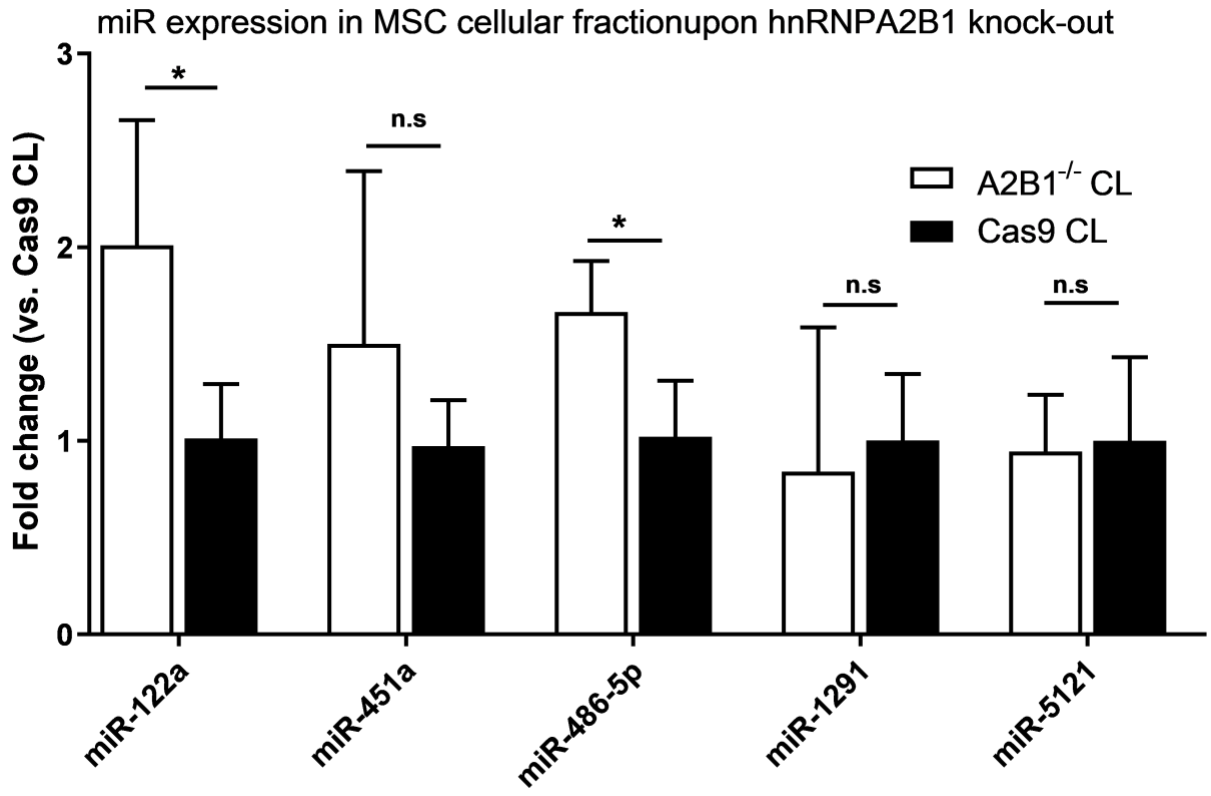

Figure 9. HnRNPA2B1 mediates the loading of miRNAs into MSC-derived EV. Analysis of the miRNA levels in cellular fractions after hnRNPA2B1 KO with miScript qRT-PCR (N=6-7/group). The values are calculated by the ΔΔCt method, normalized to small nuclear RNA (snRNA) U6 levels, and expressed as fold change. All data are presented as the mean ± SD and analyzed using two-tailed, unpaired t-test, $^{*}P \leq 0.05$, n.s. non-significant, $P > 0.05$ vs. Cas9 CL group.

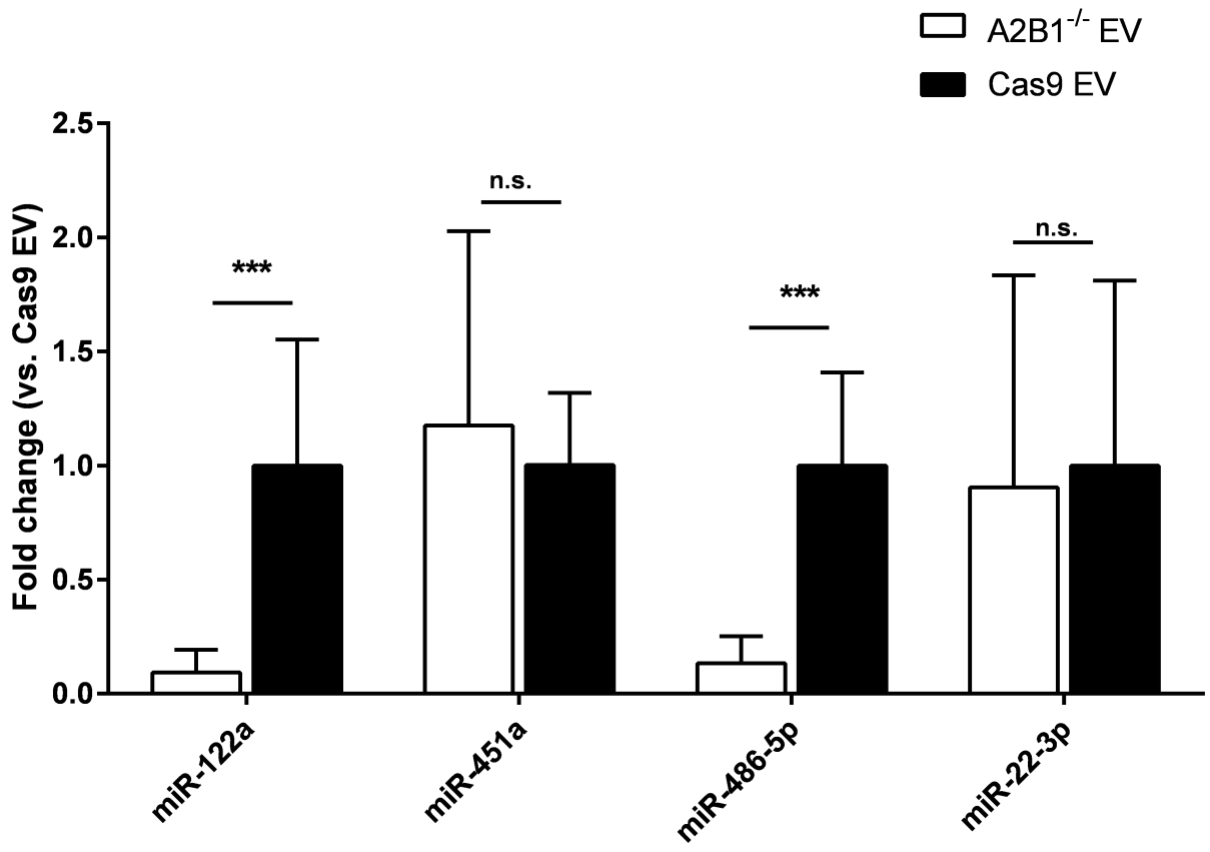

Figure 10. HnRNPA2B1 mediates the loading of miRNAs into MSC-derived EV. Analysis of the miRNA level in vesicular fraction after hnRNPA2B1 knockout with miScript qRT-PCR (N=6-7/group) via quantification of absolute copy number of miR-122a, miR-451a, miR-486-5p, and miR-22-3p. The values are calculated All data are presented as the mean ± SD and analyzed using two-tailed, unpaired t-test, ****P* ≤ 0.001, n.s. non-significant, *P* > 0.05 *vs.* Cas9 EV group.

We also employed RNA-sequencing to evaluate differential expression of miRNAs over a broader dynamic range. Principal-component analysis (PCA) showed a considerable diversity between miRNA populations of A2B1-/- and Cas9 EV (**Fig. 13A**). In particular, detailed RNA-sequence analysis revealed that stable knockout of hnRNPA2B1 caused a significant reduction in levels of several WT-EV-enriched miRNAs, including miR486-5p, miR-369 and miR-150a, compared to the Cas9 cells control **(Fig. 13B**). We also observed a

trend toward reduction in miR-122a level after hnRNPA2B1 was depleted (p=0.186). These data confirm that hnRNPA2B1 mediates the loading of a specific group of miRNAs into MSC-derived EVs. We confirmed by qPCR that this group includes miR-486-5p, miR-122a, and by RNA-sequencing, may also include miR-369 and miR-150a.

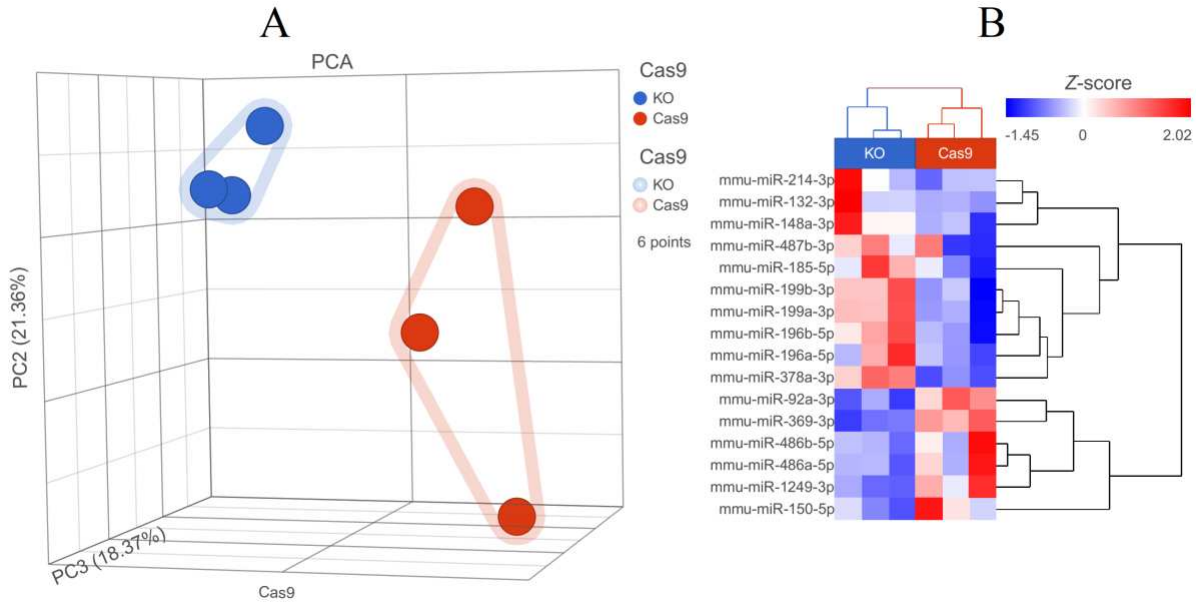

Figure 11. The sorting of miRNAs into MSC-derived EVs is mediated by protein hnRNPA2B1. (A) Principal-component analysis (PCA) (Methods) for sample-to-sample distance performed on mature miRNAs identified in KO and Cas9 EVs in three independent biological replicates. (B) Heat map showing expression values, expressed as fold enrichment (FE; blue-red) of mature miRNAs in hnRNPA2B1 knockout EV (KO) versus Cas9 control cells (Cas9).

Interaction of hnRNPA2B1 and EV-enriched miRNAs

Because hnRNPA2B1 is a well-known RNA-binding protein, we selected miRNAs shown to be EV-sorted, miR-486-5p, miR-122a (**Fig. 2, 3, 12**) and miR-451a which was shown in initial assays to be sorted (**Figs. 2,3**), but not validated by PCR (**Fig. 12**) for studies of interaction (*i.e.* binding) with hnRNPA2B1. The binding of hnRNPA2B1 to miR-486-5p, miR-451a, and miR-122a were first tested by electrophoretic mobility gel-shift

assay. The protein-miRNA complex was detected based on their mobility shift relative to controls. The specificity of the interaction was evaluated by competition and super-shift assays. In the competition assay, reduction in the shifted band was observed when excess amount (50-fold) of unlabeled miR-122a, miR-486-5p and miR-451a was added to the binding reaction, indicating the unlabeled miRNA can compete with labeled miRNA for binding to RBPs (**Fig. 14**). The protein specificity of interaction was determined by gel super-shift assay (**Methods**). The addition of the monoclonal antibody against hnRNPA2B1 to the mixture of nuclear lysate and biotinylated miRs causes a super-shift, resulting in a reduction in intensity of the initially shifted bands (RNA and protein) and accumulation of complexes in the well (RNA-protein-antibody). Moreover, the nuclear lysate of A2B1$^{-/-}$ did not cause a shift in the presence or absence of antibody for hnRNPA2B1 (**Fig. 15**). Although we tried to get the super shift complexes into the gel by changing the acrylamide gel percentage or charge of the protein-RNA complex, we could not resolve the complex in the gel, which made it difficult to make even a semi-quantitative analysis.

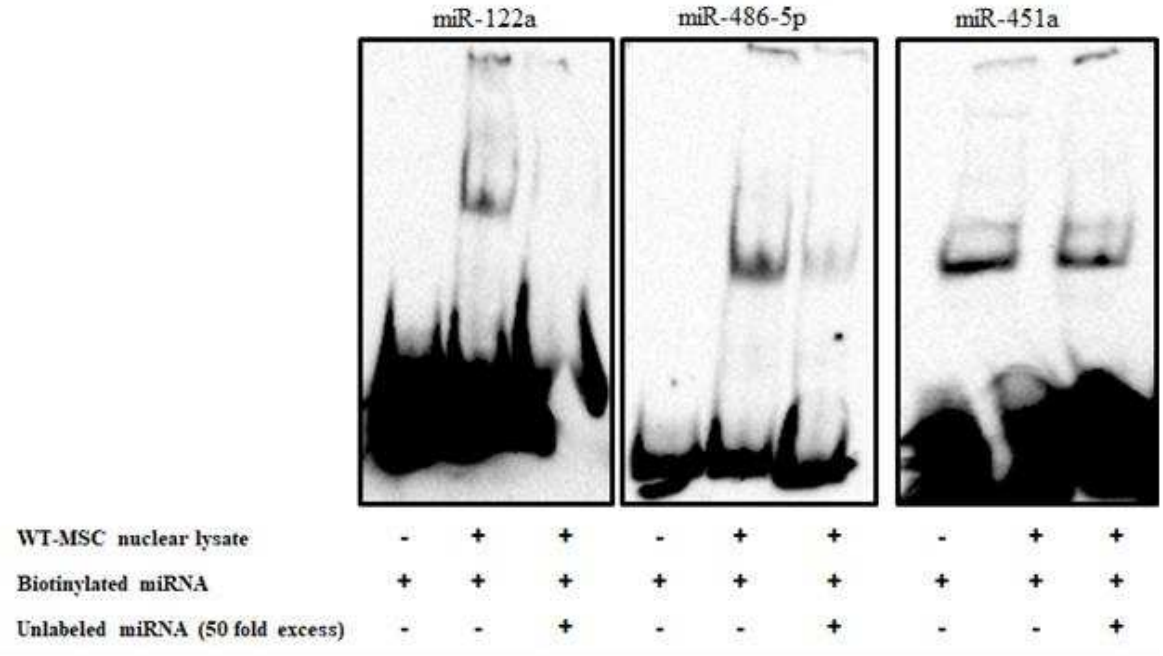

Figure 12. Specificity of *in vitro* interaction between EV-enriched miRNA and RNA-binding proteins in WT-MSC nuclear lysate. Biotinylated miRNAs were incubated with nuclear lysates from WT-MSC in the absence or presence of 50-fold excess of unlabeled cognate miRNA. Electrophoretic shift showed the binding of hnRNPA2B1 to miR-122a, miR-486-5p, and miR-451a. The specificity of protein-RNA interaction was determined by the competition assay with unlabeled miRNA.

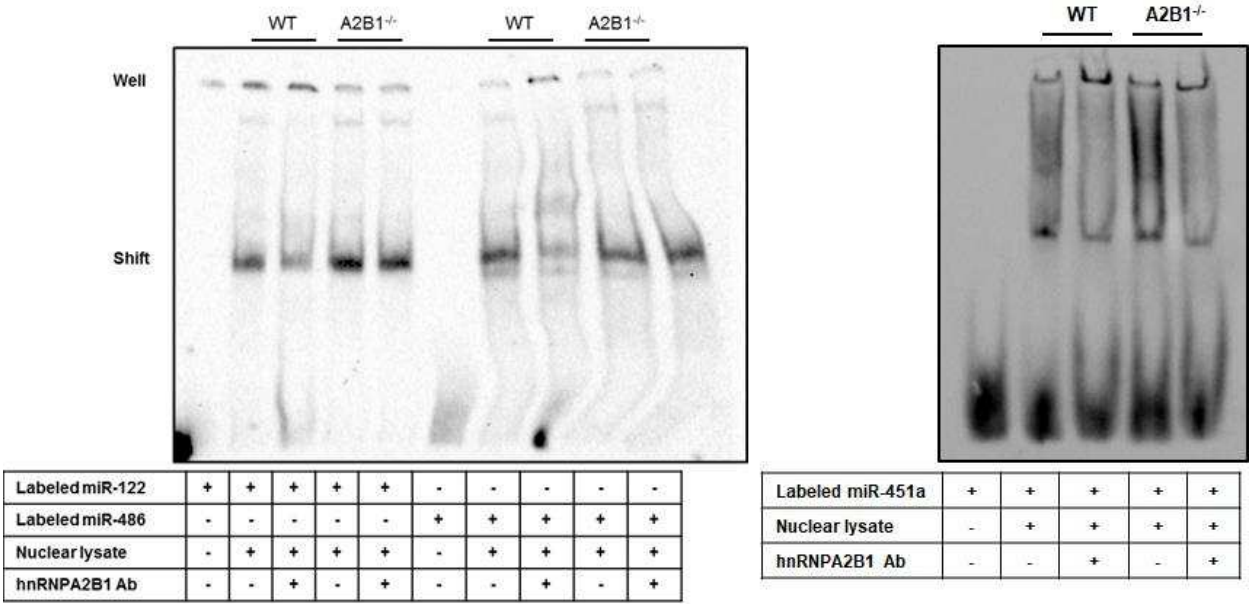

Labeled miR-122	+	+	+	+	+	-	-	-	-	-
Labeled miR-486	-	-	-	-	-	+	+	+	+	+
Nuclear lysate	-	+	+	+	+	-	+	+	+	+
hnRNPA2B1 Ab	-	-	+	-	+	-	-	+	-	+

Labeled miR-451a	+	+	+	+	+
Nuclear lysate	-	+	+	+	+
hnRNPA2B1 Ab	-	-	+	-	+

Figure 13. HnRNPA2B1 interacts with EV-enriched miRNAs in vitro. Electrophoresis mobility super-shift assay (EMSA) shows the binding of proteins to miR-122a, miR-486-5p, and miR-451a. Biotinylated miRNAs were incubated with either nuclear lysate from WT or hnRNPA2B1 knockout nuclear lysate with or without antibody against hnRNPA2B1 as indicated.

The specific binding of hnRNPA2B1 to EV-associated miRNAs was verified by RNA immunoprecipitation (RIP) assay of hnRNPA2B1 using magnetic beads and nuclear lysates as input, followed by qRT-PCR for mature miRNAs. We detected the presence of hnRNPA2B1 protein in the sample immunoprecipitated with antibody against hnRNPA2B1, but not in the anti-IgG control antibody (**Fig. 16A**). The miR-486-5p was significantly enriched in hnRNPA2B1 precipitates ($P \leq 0.05$) (**Fig. 16B**). In contrast, no significant difference was observed in enrichment of cell-retained miR-1291 and miR-5121 (**Fig. 16B**).

We also could not detect significant enrichment for miR-451a and miR-122a, though trends in that direction were noted.

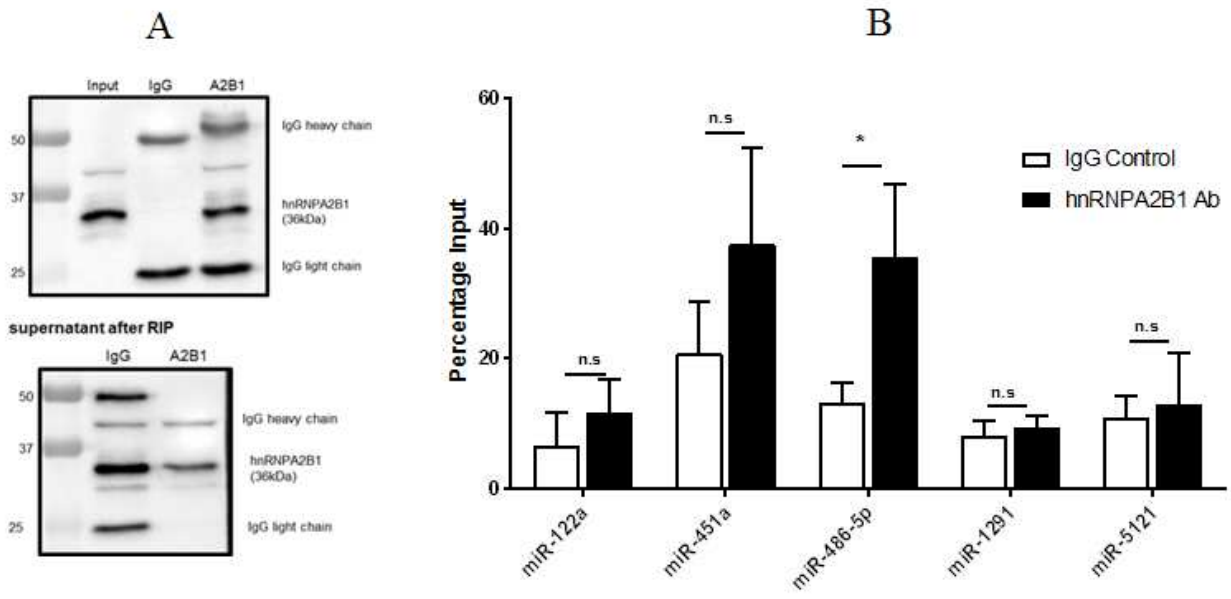

Figure 14. Association of hnRNPA2B1 and EV-enriched miRNAs by RIP assay. (A). Immunoblots for hnRNPA2B1 (36 kDa) in elutants and supernatants following RNA immunoprecipitation assay. (B) qPCR analysis of miRNAs contained in hnRNPA2B1 immunoprecipitates from WT-MSC nuclear lysates as a percentage of 10% input. Immunoprecipitation was performed with mouse anti-hnRNPA2B1 or anti-IgG control antibody (N=6/group) (Methods). All data are presented as the mean ± SD, and analyzed using two-tailed, unpaired t-test, *$P \leq 0.05$, n.s. non-significant, $P > 0.05$ *vs.* IgG control group.

To validate the observations from the RIP assay, the predicted binding of hnRNPA2B1 and miR-122a, miR-451a and miR-486-5 were confirmed with the biotinylated miRNA-mediated pull-down assay (RNA/protein pull-down assay). The hnRNPA2B1 protein was detected in samples precipitated with labeled miR-122a, miR-451a and miR-486-5p but not with labeled miR-1291 (**Fig. 17A**). To confirm the specificity of interaction between miR-486-5p and hnRNPA2B1, we performed a competition assay with excess unlabeled miR-486-5p. Binding of hnRNPA2B1 and miR-486 was reduced

when an excess amount (20X) of unlabeled miR-486-5p was added to the reactions (**Fig. 17B**). These data strongly support the association of hnRNPA2B1 and miR-486-5p, the most enriched miRNA in MSC-derived EVs.

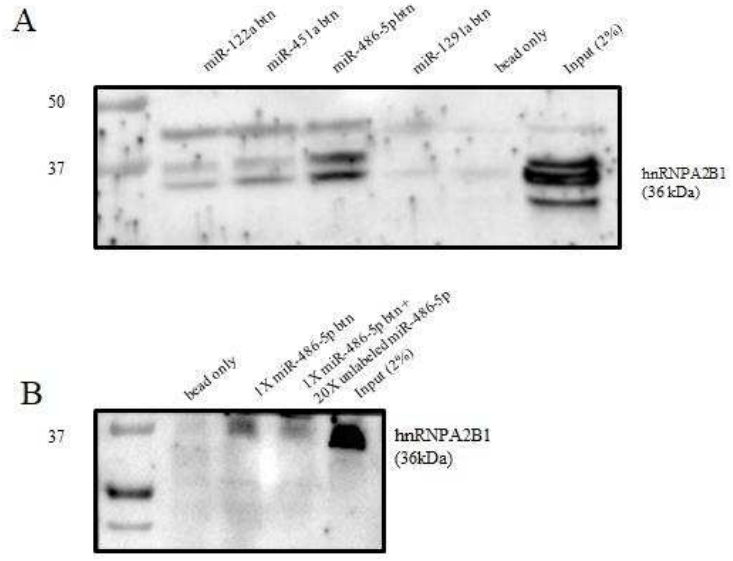

Figure 15. Pulldown of hnRNPA2B1with biotinylated miRNAs. For RNA/protein pull-down assay (A) and for competition assay (B), nuclear extracts were mixed with biotinylated miR-122a, miR-451a, miR-486-5p, miR-1291a or nonbiotinylated miR-486-5p, respectively.

Summary of the Findings

The mRNA content of extracellular vesicles is important for intercellular communication. Deep sequencing data for small non-coding RNA from our lab demonstrates that specific miRNAs are selectively loaded such that relative levels differ between EVs and producer MSCs. Several miRNAs (including miR-486-5p, miR-122a) had high abundance in EVs and yet low levels in the producer cells. The difference between the miRNA profiles of cells and EVs suggests the existence of active processes directing the sorting of miRNAs into EVs. We hypothesized that RNA-binding proteins are key components of the miRNA selective sorting apparatus. From mass-spec and bioinformatic

analyses, we selected the hnRNPA2B1 protein as a good candidate for mediating the sorting of EV-enriched miRNAs. To this aim, we knocked-out transcripts encoding hnRNPA2B1 using CRISPR-Cas9. The expression of hnRNPA2B1 was completely knocked out, as far as we could tell from Western blot validation. Knocking out of hnRNPA2B1 does not affect other RNPs that might be involved in miRNA sorting, including hnRNPA1, hnRNPQ and YBX1. Deletion of hnRNPA2B1 also does not alter EV production, size, or expression of EV markers (TSG101, HSP70, CD63). Analysis of miRNA levels by qRT-PCR showed that levels of miR-122a and miR-486-5p were significantly reduced in the EV fractions, and that their cellular levels were increased, supporting dysfunction of EV sorting of these miRNAs. Levels of cell-retained miRNAs (miR-1291a and miR-5121a) did not change in either knock-out or control cells. We showed that hnRNPA2B1 binds to miR-486-5p, which was confirmed by independent assays, including, RNA immunoprecipitation and the miRNA-mediated pulldown assays (**Fig. 18**). The status of miR-451a and miR-122a were ambiguous due to the fact that results were not uniformly supportive of sorting and hnRNPA2B1 interaction.

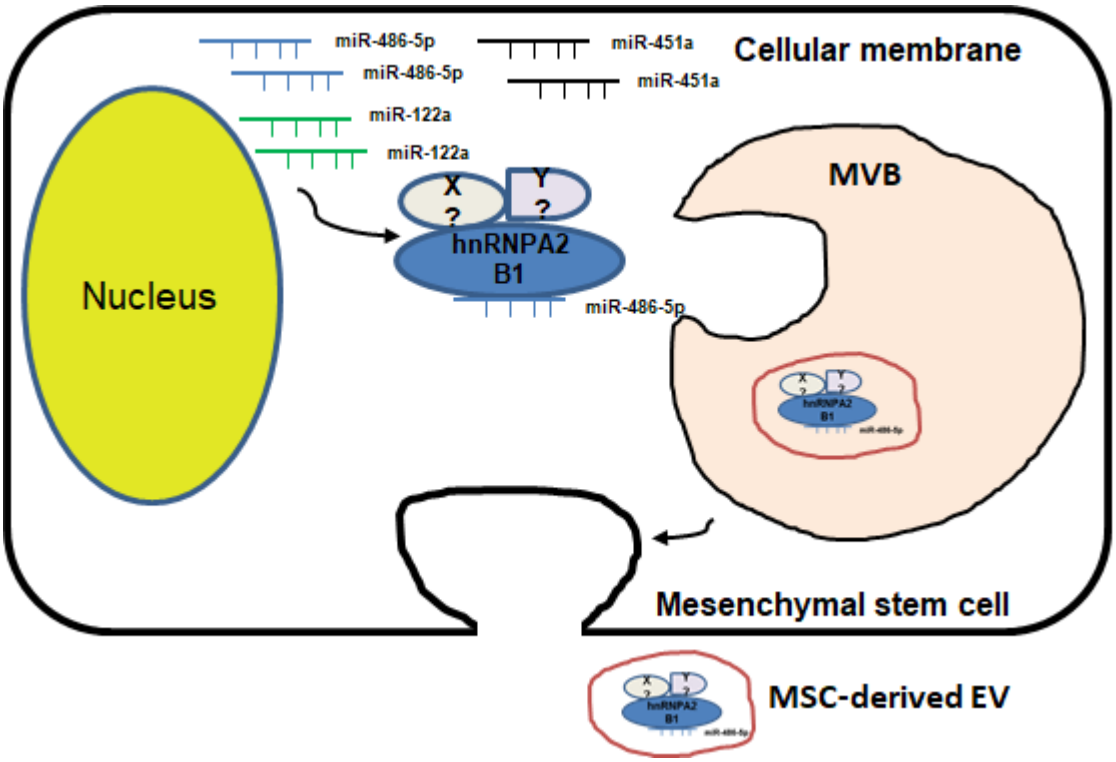

Figure 16. Graphical summary of the study findings in the Aim 1. The hnRNPA2B1protein binds to a specific group of miRNAs, including miR-486-5p. Downregulation of hnRNPA2B1 causes a decrease in EV levels of miR-486-5p, thus leading to an accumulation of the miRNA in the intracellular compartment. This supports our hypothesis of a role for hnRNPA2B1 in EV sorting of miR-486-5p.

Cardioprotective effects of EV selectively sorted miR-486-5p

Extracellular vesicles are known to package and transfer miRNA from producer cells to recipient cells to modulate gene/protein expression and contribute to the survival and/or reparative processes during and after I/R injury. In the current study, we found high levels of miR-486-5p within the MSC-derived EV, evidenced by deep RNA-sequencing (**Fig. 4**) and qRT-PCR (**Fig. 19**). This finding is consistent with other studies that show miR-486-5p was among top over-expressed miRNAs in EVs isolated from human adipose and bone-marrow MSCs[190]. Additionally, we reported previously that the protective effects of MSC-derived EVs was mediated largely by miR-21-5p. Removal of miR-21-5p did not however, completely abolish the protection, indicating other miRNAs also contributed to this beneficial effect. We identified miR-486-5p as a candidate in mediating cell survival effects. In Aim 2, we used different assays to address the hypothesis that miR-486-5p, a selectively sorted EV miRNA, can reduce cell death-associated with I/R injury, resulting in less cellular damage and smaller infarct size. To examine the protective effect of this EV-enriched miRNA against MI-mediated damage, we verified function using *in vitro* and *in vivo* models, identified targets of miR-486-5p, and determined the biological significance of miR-486-5p after I/R injury.

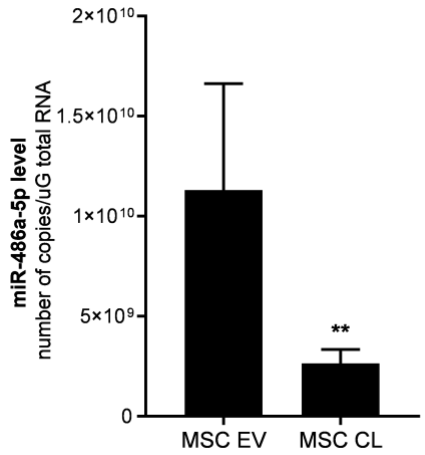

Figure 17. Validation of miR-486-5p expression in MSC cells (MSC CL) and extracellular vesicle (MSC EV) samples. miScript small RNA qRT-PCR results expressed as number of miR-486a-5p copies using a standard curve of miR-486-5p mimetic. Data is represented as mean ± SD (N=7/group) and analyzed using a two-tailed, unpaired t-test. ** $P \leq 0.01$ vs. MSC CL

Prediction and Selection of Targets for miR-486-5p Involved in Regulation of Cell Death in MI

miRNAs have been shown to regulate multiple mRNA targets to exert their biological functions. Because the consistency and accuracy of commonly used algorithms in miRNA target prediction are typically low[191], we decided to combine two algorithms (MiRanda[192] and Targetscan 7.1[69]) for predicting miRNA-mRNA target interactions, resulting in 1687 miRNA-target pairs. From theses putative targets, our gene ontology analysis (StudioPathway[193]) (targets contributing to cell survival or cell death) resulted in a final set of 64 miRNA-target pairs. Based on cumulative interaction context scores[69], Programed cell death 4 (PDCD4) and Pten, a well-known target of miR-486-5p[194; 195] were chosen to study further (**Fig. 20**).

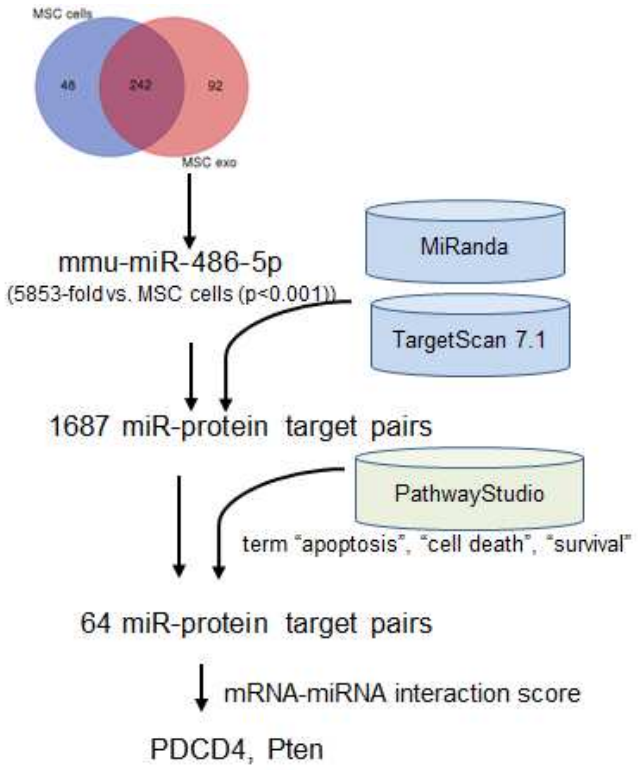

Figure 18. Scheme for selecting and prioritizing miR-486-5p and potential targets linked to cell survival. Starting with EV-enriched miR-486-5p and its associated targets defined by MiRanda and TargetScan (version 7.1) databases, we narrowed down our analysis to candidates with annotation pertaining to "apoptosis", "cell death", and "survival" pathways from PathwayStudio.

miR-486-5p Targets PDCD4 through Binding with the 3'UTR and Inhibits Protein Levels

The profound effect of miRNAs on protein levels is usually through binding of its seed sequence to complementary regions of the mRNA targets, most often in the 3' un-translated region (3'-UTR). Bioinformatic search indicated target sequences for miR-486-5p at nucleotide (nt) 63-69 and nt 721-728 of the 3'-UTRs of PDCD4 and Pten respectively. We also found that the miR-486-5p target sequences of PDCD4 and Pten-3'-UTRs are highly conserved among seven species, including humans (**Fig. 21**). Such sequence conservation may be indicative of conserved function. We next used a reporter luciferase assay to test

whether miR-486-5p directly targeted the 3'-UTRs of PDCD4 and Pten. We cloned the 3'-UTRs of PDCD4 and Pten into a *luc2*-SV40 reporter vector. This vector puts the luc gene under control of the cloned 3'UTR and repression of the reporter luc signal is due to repressed translation of luc[196]. We observed a profound reduction of luciferase activity by miR-486-5p mimic compared to the scrambled miRNA controls ($P \leq 0.0001$) (**Fig. 22**) when H9c2 cells were co-transfected with the reporter vector and different doses of miR-486-5p mimetic or siRNA against *luc2* gene as positive control. We also observed similar result with the construct of 3'-UTR of Pten (**Fig. 22**), indicating both 3'-UTRs of PDCD4 and Pten are definite targets for miR-486-5p binding and suppression of post-transcriptional regulation.

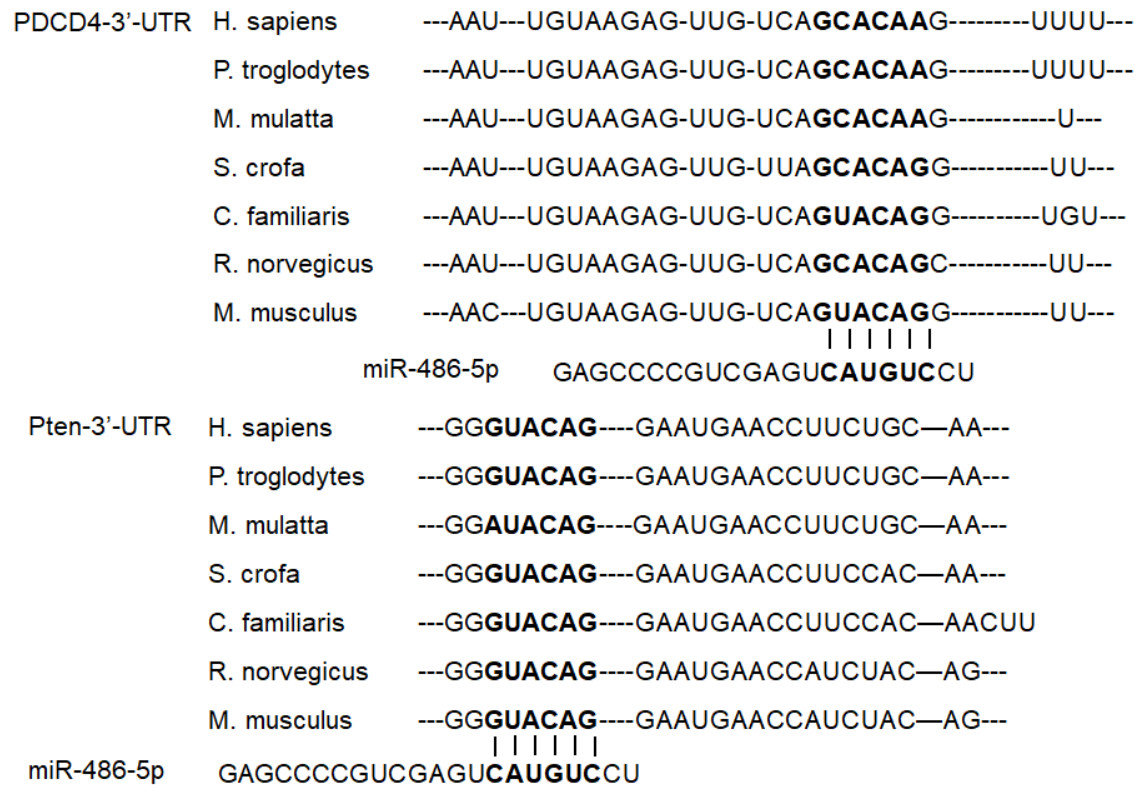

Figure 19. Binding Site of miR-486-5p on the 3'-UTR of PDCD4 and Pten is Highly Conserved in Seven Species. Comparison of nucleotides between the seed sequence of miR-486-5p and its targets in seven species. Data were retrieved from targetscan.org, release 7.1.

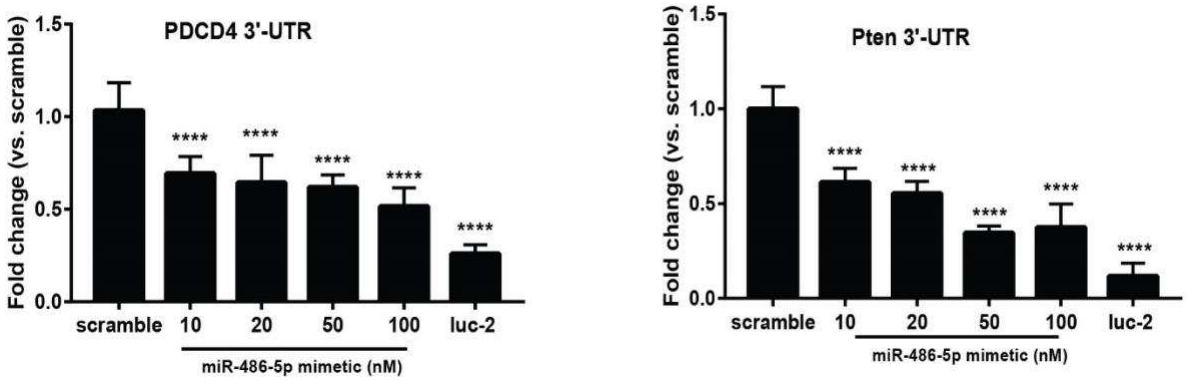

Figure 20. miR-486-5p Targets the 3'-UTRs of PDCD4 and Pten. 1 x 10^4 H9c2 cells were co-transfected with PDCD4 or Pten firefly luciferase reporter plasmids, Renilla luciferase plasmid (50:1) and amounts to comprise a dose curve of miR-486-5p mimic. Scrambled non-targeting miRNA was used as negative control (scramble) and siRNA against the luc2 gene (100nM) was used as positive control. After 24h, cells were lysed and both firefly and Renilla luciferase activities were measured. Data are presented as the relative ratio of firefly:Renilla luciferase, normalized to scramble treated group, with error bars representing SD (N=4/group) and analyzed using one-way ANOVA. ****$P \leq 0.0001$ *vs.* scramble group.

We next asked if the potential of miR-486-5p to regulate PDCD4 and Pten was functional for the endogenous genes products. H9c2 cells were transfected with miR-486-5p mimic, and scrambled miRNA and the effect of these manipulations upon mRNA and protein levels of PDCD4, Pten, and phosphorylated Akt (Pten's downstream targets), were measured by qRT-PCR and Western blotting. We found the transfection of miR-486-5p mimetic significantly increased levels of mature miR-486-5p (**Fig. 23A**). We observed that mRNA levels of PDCD4 and Pten were significantly reduced in the group transfected with miR-486-5p mimetic, compared to the scramble control group ($P \leq 0.05$) (**Fig. 23B**). Subsequently, PDCD4 protein levels were reduced by approximately 50% (**Fig. 23C-D**). On

the other hand, the miR-486-5p mimic did not affect protein levels of Pten or phosphorylated Akt (**Fig. 23C-D**). These findings demonstrated that miR-486-5p inhibits PDCD4 via targeting the PDCD4 mRNA and limiting the production of PDCD4 protein.

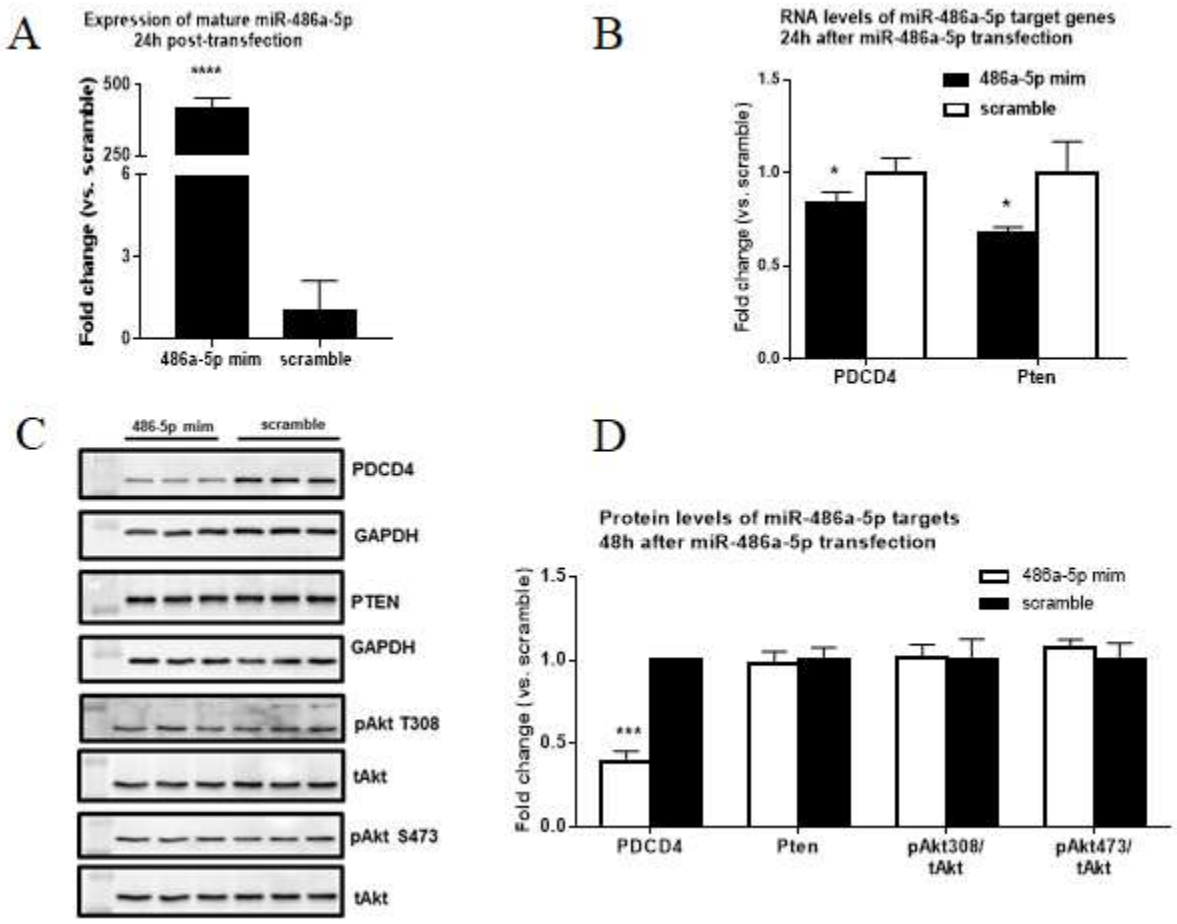

Figure 21. miR-486-5p Mimic Decrease mRNA and Protein Levels of PDCD4. 1 x 10^4 H9c2 cells were transfected with 50 nM of synthetic miR-486-5p mimic for 24 hours (for RNA isolation) or 48 hours (for protein isolation). Scrambled non-targeting miRNA was used as negative control (A) mature miR-486-5p levels in transfected cells 24 hours post-transfection detected by qRT-PCR. The values are calculated by the ΔΔCt method and normalized to U6 (B, C, D) Expression of miR-486-5p targets (PDCD4 and Pten) RNA (B) and protein levels (PDCD4, Pten, phosphorylated Akt (pAkt), total Akt (tAkt) (C, D) 24 hours after miR-486-5p transfection. The qRT-PCR data are calculated by the ΔΔCt method and normalized to 18S. Protein bands signal intensities were normalized to GAPDH. Results are presented as the average fold change ± SD (N=3/group) and analyzed using two-tailed, unpaired t-test. *$P \leq 0.05$; **$P \leq 0.01$, ****$P \leq 0.0001$ *vs.* scramble group

miR-486-5p Mimetic Increases Cell Survival after Simulated I/R Injury

In order to study the effect of miR-486-5p mimetic treatment on I/R injury, we next performed the simulated ischemia reperfusion injury (sim I/R). We transfected H9c2 cells with either miR-486-5p mimetic, or non-targeting scrambled RNA. 48h after transfection, cells were challenged with sim I/R by hypoxia for 12 hours in ischemia mimetic solution, followed by 2 hours reperfusion in normal growth medium (**Methods**). The number of I/R-induced necrotic cells was evaluated by Hoechst 33258 – propidium iodide staining. We found that pretreatment with miR-486-5p mimetic did not change the cell viability in normal conditions (**Fig. 24**). However, a significant increase in cell survival was observed for the miR-486-5p mimetic treated group (**Fig. 26A-B**) after sim I/R ($P \leq 0.05$). Representative images of Hoechst/PPI double-staining of H9c2 cells treated with scrambled non-targeting control, or miR-486-5p mimic are shown in **Fig. 26A**. Additionally, released lactate dehydrogenase (LDH) into cell culture medium was used as additional indicator for damaged plasma membrane. In accordance with results in cell viability measurement with Hoechst/PPI staining, transfection of miR-486-5p mimetic at 50 and 100nM significantly reduced LDH release, relative to scrambled group ($P \leq 0.05$) (**Fig. 25**). These data suggested that miR-486-5p pretreatment promotes cell survival of H9c2 cells after sim I/R.

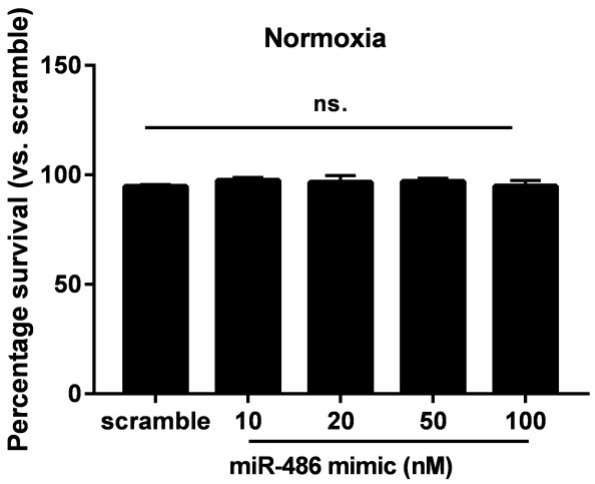

Figure 22. The miR-486-5p does not Affect Cell Survival in Normoxic Conditions. 1 x 10^4 H9c2 cells were transfected with a dose curve of miR-486-5p mimic for 48 hours. Scrambled non-targeting miRNA was used as negative control (scramble). Percentage (%) of cell viability was measured by number of viable cells using Hoechst and PPI staining before and after 16 hours in normoxia condition. Data are represented as mean ± SD (N=4/group) and analyzed using one-way ANOVA. n.s., non-significant, $P > 0.05$ *vs.* scramble group.

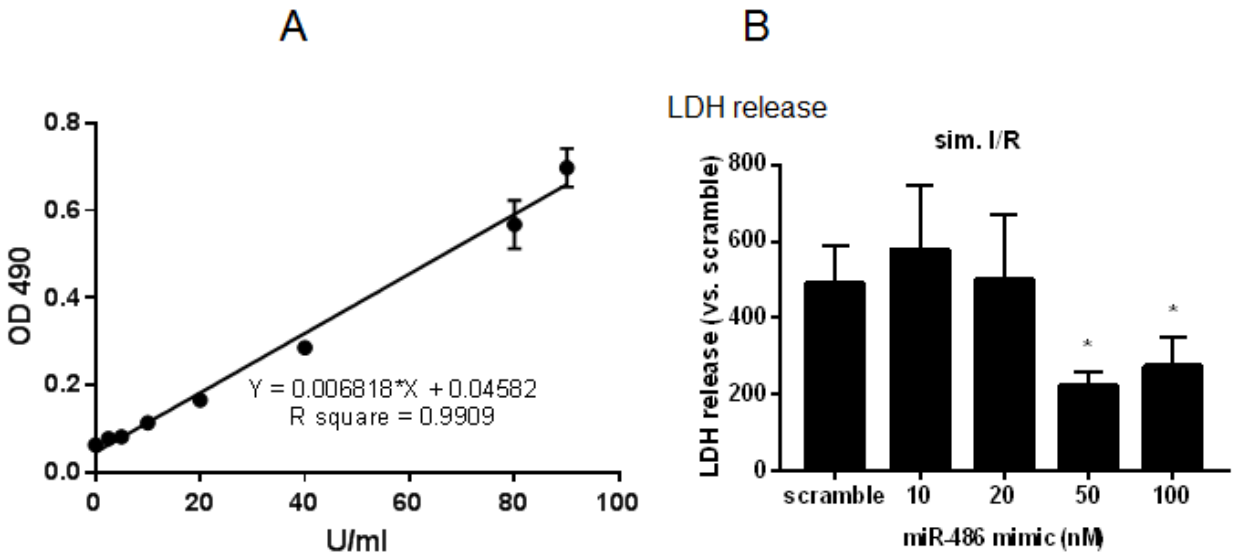

Figure 23. Measure LDH Release after sim I/R. (A). Standard curve of LDH. (B) Quantification of LDH release (mU/mL) by H9c2 cells into the medium after sim I/R using a standard curve of LDH. Results are represented as mean ± SD. (N=4/group) and analyzed using one-way ANOVA. *$P \leq 0.05$ *vs.* scramble group. LDH, Lactate dehydrogenase, sim I/R, simulated Ischemia/reperfusion.

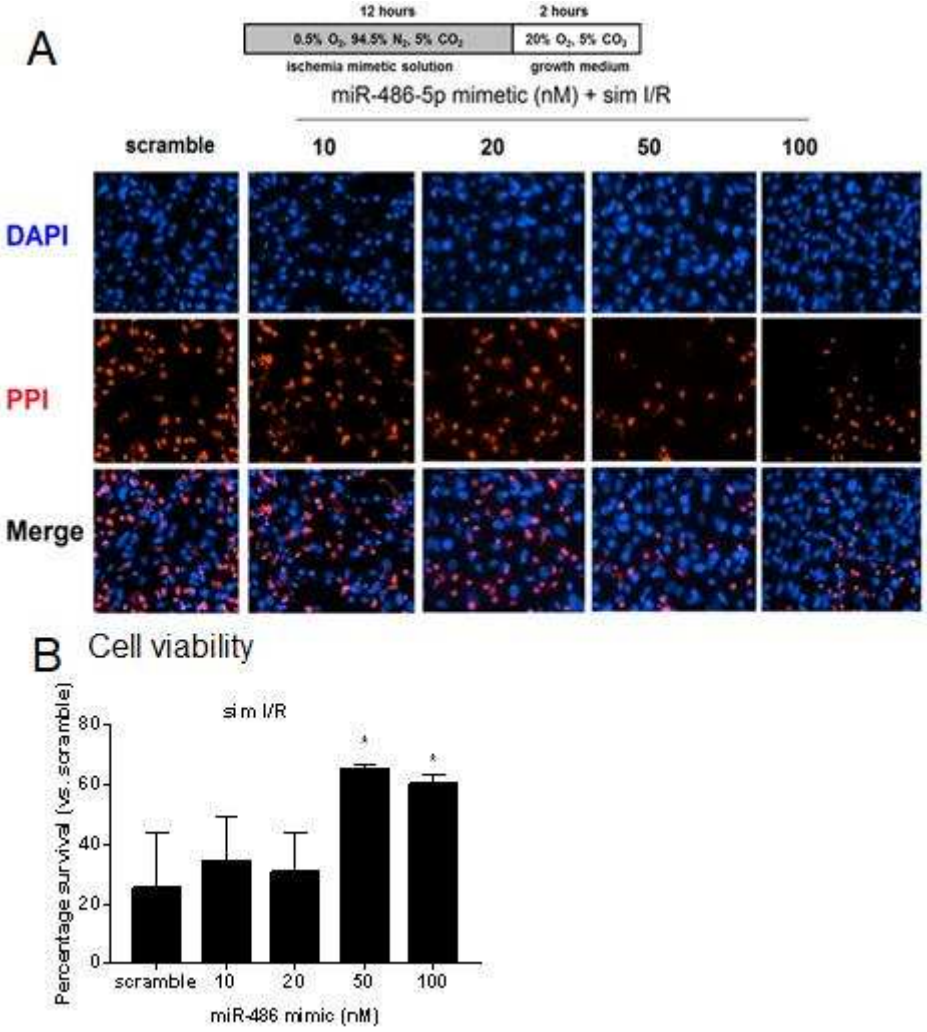

Figure 24. miR-486-5p Mimic Increases Cell Survival after sim I/R. 1 x 10^4 H9c2 cells were transfected with a dose curve of miR-486-5p mimic for 48 hour before subjected to 12 hours ischemia and 2 hours reperfusion (Methods). Scrambled non-targeting miRNA was used as negative control (scramble). (A) Representative images demonstrate PPI-positive nuclei (red color) of dead cells, all nuclei, Hoechst-positive (blue color) after sim I/R (×4 magnification). Scale bar = 1000 μm (B). Quantification of cell viability, the percentage (%) of cell survival was measured by number of viable cells using Hoechst and PPI staining before and after sim I/R (C) Quantification of LDH release (mU/mL) by H9c2 cells into the medium after sim I/R using a standard curve of LDH. Results are represented as mean ± SD. (N=4/group) and analyzed using one-way ANOVA. *$P \leq 0.05$ *vs.* scramble group. LDH, Lactate dehydrogenase, sim I/R, simulated Ischemia/reperfusion.

miR-486-5p Down Regulates PDCD4 Levels and Inhibits I/R Injury-induced Apoptosis *In vitro*

Since EV-derived miR-486-5p targets PDCD4[195], a mediator of apoptosis, and increases cell viability after sim I/R (**Fig. 25-26**), we hypothesized that miR-486-5p functions by inhibiting cell apoptosis of H9c2 cardiomyocyte. DNA fragmentation as a characteristic hallmark of apoptosis was identified and quantified using TUNEL (terminal deoxynucleotidyl transferase dUTP nick end labeling) staining. TUNEL assay after sim I/R revealed that sim I/R challenge significantly increased the number of apoptotic cells ~40% compared with control cells in the normoxic condition. In accordance with the data observed in the simulated I/R, pretreatment with miR-486-5p significantly inhibited sim I/R-induced apoptosis ($P \leq 0.05$) (**Fig. 27 A-B**). In addition, PDCD4 has been reported to induce apoptosis via activation of caspase-3 and Bax[196,197]. We found miR-486-5p treatment effectively reduces the protein levels of the pro-apoptotic proteins PDCD4, cleaved caspase-3/total caspase-3 and Bax, after sim I/R (**Fig. 28 A-B**). Therefore, we concluded that miR-486-5p increases cell survival in H9c2 cells by inhibiting apoptosis via PDCD4 repression.

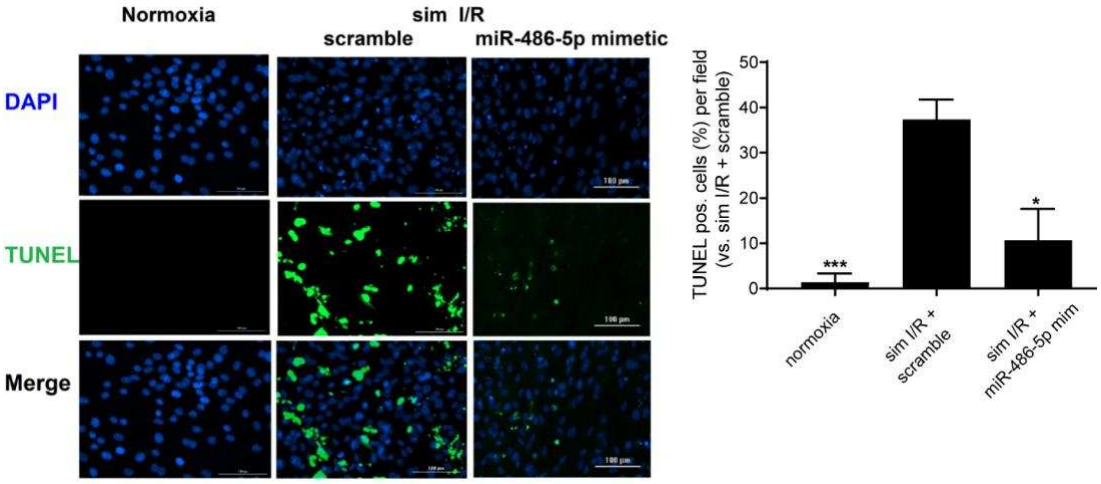

Figure 25. miR-486-5p Reduces Apoptotic Cell Death after sim I/R. 1 x 10^4 H9c2 cells were transfected with 50 nM miR-486-5p mimic for 48 hours. Scrambled non-targeting miRNA was used as negative control (scramble). They were then subjected to sim I/R challenge (**Methods**). After sim I/R, cells were fixed for TUNEL assay. (A) Representative images demonstrate TUNEL-positive nuclei (green color) (×20 magnification). Scale bar = 100 µm. (B) quantification of percentages (%) of TUNEL-positive cells relative to DAPI-positive total nuclei. Results are represented as mean ± SD (N=4/group) and analyzed using one-way ANOVA. *$P \leq$ 0.05, ***$P \leq$ 0.001 *vs.* scrambled group. TUNEL, Terminal deoxynucleotidyl transferase dUTP nick end labeling, Sim I/R, simulated ischemia/reperfusion.

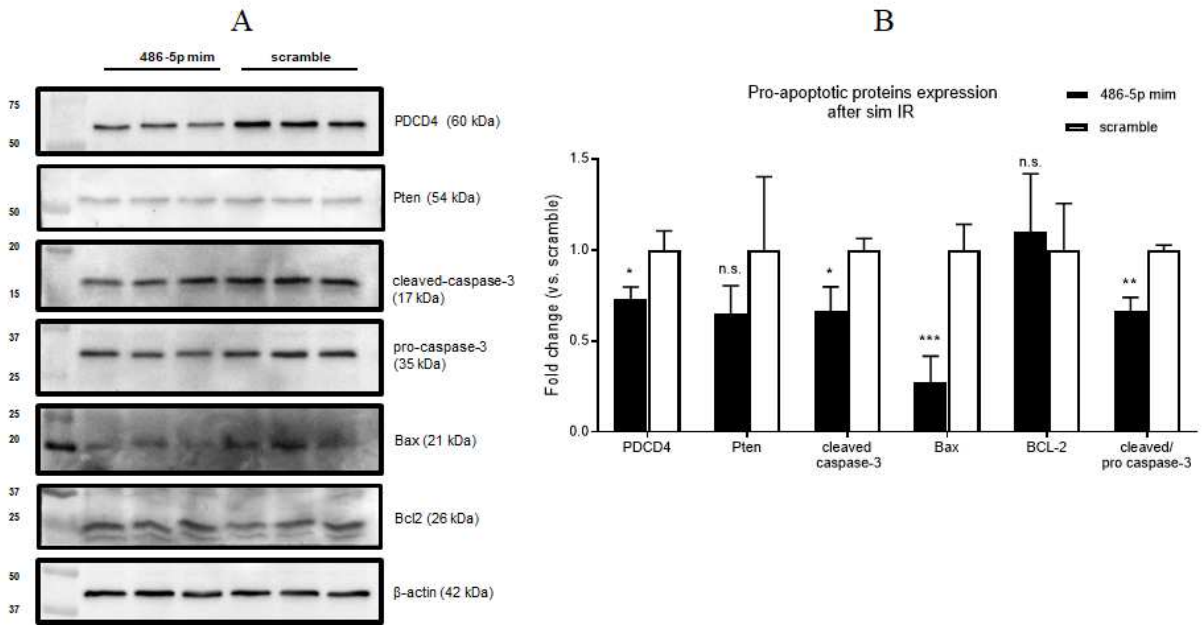

Figure 26. miR-486-5p Reduces Pro-apoptotic Protein Levels after sim I/R. 1 x 10^4 H9c2 cells were transfected with 50 nM miR-486-5p mimetic or non-targeting miRNA for 48 hours. Scrambled non-targeting miRNA was used as negative control (scramble). They were then subjected to sim I/R challenge. After sim I/R, cells were lysed for Western blot using RIPA buffer (**Methods**). (A) Levels of PDCD4, Pten, cleaved caspase-3, Bcl-2 and Bax via Western blot analysis. (B) Protein levels were normalized to that of β-actin. Results are represented as mean ± SD (N=3/group) and are analyzed using a two-tailed, unpaired t-test. n.s., non-significant *$P \leq 0.05$, **$P \leq 0.01$, ***$P \leq 0.001$ *vs*. scramble group. Sim I/R, simulated ischemia/reperfusion

miR-486-5p Mimetic Reduces Infarct Size *In vivo*

The potential effect of EV-enriched miR-486-5p in protection against I/R injury *in vivo* was examined in B6/129 mice. Mice were treated with miR-486-5p mimetic or scramble non-targeting miRNA control by pericardial sac injection of a mimic/lipid complex (**Methods**) and subjected to I/R injury (**Methods)** (**Fig. 29A**). There was a significant 28% reduction ($P \leq 0.05$) in infarct size as percentage of the area at risk in group treated with miR-486-5p mimic, compared to non-targeting scramble control (**Fig. 29B-C**). Taken together, both the *in vitro* and the *in vivo* data support the hypothesis that miR-486-5p is protective against ischemia reperfusion-induced injury.

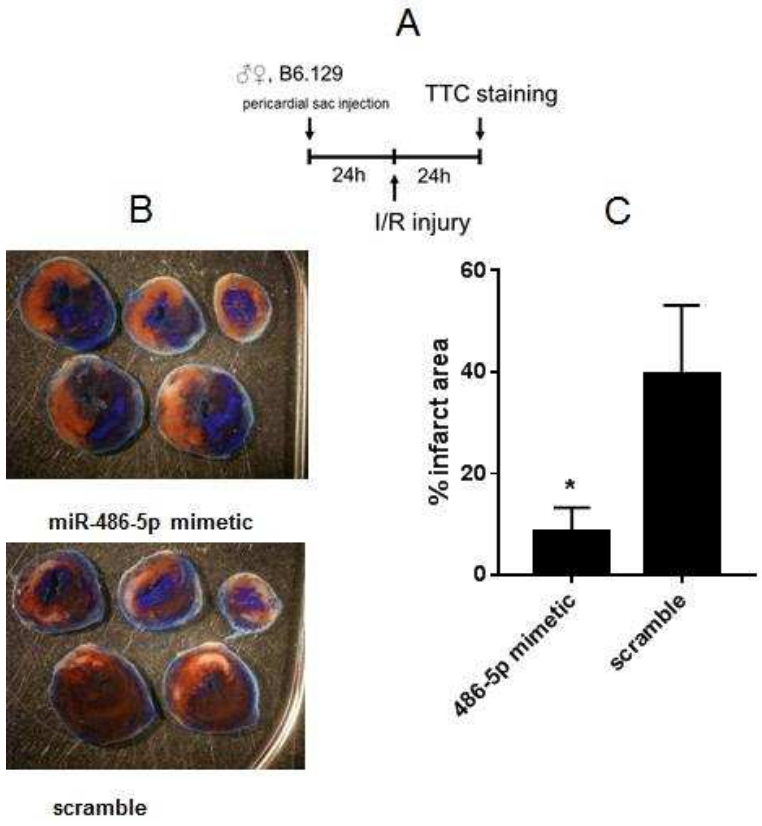

Figure 27. miR-486-5p Reduces Infarct Size in an *in vivo* Model of MI. (A) Timeline for *in vivo* experiment: 24 hours prior to I/R injury, mice were injected with either miR-486-5p mimic/lipid complex (**Methods**) or scrambled complex into the pericardial sac and were recovered overnight. Scrambled non-targeting miRNA was used as negative control (scramble). 24 hours after I/R injury, hearts were collected and stained with TTC, and sectioned for infarct size, and risk region measurements. (B) Representative images of phthalo blue dye and TTC-stained heart slices from the mice pre-treated with scrambled or miR-486-5p mimic after 45 min. ischemia and 24 hours reperfusion. Blue color is the area not at risk; red color is TTC staining indicating the areas at risk (red plus white); white color is the infarcted area. (C) Infarct sizes were measured as the average infarcted percent of the risk region (white/red), error bars represent SD (N=7/group). **P*=0.0175 vs. scrambled group (two-tailed, unpaired t-test). MI, myocardial infarction, I/R, ischemia/reperfusion, TTC, triphenyltetrazolium chloride.

Summary of the Findings

We have reported that MSC-derived exosomes protect cardiomyocytes from ischemia-reperfusion (I/R) induced myocardial injury both *in vitro* and *in vivo*[17]. We found that miRNA-486-5p (miR-486-5p) was highly and selectively expressed in MSC-derived exosomes. The role of miR-486-5p in cell survival is still debated and miR-486-5p has been reported to act as either a tumor suppressor or an oncogene[192,198,199]. We hypothesized that increased levels of miR-486-5p will protect cardiomyocytes from I/R injury. Simulated ischemia/reperfusion was performed on H9c2 cells treated with miR-486 mimic or scrambled control to measure the cytoprotective effect of miR-486-5p. H9c2 cells treated with the mimic of miR-486-5p showed a significant increase in cell survival by 35% and a reduction of 20% in LDH release compared to control cells treated with non-targeting scrambled miRNA.

We searched for miR-486-5p gene targets using miRanda and Targetscan and focused upon targets involving in the cell death and survival pathways. Program cell death 4 (PDCD4), a tumor suppressor and PTEN, which negatively regulates the PI3K/Akt survival pathway, were chosen for further study based upon considerations of scores for mRNA-miRNA interaction and the predicted targets. Luciferase reporter gene assays indicated that the 3'-UTRs of PDCD4 and PTEN are targeted by miR-486-5p. Immunoblotting results showed a 50% reduction in PDCD4 protein levels with the miR-486-5p mimic. Western blot results with cell lysates after sim I/R showed marked decreased levels of PDCD4, cleaved-Caspase 3 and Bax level in the group treated with miR-486-5p mimic compared to control cells. Pericardial sac injection of miR-486-5p mimic

before animals were subjected to ischemia (45 min) followed by overnight reperfusion significantly reduced infarct size by 28% ($P \leq 0.05$) compared to the scrambled treated group. These findings support that miR-486-5p upregulation is cardioprotective by targeting PDCD4 thereby reducing apoptosis.

CHAPTER IV

DISCUSSION

Cardiovascular diseases remain the leading cause of death in the USA and globally[1]. Several types of stem cells, including mesenchymal stem cells (MSC) have been studied for potential to repair injured myocardial tissue and improve cardiac function in MI[109]. Even though stem cells had low retention rate post-transplantation, small beneficial effects were observed, though these were unrelated to transdifferentiation and replacement of dead cells by stem cell derivatives[115; 116; 118; 202]. This observation inspired the paracrine hypothesis that MSCs mediate reparative effects through secreted factors including EVs[18; 202]. EVs derived from MSCs can recapitulate cardioprotective potential of their source cells with a less immunogenic capacity. Delivery of MSC-derived EVs protects against cardiac ischemia/reperfusion injury[18; 171], and the role of small non-coding miRNA in EVs cargoes has been implicated in the salvage process[17; 84; 203]. Previously, we demonstrated the cardioprotective effects of MSC-EVs in preconditioning against I/R injury by miR-21-5p[17]. However, depletion of miR-21-5p from MSC-EVs did not completely abrogate their cardioprotective effects, suggesting the potential involvement of other cardioprotective miRNAs in the EV cargo.

In this present study, we described the mechanism that regulates the sorting of miRNAs into MSC-derived EVs and studied the functional roles of secreted miRNA in the context of I/R injury. Our results indicated miR-486-5p is a particularly enriched nucleic

acid cargo that is selectively packaged into MSC EVs in comparison to producer MSCs. In this dissertation we sought to investigate whether RNA-binding proteins in the nuclear lysate of MSCs could interact with EVs-enriched miRNAs. We identified that hnRNPA2B1 is required for the efficient loading of miR-486-5p into MSC-derived EVs. Our findings also showed that miR-486-5p in turn has a significant positive impact on viability of cardiomyocytes after MI via inhibition of PDCD4 and apoptosis post-I/R injury.

RNA Binding Protein-mediated Loading of miRNAs into EVs

Consideration of miRNA as EV cargo is increasingly of interest. The packaging of these miRNAs into extracellular vesicles is still incompletely understood. Overexpression of miRNAs enriches its expression level in EVs. In some instances, this may occur by mass action and is not selective. This is how we envision miR-21-5p is loaded into EVs as it appears not to be selectively increased in EVs relative to producer cells, and knockout MSCs and EVs both lack the miR-21-5p[17]. There have been multiple studies that have uncovered several pathways for selective loading of specific miRs into EVs and these are cell-type and situation specific[78; 79; 94; 95; 96]. Specific miRNA regions have been proposed to contain short localization signals that facilitate miRNA cargo loading[53]. Alternatively, cargo active selection may occur via an AGO2 protein association with the RISC complex for specific miRNAs[77]. The YBX1[78] and La RNA binding proteins[79] have been reported to direct specific miRNA loading into EVs, and post transcriptional modification of certain miRNAs in the form of a 3'-end uridylation also facilitates miRNA loading[96]. Analysis of RNA Seq data from MSC and MSC-derived EVs demonstrated a series of eight miRs that were increased in EVs *vs.* parental MSC, and use of MEME software[188] suggested a specific sequence motif that

was present in this set of miRs (**Fig. 5**). This motif, ugAGuu, had a perfect conservation of the core AG element, and was not present in miRNAs that were not selectively sorted to EVs (**Fig. 5A**). Importantly, this potential miRNA motif was not in miRNAs that were not selectively sorted to MSC-derived EVs has not been previously described (**Fig. 5B**). Thus, based on background information and our data, we hypothesized that a specific RNA binding protein or proteins may be involved in the selective sorting of this set of miRs into MSC EVs. Besides miR-486-5p, we also found miR-122a and miR-451a were highly enriched in MSC-EVs (**Fig. 4**) and decided to choose them to study further the active sorting mechanism, because of their levels in MSC-derived EVs.

In order to identify potential RNA binding proteins for this motif, we performed mass spectrometry and western blot analyses and discovered the presence of several potential RNA binding proteins which have been shown to mediate the sorting/trafficking of miRNAs including hnRNPA2B1, hnRNPA1, and hnRNPQ (**Fig. 7**). We hypothesized that these RBP could be involved in the packaging of miRNAs into EVs. The goals of Aim 1 were to better understand the role of RNA-binding proteins in mediating EVs-enriched miRNAs, and determine the association of RNA-binding protein with specific EVs miRNAs. Identifying mechanisms for sorting miRNA into EVs will contribute to better understanding of miRNA loading events, and help to develop new strategies to engineer the miRNAs cargo of MSC-EVs.

We focused our investigation on hnRNPA2B1 to study the regulation of miRNAs packaging into MSC-EV due to its abundance in EVs among other RNA-binding proteins and its predicted strong binding of AG core sequences (**Figs. 6-7**). The hnRNPA2B1 protein is a

multi-functional RNA binding protein that participates in RNA processing and trafficking[204]. In the nucleus, hnRNPA2B1 is a component of core particles that bind to pre-miRNAs in the nucleus, while it facilitates the transport of some localized mRNAs in the cytoplasm[204]. Through its interaction with a 21-nucleotide RNA trafficking sequence, hnRNPA2B1 has been reported to be involved in cytoplasmic RNA transport to axons in neural cells[205; 206]. A recent study showed that hnRNPA2B1 binds to mRNA carried N6-methyladenosine (m6A) modification and mediates the processing of nuclear transcripts[207]. Crystallographic analysis revealed that hnRNPA2B1 has two RNA recognition motifs (RRM) -1, -2. Both RRMs specifically recognize AG core motifs[204]. Interestingly, Villarroya-Beltri *et al.* reported that hnRNPA2B1 interacts with miRNA harboring the EXO-motif GGAU (*e.g.*, miR-198, and miR-601) and controls their loading into EV secreted by lymphocytes[94]. In a recent study, hnRNPA2B1 was identified to be necessary for the sorting of miR-17/93 into microvesicles of lung epithelial cells[208]. The AGG and UAG motifs that are necessary for the interaction of RNA molecules with the RRM1 and RRM2 domains, were present in the hnRNPA2B1-associated miRNAs (miR-17, -20a, and -93)[208]. In addition, other studies suggested the role of hnRNPA2B1 in controlling the packaging of lncRNAs into EVs. In one study, the accumulation of lncRNA H19 within EVs was dependent on hnRNPA2B1, leading to resistance to tyrosine kinase inhibitor, gefitinib in non-small cell lung cancer (NSCLC)[209]. Overexpression of hnRNPA2B1 increased expression of exosomal lncRNA H19, whereas the opposite result was reported when hnRNPA2B1 was knocked down. The binding of lncRNA H19 to hnRNPA2B1 was reduced when the specific motif GGAG located at the 5'-end of this lncRNA was mutated[209]. Another

study supported the role of hnRNPA2B1 for sorting lncRNA LNMAT2 into EVs derived from bladder cancer cells, thus promoting lymphatic metastasis[210]. The author also reported the presence of the specific motif GGAG on the hnRNPA2B1 binding sites of lncRNA LNMAT2[210]. Additionally, hnRNPA2B1 was also annotated as cargo of EVs from many cell types in the exosome database Exocarta [211].

A loss-of-function approach with CRISPR-Cas9 genome editing was used to evaluate the function of hnRNPA2B1via a loss-of-function approach. We chose to target the second exon of the hnRNPA2B1since this exon is present in all splice variants, and thus would cause loss-of-function by premature stop codon. The gene ablated MSCs and their EV derivatives showed no expression of hnRNPA2B1 by Western blot while expression of other RBPs including hnRNPA1, hnRNPQ and proteins involved in miRNA biogenesis including Drosha and Dicer were not altered (**Fig. 8**). In addition, EV markers, and EV size and distribution were unaffected (**Fig. 9**). We next sought to evaluate the effects of hnRNPA2B1 ablation upon miRNA sorting into EVs.

First, we performed RNA Seq once again, this time comparing the profiles of EVs from Cas9 control and hnRNPA2B1 KO EVs. We observed that expression levels of vesicular miRNAs including miR-486-5p and other miRNAs identified as selectively sorted by the initial RNASeq data (miR-369-3p, miR-150-5p, miR-486b-5p, miR-486a-5p) (**Figs. 12 *vs.* 4**) were suppressed in EVs by the removal of hnRNPA2B1. There was also a non-significant trend towards a reduction in expression levels of miR-122a-5p, which was initially found to be increased in EVs (**Fig. 4**). We noted, for example, that silencing of hnRNPA2B1 prevented the transfer of miR-486-5p, one of the more highly expressed miRNAs in the

original EVs, from cell to EV, resulting in an accumulation of miR-486-5p in the cellular compartment of hnRNPA2B1 knock-out cells. We performed real-time RT-PCR on selected miRNAs to confirm the results of the Cas9 PA2B1 KO analysis (**Figs. 10 and 11**), and these results confirmed the hnRNPA2B1 dependency of EV loading for miR-122a, and miR-486a-5p (**Fig. 11**).

We next sought verification for binding of hnRNPA2B1 with specific miRNAs using a variety of biochemical assays. The predicted binding of miR-486-5p to hnRNPA2B1 was confirmed via electrophoretic gel-shift assay, RNA immunoprecipitation and UV cross-linked biotinylated RNA pull-down assay (**Figs. 13-17**). Additionally, we also identified a common sequence motif shared by EV-enriched miRNAs, ugAGuu motif, with the MEME Suite program. This new motif has the same AG core motif which exists in the EXOmotif GGAG[94; 204]. Although we have evaluated the effect of complete silencing of hnRNPA2B1 upon miRNA sorting into MSC-derived EV, we were unable to test the effects of overexpression of hnRNPA2B1 or the role of ugAGuu motif with mutational approaches (see Limitations and Future Directions). Of note, miR-122a-5p also exhibits GGAG motif which has been previously described sorting motif for hnRNPA2B1 in T-cells[94]. This GGAG motif was overlapped with the ugAGuu motif we found in some of the MSC-EV enriched miRNAs, notably, miR-122-5p (**Fig. 5**). We did not observed a clear statistically significant relationship between miR-122a-5p and hnRNPA2B1 in the context of MSC cells, indicating miRNA sorting may be cell type specific. It is also possible that other proteins bind overlapping sites, reducing the hnRNPA2B1 binding in the case of miR-122-5p. A future

study will focus on the biological effects of increased/decreased miR-486-5p export into EVs in overexpression or knockout hnRNPA2B1 experiments.

Given the essential role of RBPs in RNA trafficking and metabolism as well as recent reports on the mechanism of RNA loading into EVs[94; 95], understanding the RBPs involved in EV packaging of specific miRNAs would provide our first insights into the mechanism of this phenomenon. Our data demonstrated the key role of hnRNPA2B1 in mediating miRNA sorting of a limited set of specific MSC miRNAs into EVs. Further, EV cargo miRNAs are emerging as diagnostic and prognostic biomarkers for cardiovascular diseases. New insights into the regulation of miRNA sorting can help to understand circulating miRNA biomarkers and contribute to development of new therapies based on the transfer of EV-associated miRNAs.

Physiological Role of EV-enriched MicroRNAs

As part of a paracrine mechanism, vesicles secreted from bone marrow derived stem cells have been shown to decrease infarct size and slow progression of heart failure in models of cardiac ischemia/reperfusion injury. MSC-derived EVs have demonstrated the ability to ameliorate tissue injury via their miRNA and protein cargoes[18; 171; 172]. A recent study from our laboratory showed that miR-21-5p is a key factor behind the protective effect of MSC derived EVs against MI[17]. We observed a significant protection after injection of wild-type EV, compared to saline group[17]. Pre-treatment with miR-21-5p depleted EVs produced a small but non-significant reduction of infarct size, suggesting other EV cargo also contributed to the cardioprotection[17]. The goals of Aim 2 were to investigate the effect of miR-486-5p on *in vitro* and *in vivo* ischemia/reperfusion models and identify specific

targets of miR-486-5p that are involved in the cell death/cell survival pathways. Identification of specific function of miRNAs in EV cargo will facilitate the development of novel EV RNA therapies against I/R injury[164].

MSC-EV miRNA Cargo and Their Predicted Targets and Function

Our small RNA deep sequencing data and other published profiling studies[167; 212; 213] show the EV miRNA expression levels are different from their producer cells. We detected several miRNAs that have been implicated in I/R injury including miR-21-5p[17; 214; 215; 216], miR-22a-3p[84], let-7b-5p[217] (antiapoptotic), miR-126-3p[218] (pro-angiogenic), but their levels did not change in EVs compared to parent cells. We demonstrated that miR-486-5p is the top upregulated miRNA in MSC-derived EVs, relative to producer cells. This result has confirmed earlier findings showing miR-486-5p is the most abundant miRNA in human bone marrow and adipose tissue MSC-derived EVs[190].

Table 1. Top Candidate Cardioprotective EV-sorted miRNAs Identified by miRNA-Sequencing

miRNA	Read per million		Targets	Mechanisms
	Cells	EVs		
miR-486-5p	6.35	10715.18	Pten, Stau1, Dnajc21, Afl3, Pdzm3, Cadm1, Mark1, Atg2b, PDCD4	Cell death, Angiogenesis, Adhesion, Autophagy, MAPK regulation
miR-122a-5p	1.85	5308.91	GATA4, ANKRD13C, APLNR, TLR4, SIRT6, TGFβ, CTGF, FOXO3, HNRPU	Cell proliferation, Anti-fibrotic, Collagen, RNA binding, Transcription
miR-451a	1.39	1355.29	CUGBP2, Zpf207, Ccr4, NEK2, CISD1, Arr3, Zfpm2	Cell death, Mitosis, Metabolism, Mitochondria oxidation, G-protein signaling, GATA4 modulation
miR-150-5p	0.31	1114.54	CXCR4, Zpf711, CRP, c-Myb, Map3k3, Calcr, Eif5, Cbll1	Inflammation, PKA signaling, Cadherin regulation in apoptosis, Myoblast fusion/development

To select candidate miRNAs and their potential targets involved in cardioprotection, we performed miRNA-Seq analysis of MSC-derived EVs (N=3). Sequencing data demonstrated that many miRNAs are highly enriched in the EVs compared with their parent cells. Some miRNAs were exclusively expressed in the EVs but not in the cells (**Fig. 4 and Table 2**). EV-enriched miRNAs that target genes predicted to be injurious in I/R injury were revealed by two online algorithms MiRanda and Targetscan version 7.1 *in silico* analyses. This narrowed the focus to four miRNAs of interest, of which miR-486-5p is the most highly enriched followed by miR-122a-5p, miR-451a and miR-150a (**Table 2**). This result provided preliminary data for selection candidate miRNAs and their protein targets associated with cardioprotection.

Notably, miR-122a-5p has been shown to promote apoptosis, oxidative stress, inflammation, collagen and extracellular matrix deposition in cardiovascular diseases. The gene for miR-122a-5p was located within chromosome 18 in the mouse. In an hypoxia/reoxygenation model employing rat cardiomyocytes, increased expression of miR-122a-5p was associated with increased apoptosis and generation of ROS, whereas inhibition of miR-122a-5p with antagomir was cardioprotective through modulating its target GATA-4[219]. Inhibition of miR-122a-5p also alleviated lipid accumulation and reduced secretion of inflammatory cytokines through the TLR4/MyD99/NF-kBp65 axis[220]. Further, miR-122a-5p has been confirmed to target the important regulator of cardiac fibrosis and remodeling Sirtuin 6 (SIRT6), promoting autophagy and apoptosis in rat aortic adventitial fibroblasts[221]. The upregulation of miR-122a-5p was associated with the development of cardiac hypertrophy with Angiotensin II stimulation through attenuation of FOXO3 and

activation of calcineurin signaling pathway[222]. However, miR-122a-5p was reported to inhibit ischemic neuronal cell death through HSP-70 mediated NF-κB pathway by targeting FOXO3[223].

Previous studies have suggested the protective role of miR-451a in the heart. miR-451a works in a synergistic manner with miR-144, to which it is linked in a miRNA cluster, to confer protection against MI-induced cardiomyocyte death through targeting CUG triplet repeat-binding protein 2 (CUGBP2)-COX2 pathway[224]. Genetic deletion of miR-144/451a cluster impaired the efficacy of IPC-mediated cardioprotection on infarct size and functional recovery after I/R[225]. Rac-1, a downstream effector of CUGBP2-COX2, was targeted by miR-144/451a to contribute to IPC-elicited action[225]. In another study, upregulation of miR-451a was demonstrated to be cardioprotective in reduction of infarct size, release of creatine kinase, LDH and apoptotic index through inhibition of HMGB1, a non-histone nucleoprotein that can promote autophagy and inflammation[226]. Furthermore, miR-451a was down-regulated in heart tissue of hypertrophic cardiomyopathy patients[227]. Knockdown miR-451a increased the cell size, whereas overexpression of miR-451a reduced the cell surface area in neonatal rat cardiomyocytes via targeting tuberous sclerosis complex 1 (TSC1)[227].

Lastly, miR-150 is another miRNA that has been shown to underlie the progress of cardiac disease. Circulating levels of miR-150 were reported to be down-regulated in patients with LV-remodeling after first ST-segment-elevated acute MI event[228]. CRP and ADRB1, two genes associated with LV remodeling, were confirmed to be regulated by miR-150[228]. On the other hand, miR-150 deficient mice had impairment in cardiac function and

structure as well as increased in mortality after permanent ligation of LAD[229]. This effect appeared to be via direct suppression of egr2 and p2x7r, pro-apoptotic proteins[229]. In one study, ectopic expression of miR-150 significantly reduced infarct size, inhibited apoptosis and alleviated inflammation after acute MI[230]. The author reported that mechanistically miR-150 promoted monocyte migration by targeting chemokine receptor 4 (CXCR4)[230]. However, there was a report about the up-regulation of miR-150 in cardiomyocytes after H_2O_2 treatment and aggravated oxidative stress-induced injury by inhibiting c-Myb, whereas opposite effects were observed when miR-150 was silenced[231].

Overall, it seems the function of extracellular miRNAs is still a matter that requires further research in different cell types. The functional studies described above suggested that some EV derived-miRNAs such as miR-150a, miR-451a are protective and beneficial to target cells, whereas other miRNAs such as miR-122a are ineffective or injurious. Thus, we would hypothesize that modulation of EV-miRNA sorting will increase the loading into EVs of beneficial miRNA and apply them to clinical settings as well as interest to decrease the production and release of detrimental miRNAs in EVs.

Target Genes that Mediate miR-486-5p Function in Cardiomyocytes

The most highly enriched miRNA in MSC-EVs was miR-486-5p, 5853-fold higher in EVs than in cells (**Fig. 4**). After miR-486-5p levels in EVs were validated by qRT-PCR (**Fig. 19**), we chose miR-486-5p to determine whether this miRNA contributes to the cardioprotective effects of EVs. Recently, the link between miR-486-5p and MI has become more apparent. It was reported that miR-486-5p is positively regulated by hypoxia-inducible factor-1a (HIF-1a), a transcriptional regulator in cellular response to hypoxic

conditions[201]. Expression of miR-486-5p was reduced in H9c2 cells after hypoxia treatment[232; 233] or in H_2O_2-induced cardiomyocyte apoptosis[234]. Overexpression of miR-486-5p with lentiviral vector increased cell viability and decreased cell apoptosis by targeting Pten[233], NDRG2[232], or p53[234]. In the current study, we predicted PDCD4 and Pten as the most likely potential target genes of miR-486a-5p using bioinformatic analysis (**Fig. 20**). Results if luciferase assay using the 3'-UTRs of PDCD4 and Pten showed a dose-response relationship in reducing luciferase activities by miR-486-5p mimic (**Fig. 22**). Transfection with miR-486-5p mimetic into H9c2 cells significantly reduced both mRNA and protein level of PDCD4. Pten protein level did not change significantly after 48 hours though there was a reduction in its mRNA levels after 24 hours post-transfection. These results suggested PDCD4 is a definite target of miR-486-5p (**Fig. 23**). It is of note that our result is in contrast with previous studies, in which miR-486-5p was reported to suppress protein expression of Pten, and its downstream target, pAkt[194; 195; 233]. We did investigate PTEN, since it was the second most likely miR-486-5p target, and in fact found an effect upon PTEN mRNA levels of miR-486-5p treatment. However, we did not find effects upon protein levels of PTEN, or its target Akt, at least in the time frame we chose, which is relevant to cell death and survival in our models (**Fig. 23**). We observed a trend toward reduction of Pten in the group treated with miR-486-5p mimic after simulated I/R injury (**Fig. 27**). A post-hoc power analysis indicated that this decrease was significant if we had increased the sample size to approximately 8 per group. So it may be that the lack of significance in our study was due to sampling error. Another possible explanation for the difference between the studies is the longer half-lives for Pten (10 hours)[235] than PDCD4

(4 hours)[236] or the difference in method of overexpressing miR-486-5p. It may be that the link between miR-486-5p and protein expression of Pten is cell type-specific, or that we simply did not detect an effect that occurred at a slightly later time point. However, if the latter is true, we would question the relevance of this effect to cardioprotection in our model and our results support that PDCD4 is the more relevant target.

Some studies have suggested a regulatory loop between Pten, PDCD4, miR-21-5p/miR-486-5p. Downregulation of Pten by miR-21-5p and miR-486-5p enhance Akt activity[17; 195]. Akt can directly phosphorylate PDCD4, causing its inactivation and nuclear localization. The phosphorylation of PDCD4 by Akt reduces the ability of PDCD4 to suppress the activation of activator protein 1 (AP-1) in initiating protein synthesis[237] and to induce cyclin-dependent kinase inhibitor p21 in reducing cell proliferation[238]. Additional studies are needed to dissect the coordinated suppression of Pten and PDCD4 in the context of cardiomyocytes.

Because a single miRNA can target more than 1,000 target mRNAs, and each gene in turn can be regulated by many different miRNAs[239], the relationship between miR-486-5p and PDCD4 has not been investigated before. In this study, we aimed to explore whether miR-486-5p can induce cardioprotection against cell death-mediated by I/R injury by attenuating PDCD4. This is the first study demonstrating miR-486-5p negatively regulates the tumor suppressor PDCD4 at the post-transcriptional level via binding in the 3'-UTR of the mRNA. PDCD4 is a known tumor suppressor, regulating apoptosis via interaction with initiation factor eIF4A and eIF4G to suppress their translation[240]. Besides that, PDCD4 was reported to be upregulated in cellular senescence and apoptosis[241]. PDCD4 deregulation

has been found to be associated with several types of CVD. Myocardial expression of PDCD4 increases up to 24 hours after coronary microembolization induction in pig[242]. In coronary arteries of atherosclerotic rats, PDCD4 is up-regulated and contributes to the formation of coronary plaques and promotes inflammation[243]. Genetic knockdown of PDCD4 improves left ventricular function and reduces myocardial apoptosis in a type 2 diabetic rat[244]. Also atorvastatin therapy has been shown to reduce myocardial inflammation by inhibiting PDCD4 expression in CD4+ T lymphocytes of patients with unstable angina who received percutaneous coronary intervention[245]. Data from several studies suggest the protective effect of miRNAs in MI is through targeting PDCD4. For example, PDCD4 is a direct target of several miRNA including miR-21-5p[17; 215], and miR-499[246; 247] in cardiomyocytes resulting in inhibition of apoptosis-induced cardiomyocytes death in response to H_2O_2 stimulation or simulated I/R in cell culture. In this study, we also found miR-486-5p protected cardiomyocytes from ischemia reperfusion-induced apoptosis via targeting PDCD4.

Myocardial apoptosis is associated with cardiac dysfunction after MI[248]. The apoptotic process is mediated by the regulation of many genes, including Caspase-3 and members of the Bcl-2 family. Our *in vitro* data showed that pretreatment with miR-486-5p reduces cleaved caspase-3 and Bax expression after simulated I/R. This finding is consistent with previous studies which demonstrated PDCD4 signals through the caspase-3, Bax pathway[198; 199]. Furthermore, *in vivo* administration of miR-486-5p mimic via pericardial sac injection was protective against I/R injury *in vivo* (**Fig. 28**). These results suggest that miR-486-5p has cardioprotective effect and may act as anti-apoptotic miRNA via its functional target PDCD4. Given previous roles of miR-21-5p in other studies[17; 215]

and miR-486-5p in this study in alleviating cardiomyocyte cell death via suppressing PDCD4, we would propose that the common action at this target by MSC-EV associated miRNAs is a key part of the powerful cardioprotective effect of MSC-derived EVs.

Limitations and Future Directions

Recently, the interaction of RBPs and miRNA has been shown as an important sorting mechanism for vesicular miRNAs[77; 78; 79; 94; 95]. In this study we identified hnRNPA2B1 binds to miR-486-5p and facilitates the sorting of miR-486-5p in EVs. However, we may not have a clear picture on how many RBPs may form complexes with miR-486-5p and other EV-enriched miRNAs to shuttle them into EVs. For example, caveolin-1 was found to form a complex with hnRNPA2B1 to bind with miR17/93 [208], while microtubule-associated protein 1A/1B-light chain 3 (LC3) was reported as a interactor of hnRNPK to control the loading of EV cargo[249]. This could be due to their slight expression in EVs or their decent affinity to specific small non-coding RNA molecules. As a result, we may miss identifying all RBPs that are essential for the sorting of miRNAs into EVs. Future studies on the relationship of RBPs and mechanism of trafficking of miRNAs to secreted vesicles will involve quantitative measurement of protein localization, efficiency of RNA-protein interaction at intracellular and vesicular level. In addition, the role of secondary RNA structures in binding of miRNAs and RBPs is another important future direction. For instance, YBX1 was suggested to recognize miR-233 for sorting into HEK293T-derived EVs via recognition motif on secondary structure rather than primary RNA sequence. Taken together, these approaches will elucidate how the loading of miRNAs into EVs is modulated.

One of the limitations in our study is the physiologically relevant amount of miR-486-5p mimic used in experiments. To study the function of miR-486-5p in recipient cells, we transfected H9c2 cells with 50-100 nM of miRNA mimetics or scramble non-targeting miRNA, corresponding to 50-100 pmol or $3x10^{13}$- $6x10^{14}$ copies of miRNA in the medium. Transient transfection miR-486-5p mimics led to 400 fold increase in mature miR-486-5p levels (**Fig. 23A**) and 50% inhibition in protein level of PDCD4 (**Fig. 23D**). In a previous study, we observed a protective effect when cells were pre-treated with 300 μg proteins of WT-MSC-derived EVs[17]. The number of particles that corresponds to 1 μg EVs protein has been estimated at $2x10^{9}$- $2x10^{10}$ particles[250; 251] in the conditioned medium. If there was an average of 0.01 copy of miRNA of interest per particle based on previous stoichiometric studies[252; 253], a maximum of $6x10^{9}$ to $6x10^{10}$ copies of specific miRNA were present in the medium. Comparison of the miRNA mimics used for transfection and the miRNA content in the EVs showed a large difference in miRNA copy number in the order of 10^{4}- 10^{5}, indicating the superior transfer efficiency of EVs over conventional transfection reagents.

Another limitation is that no single RNA species can account for all the benefits of EVs. Administration of miR-486-5p alone might mask the protective effect of other miRNAs, as well as other RNA species and proteins found in EVs. This has been seen in the case of miR-146a, the most highly enriched miRNA in CDC-derived EVs relative to producer cells[19]. CDC-EVs containing miR-146a reduced apoptosis and enhanced angiogenesis *in vitro*, as well as improved cardiac functions and increased viable mass after MI *in vivo*. Level of miR-146a elevated in infarcted animals treated with CDC-derived EVs, suggesting the critical role of miR-146a in CDC-EVs' protective properties. However, administration of miR-146a

mimic alone did not reproduce all therapeutic effects of CDC and CDC-EVs. While miR-146a mimetic protected neonatal cardiomyocytes against oxidant stress, EVs deficient in miR-146a are still suppressed apoptosis, much as our miR-21-5p deficient EVs[17]. In a chronic model of MI, miR-146a mimic failed to decrease scar mass and improve global function, while increasing viable mass. From these studies and from our own, it seems that multiple miRNAs may be needed to confer comprehensive cardioprotective benefits of CDC-EVs. The author of the abovementioned work suggested that detailed analysis of active components within EVs is worthwhile, but intact particles may be required for therapeutic application[19]. Our small RNA sequencing data demonstrated the presence of other miRNAs that may work synergically with miR-21-5p and miR-486-5p. For example, miR-22 modulates the adaptive responses to cardiac stress via cardiac expression of SERCA and myofibrillar genes[254]. Likewise, miR-24 has been shown to be critical for cardiac fibrosis after MI by targeting furin, a protease which participates in the activation of TGF-β. Overexpression of miR-24 reduced formation of fibrosis in the infarct border zone in a model of MI[255].

On the other hand, we also detected the presence in EVs of miR-122a whose deleterious role in cardiomyocyte apoptosis has been reported in several studies. This observation suggests that EVs can serve as a carrier for unnecessary or even injurious cargo as well as beneficial cargo. This raises the question whether EV selectively sorted miRNAs work together or not. There could, if course, be other functions of miR-122a that outweigh the injurious aspects. It also could be that different EV subpopulations contain somewhat different populations of miRNAs; to date there are not good procedures for isolating homogenous EVs in the numbers needed for these types of experiments. New and

standardized methods for EV isolation and purification are needed. Perhaps affinity purification based on antibodies against EV surface markers such as CD9, CD81, TSG101, or Alix may reveal EV subpopulations carrying unique miRNA cargo and allow us to further refine our work.

In addition to identifying potential miRNA candidates controlling the cardioprotection, future studies of other non-coding RNA subtypes will be needed. In fact, miRNAs are a minority of exosomal RNA. For example, less than 7% of RNA in CDC-derived EV is miRNAs, but 18% were Y-RNA[256]. In one study, EV-derived Y-RNA fragment 1 (EV-YF1) was found to be anti-hypertrophic, and anti-fibrotic and to improve renal function in a model of cardiac hypertrophy and renal damage induced by Angiotensin II infusion[257]. The hypertrophy associated with Ang.II infusion was antagonized by EV-YF1 to the same extent that it was antagonized by EVs. The anti-fibrotic effect was also reproduced by YF1, and the renal function was improved by a reduction in proteinuria into similar degrees by YF1 as compared to the parent EVs. Additionally, long non-coding RNAs are another EVs cargo that needs to be studied further. Recently a study has demonstrated that EVs isolated from human MSC pretreated with macrophage migration inhibitory factor can horizontally transfer lncRNA nuclear assembly transcript 1 (NEAT1) to cardiomyocytes[142]. LncRNA-NEAT1 exerted cellular protection against H_2O_2-induced oxidative stress through suppression miR-142-3p, leading to activation of this miRNA downstream target, FOXO1 transcription factor, an important factor in cardiac metabolism and cell survival. Silencing lncRNA-NEAT1 or FOXO1, or over-expressing miR-142-3p blocked these antioxidant effects of EVs. In another study, EVs isolated from atorvastatin-pretreated MSC protected

cardiomyocytes from apoptosis induced by hypoxia and serum deprivation condition in vitro, and reduced infarct size and improved cardiac function in a rat acute MI model. In addition inflammation and expression of fibrosis genes were down-regulated while the angiogenesis was promoted in MI hearts. MSC-EVs derived lncRNA H19 was thought to functionally act through the activation of miR-675, VEGF and ICAM-1[258].

In this project, we focused on the sorting mechanism and function of miRNA in recipient cells. Ongoing projects in our laboratory are studying whether the internalization of EVs occurs through direct membrane fusion/receptor-mediated endocytosis and how EVs can be used in drug delivery. With the explosion of RNA-based therapeutics that we are seeing, including mRNA vaccines against Covid-19, this is one of the most exciting opportunities that biotechnology has seen in a long time.

Clinical Significance

Coronary heart diseases, including myocardial infarction, are the leading cause of all cardiovascular diseases in both industrialized and developing countries. As a result, novel cardioprotective therapies are desperately needed to prevent the detrimental adverse effects of ischemia/reperfusion injury, thus attenuating adverse left-ventricle remodeling, reducing heart failure and mortality in patients after acute MI. However, many cardioprotective interventions for reducing infarct size in the laboratory settings failed or yielded neutral results in the clinical settings. Stem cell transplantation has been an attractive promising therapy for CVD. Several types of adult stem cells, including mesenchymal stem cells, have been studied both pre-clinically and clinically for their potential to repair injured myocardium, and improve cardiac function as well as patient

outcome in MI. However, poor cell engraftment and the lack of transdifferentiation potential of stem cells to cardiomyocytes have inspired the paracrine hypothesis that stem cells have beneficial effects on the infarcted heart through secreted factors including extracellular vesicles (exosomes and microvesicles). EVs are potential players in interaction between different cell types and in inter-organ communication. Accordingly, stem cell-free therapies offer an alternative to such cardioprotective strategies. There are several advantages of using EVs instead of stem cells in MI. First, EVs can recapitulate beneficial properties of their source cells while being more physiologically stable than cells in terms of viability. Second, EVs are associated with low immunogenicity, therefore they are not cleared from the blood by the immune system. Third, EVs can deliver bioactive molecules including mRNA, non-coding RNAs, and proteins to recipient cells, and this cargo can be modified by manipulating parent cells or by external means such as electroporation or transfection. All of these features show promise for their application of EVs over conventional cell-based approaches for myocardial salvage and repair.

We believe EVs hold great potential as the next generation of therapeutic candidates and could have a large impact in clinical settings. The toxicity, biodistribution, half-life, and dose estimation should be assessed in EV-mediated cardioprotection experiments to determine the safety and procedures for EV delivery, dosing, and elimination. Future studies should also investigate how long the beneficial effects of EVs might last for and what factors are required to maintain these effects in the long term as well as multiple dosing study. Furthermore, EVs could be used in combination with other cardioprotective agents directed to different unrelated targets for complementary effects. This multi-

targeted approach directed to different signaling pathways can be more effective in cardioprotection.

Conclusions

In summary, the results represented here demonstrate that a selective group of miRNAs are actively loaded into MSC-EVs and are cardioprotective. We found MSC-derived EVs exhibit a distinctive miRNA profile, relative to parental cells, which might implicate their biological function and therapeutic applications. We were able to identify miR-486-5p as the most highly enriched in MSC-derived EVs and its sorting mechanism can be explained by the interaction with RNA binding protein, hnRNPA2B1. The protective features of miR-486-5p are mediated, at least in part through modulation of cardiomyocyte apoptosis via PDCD4, in ischemia/reperfusion injury.

We provided evidence that EV enrichment of miR-486-5p and other miRNAs that share a common sequence motif ugAGuu required hnRNPA2B1. The role of hnRNPA2B1 for miRNA loading into EVs was confirmed by loss-of-function experiments. In the group of MSC-EV-enriched miRNAs, miR-486-5p was the miRNA whose sorting was most significantly modulated by hnRNPA2B1. We demonstrated interaction between miR-486-5p and hnRNPA2B1 through several different in vitro binding assays, including electrophoretic mobility shift assay, RNA immunoprecipitation and reciprocal biotinylated RNA pull-down. The data demonstrate an important role of hnRNPA2B1 in the secretion of miRNA in EVs derived from MSC cells. Understanding the machinery involved in EV loading of miRNAs will provide targets for manipulating miRNA cargo of MSC-EVs.

On the functional role of secreted miRNA in the MSC-EV cargo, several of the miRNAs loaded into EVs share potential targets that may play roles in cell survival, anti-apoptosis, and angiogenesis. We focused upon miR-486-5p and were able to predict the biological targets using bioinformatic analysis. Luciferase assay showed that miR-486-5p targets 3'-UTR of PDCD4 and represses mRNA and protein expression *in vitro*. We did not find evidence of cell toxicity of miR-486-5p in normoxic conditions. Pretreatment of miR-486-5p mimetics increased H9c2 viability, and reduced the release of LDH as well as the number of apoptotic cells after sim I/R. Meanwhile, the cardioprotective effects of miR-486-5p were further confirmed *in vivo* by demonstrating infarct size reduction in an animal model of MI after I/R injury. We validated the role of signaling pathway PDCD4/caspase-3/Bax in the cytoprotective properties of miR-486-5p action. Collectively, the data indicated that miR-486-5p regulates cell survival after I/R injury through suppressing tumor suppressor PDCD4. Our laboratory previously demonstrated that miR-21-5p also reduced apoptosis primarily through PDCD4 repression. Thus, the miR-486-5p:PDCD4 axis may be a critical regulatory axis for apoptosis that is additively repressed by cooperative action of several miRNAs from MSC-EVs, producing strong protection against cardiac I/R injury.

Future studies in our laboratory will continue to identify and validate other factors including RNA-binding proteins, specific sequence motifs or post-transcriptional modifications that mediate the loading of miRNAs into MSC-EVs as well as investigate functions of other EVs-enriched miRNAs whose expression levels were significant reduced in hnRNPA2B1 knock-out experiment including miR-150 and miR-369. In humans, more

than 1500 proteins have been predicted and experimentally determined to modulate RNA metabolism through binding and processing RNA or being essential part of the ribonucleoprotein complex[259]. Thus we speculate that the binding preference of RNA binding proteins to miRNAs is cell type specific, depending upon which miRNAs and proteins are present in a specific cellular compartment. In addition, some cell types may use multiple RNA-binding proteins to load RNAs into EVs. Furthermore, we will continue mining of EV contents beyond miRNAs to identify defined factors that mediate beneficial and injurious effects of MSC-derived EVs. Finally, we can combine understanding of sorting mechanisms, function of RNA species with uptake mechanisms for potential recipient cells from other ongoing projects in our laboratory to create a comprehensive profile of MSC-derived EV cargos by function. We predict that new insight into small vesicles released from MSC and their cargoes may regulate protection of the heart following myocardial infarction will lead to new cell-free therapies that can improve long-term patient outcomes.

MSC-EVs mediated cardioprotection is highly translational as MSC-EVs can recapitulate the benefits of MSC therapies while possessing emergent properties such as extended shelf-life, less immunogenicity, and readily manipulable post-production. Initially regarded as means to dispose of cellular waste, EVs are now considered as potential therapeutic and diagnostic markers. It is my hope that data from this dissertation will help establish a rationale and new targets for the development of EV therapies engineered to maximize therapeutic effects, minimize adverse effects and improve patient outcome in the cardiovascular diseases area and beyond.

REFERENCE LIST

1. Virani, S. S., Alonso, A., Aparicio, H. J., Benjamin, E. J., Bittencourt, M. S., Callaway, C. W., . . . null, n. (2021). Heart Disease and Stroke Statistics—2021 Update. *Circulation, 143*(8), e254-e743. doi:10.1161/CIR.0000000000000950

2. Yeh, R. W., Sidney, S., Chandra, M., Sorel, M., Selby, J. V., & Go, A. S. (2010). Population Trends in the Incidence and Outcomes of Acute Myocardial Infarction. *New England Journal of Medicine, 362*(23), 2155-2165. doi:10.1056/NEJMoa0908610

3. Sulo, G., Igland, J., Vollset, S. E., Nygård, O., Ebbing, M., Sulo, E., . . . Tell, G. S. (2016). Heart Failure Complicating Acute Myocardial Infarction; Burden and Timing of Occurrence: A Nation-wide Analysis Including 86 771 Patients From the Cardiovascular Disease in Norway (CVDNOR) Project. *Journal of the American Heart Association, 5*(1), e002667. doi:10.1161/JAHA.115.002667

4. Turer, A. T., & Hill, J. A. (2010). Pathogenesis of Myocardial Ischemia-Reperfusion Injury and Rationale for Therapy. *The American journal of cardiology, 106*(3), 360-368. doi:10.1016/j.amjcard.2010.03.032

5. Epstein, A. M., Jha, A. K., & Orav, E. J. (2011). The Relationship between Hospital Admission Rates and Rehospitalizations. *New England Journal of Medicine, 365*(24), 2287-2295. doi:10.1056/NEJMsa1101942

6. Kloner, R. A., Hale, S. L., Dai, W., & Shi, J. (2017). Cardioprotection: Where to from here? *Cardiovascular Drugs and Therapy, 31*(1), 53-61. doi:10.1007/s10557-016-6691-0

7. Hausenloy, D. J., Garcia-Dorado, D., Bøtker, H. E., Davidson, S. M., Downey, J., Engel, F. B., . . . Ferdinandy, P. (2017). Novel targets and future strategies for acute cardioprotection: Position Paper of the European Society of Cardiology Working Group on Cellular Biology of the Heart. *Cardiovascular research, 113*(6), 564-585. doi:10.1093/cvr/cvx049

8. Murry Charles, E., Reinecke, H., & Pabon Lil, M. (2006). Regeneration Gaps. *Journal of the American College of Cardiology, 47*(9), 1777-1785. doi:10.1016/j.jacc.2006.02.002

9. Roger, V. L. (2013). Epidemiology of heart failure. *Circulation Research, 113*(6), 646-659. doi:10.1161/CIRCRESAHA.113.300268

10. Heusch, G., Libby, P., Gersh, B., Yellon, D., Böhm, M., Lopaschuk, G., & Opie, L. (2014). Cardiovascular remodelling in coronary artery disease and heart failure. *The Lancet, 383*(9932), 1933-1943. doi:https://doi.org/10.1016/S0140-6736(14)60107-0

11. Sobel, B. E., Bresnahan, G. F., Shell, W. E., & Yoder, R. D. (1972). Estimation of Infarct Size in Man and its Relation to Prognosis. *Circulation, 46*(4), 640-648. doi:10.1161/01.CIR.46.4.640

12. Bolli, R., Becker, L., Gross, G., Mentzer, R., Balshaw, D., & Lathrop, D. A. (2004). Myocardial Protection at a Crossroads. *Circulation Research, 95*(2), 125-134. doi:10.1161/01.RES.0000137171.97172.d7

13. Heusch, G. (2015). Molecular Basis of Cardioprotection. *Circulation Research, 116*(4), 674-699. doi:10.1161/CIRCRESAHA.116.305348

14. Giustino, G., & Dangas, G. D. (2017). Ischemia-reperfusion injury and ischemic post-conditioning in acute myocardial infarction: Lost in translation. *Catheterization and Cardiovascular Interventions, 90*(7), 1068-1069. doi:https://doi.org/10.1002/ccd.27436

15. Kloner, R. A. (2013). Current State of Clinical Translation of Cardioprotective Agents for Acute Myocardial Infarction. *Circulation Research, 113*(4), 451-463. doi:10.1161/CIRCRESAHA.112.300627

16. Miura, T., & Miki, T. (2008). Limitation of myocardial infarct size in the clinical setting: current status and challenges in translating animal experiments into clinical therapy. *Basic Research in Cardiology, 103*(6), 501-513. doi:10.1007/s00395-008-0743-y

17. Luther, K. M., Haar, L., McGuinness, M., Wang, Y., Lynch, T., Phan, A., . . . Keith Jones, W. (2018). Exosomal miR-21a-5p mediates cardioprotection by mesenchymal stem cells. *Journal of Molecular and Cellular Cardiology*. doi:10.1016/j.yjmcc.2018.04.012

18. Lai, R. C., Arslan, F., Lee, M. M., Sze, N. S. K., Choo, A., Chen, T. S., . . . Lim, S. K. (2010). Exosome secreted by MSC reduces myocardial ischemia/reperfusion injury. *Stem Cell Research, 4*(3), 214-222. doi:https://doi.org/10.1016/j.scr.2009.12.003

19. Ibrahim, A. G.-E., Cheng, K., & Marbán, E. (2014). Exosomes as critical agents of cardiac regeneration triggered by cell therapy. *Stem cell reports, 2*(5), 606-619. doi:10.1016/j.stemcr.2014.04.006

20. Théry, C., Witwer, K. W., Aikawa, E., Alcaraz, M. J., Anderson, J. D., Andriantsitohaina, R., . . . Zuba-Surma, E. K. (2018). Minimal information for studies of extracellular vesicles 2018 (MISEV2018): a position statement of the International Society for Extracellular Vesicles and update of the MISEV2014 guidelines. *Journal of Extracellular Vesicles, 7*(1), 1535750. doi:10.1080/20013078.2018.1535750

21. Colombo, M., Raposo, G., & Théry, C. (2014). Biogenesis, Secretion, and Intercellular Interactions of Exosomes and Other Extracellular Vesicles. *Annual Review of Cell and Developmental Biology, 30*(1), 255-289. doi:10.1146/annurev-cellbio-101512-122326

22. Gould, S. J., & Raposo, G. (2013). As we wait: coping with an imperfect nomenclature for extracellular vesicles. *Journal of Extracellular Vesicles, 2*(1), 20389. doi:10.3402/jev.v2i0.20389

23. Harding, C., Heuser, J., & Stahl, P. (1983). Receptor-mediated endocytosis of transferrin and recycling of the transferrin receptor in rat reticulocytes. *The Journal of cell biology, 97*(2), 329-339. doi:10.1083/jcb.97.2.329

24. Wang, B., Xing, D., Zhu, Y., Dong, S., & Zhao, B. (2019). The State of Exosomes Research: A Global Visualized Analysis. *BioMed Research International, 2019*, 1495130. doi:10.1155/2019/1495130

25. Zitvogel, L., Regnault, A., Lozier, A., Wolfers, J., Flament, C., Tenza, D., . . . Amigorena, S. (1998). Eradication of established murine tumors using a novel cell-free vaccine: dendritic cell derived exosomes. *Nature Medicine, 4*(5), 594-600. doi:10.1038/nm0598-594

26. Isola, A. L., & Chen, S. (2017). Exosomes: The Messengers of Health and Disease. *Current neuropharmacology, 15*(1), 157-165. doi:10.2174/1570159x14666160825160421

27. Kim, M. S., Haney, M. J., Zhao, Y., Mahajan, V., Deygen, I., Klyachko, N. L., . . . Batrakova, E. V. (2016). Development of exosome-encapsulated paclitaxel to overcome MDR in cancer cells. *Nanomedicine : nanotechnology, biology, and medicine, 12*(3), 655-664. doi:10.1016/j.nano.2015.10.012

28. Booth, A. M., Fang, Y., Fallon, J. K., Yang, J.-M., Hildreth, J. E. K., & Gould, S. J. (2006). Exosomes and HIV Gag bud from endosome-like domains of the T cell plasma membrane. *Journal of Cell Biology, 172*(6), 923-935. doi:10.1083/jcb.200508014

29. Colombo, M., Moita, C., van Niel, G., Kowal, J., Vigneron, J., Benaroch, P., . . . Raposo, G. (2013). Analysis of ESCRT functions in exosome biogenesis, composition and secretion highlights the heterogeneity of extracellular vesicles. *Journal of Cell Science, 126*(24), 5553-5565. doi:10.1242/jcs.128868

30. Wollert, T., & Hurley, J. H. (2010). Molecular mechanism of multivesicular body biogenesis by ESCRT complexes. *Nature, 464*(7290), 864-869. doi:10.1038/nature08849

31. Guo, B. B., Bellingham, S. A., & Hill, A. F. (2015). The neutral sphingomyelinase pathway regulates packaging of the prion protein into exosomes. *The Journal of biological chemistry, 290*(6), 3455-3467. doi:10.1074/jbc.M114.605253

32. van Niel, G., D'Angelo, G., & Raposo, G. (2018). Shedding light on the cell biology of extracellular vesicles. *Nature Reviews Molecular Cell Biology, 19*(4), 213-228. doi:10.1038/nrm.2017.125

33. Ostrowski, M., Carmo, N. B., Krumeich, S., Fanget, I., Raposo, G., Savina, A., . . . Thery, C. (2010). Rab27a and Rab27b control different steps of the exosome secretion pathway. *Nature Cell Biology, 12*(1), 19-30. doi:10.1038/ncb2000

34. Fader, C. M., Sánchez, D. G., Mestre, M. B., & Colombo, M. I. (2009). TI-VAMP/VAMP7 and VAMP3/cellubrevin: two v-SNARE proteins involved in specific steps of the autophagy/multivesicular body pathways. *Biochimica et Biophysica Acta (BBA) - Molecular Cell Research, 1793*(12), 1901-1916. doi:https://doi.org/10.1016/j.bbamcr.2009.09.011

35. Savina, A., Furlán, M., Vidal, M., & Colombo, M. I. (2003). Exosome Release Is Regulated by a Calcium-dependent Mechanism in K562 Cells*. *Journal of Biological Chemistry, 278*(22), 20083-20090. doi:https://doi.org/10.1074/jbc.M301642200

36. Morelli, A. E., Larregina, A. T., Shufesky, W. J., Sullivan, M. L. G., Stolz, D. B., Papworth, G. D., . . . Thomson, A. W. (2004). Endocytosis, intracellular sorting, and processing of exosomes by dendritic cells. *Blood, 104*(10), 3257-3266. doi:https://doi.org/10.1182/blood-2004-03-0824

37. Andreu, Z., & Yáñez-Mó, M. (2014). Tetraspanins in extracellular vesicle formation and function. *Frontiers in immunology, 5*, 442-442. doi:10.3389/fimmu.2014.00442

38. Raposo, G., Nijman, H. W., Stoorvogel, W., Liejendekker, R., Harding, C. V., Melief, C. J., & Geuze, H. J. (1996). B lymphocytes secrete antigen-presenting vesicles. *The Journal of experimental medicine, 183*(3), 1161-1172. doi:10.1084/jem.183.3.1161

39. Denzer, K., van Eijk, M., Kleijmeer, M. J., Jakobson, E., de Groot, C., & J. Geuze, H. (2000). Follicular Dendritic Cells Carry MHC Class II-Expressing Microvesicles at Their Surface. *The Journal of Immunology, 165*(3), 1259. doi:10.4049/jimmunol.165.3.1259

40. Mulcahy, L. A., Pink, R. C., & Carter, D. R. F. (2014). Routes and mechanisms of extracellular vesicle uptake. *Journal of Extracellular Vesicles, 3*(1), 24641. doi:10.3402/jev.v3.24641

41. Bissig, C., & Gruenberg, J. (2014). ALIX and the multivesicular endosome: ALIX in Wonderland. *Trends in Cell Biology, 24*(1), 19-25. doi:https://doi.org/10.1016/j.tcb.2013.10.009

42. Jahn, R., & Südhof, T. C. (1999). Membrane Fusion and Exocytosis. *Annual Review of Biochemistry, 68*(1), 863-911. doi:10.1146/annurev.biochem.68.1.863

43. Parolini, I., Federici, C., Raggi, C., Lugini, L., Palleschi, S., De Milito, A., . . . Fais, S. (2009). Microenvironmental pH Is a Key Factor for Exosome Traffic in Tumor Cells*. *Journal of Biological Chemistry, 284*(49), 34211-34222. doi:https://doi.org/10.1074/jbc.M109.041152

44. Vargas, A., Zhou, S., Éthier-Chiasson, M., Flipo, D., Lafond, J., Gilbert, C., & Barbeau, B. (2014). Syncytin proteins incorporated in placenta exosomes are important for cell uptake

and show variation in abundance in serum exosomes from patients with preeclampsia. *The FASEB Journal, 28*(8), 3703-3719. doi:https://doi.org/10.1096/fj.13-239053

45. Mathivanan, S., Fahner, C. J., Reid, G. E., & Simpson, R. J. (2012). ExoCarta 2012: database of exosomal proteins, RNA and lipids. *Nucleic Acids Research, 40*(D1), D1241-D1244. doi:10.1093/nar/gkr828

46. Simons, M., & Raposo, G. (2009). Exosomes – vesicular carriers for intercellular communication. *Current Opinion in Cell Biology, 21*(4), 575-581. doi:https://doi.org/10.1016/j.ceb.2009.03.007

47. Choi, D.-S., Kim, D.-K., Kim, Y.-K., & Gho, Y. S. (2015). Proteomics of extracellular vesicles: Exosomes and ectosomes. *Mass Spectrometry Reviews, 34*(4), 474-490. doi:https://doi.org/10.1002/mas.21420

48. Zhang, Y., Meng, J., Zhang, L., Ramkrishnan, S., & Roy, S. (2019). Extracellular Vesicles with Exosome-like Features Transfer TLRs between Dendritic Cells. *ImmunoHorizons, 3*(6), 186. doi:10.4049/immunohorizons.1900016

49. Smalheiser, N. R. (2007). Exosomal transfer of proteins and RNAs at synapses in the nervous system. *Biology direct, 2*, 35-35. doi:10.1186/1745-6150-2-35

50. Subra, C., Grand, D., Laulagnier, K., Stella, A., Lambeau, G., Paillasse, M., . . . Record, M. (2010). Exosomes account for vesicle-mediated transcellular transport of activatable phospholipases and prostaglandins. *Journal of lipid research, 51*(8), 2105-2120. doi:10.1194/jlr.M003657

51. Tan, N.-S., Shaw, N. S., Vinckenbosch, N., Liu, P., Yasmin, R., Desvergne, B., . . . Noy, N. (2002). Selective Cooperation between Fatty Acid Binding Proteins and Peroxisome Proliferator-Activated Receptors in Regulating Transcription. *Molecular and Cellular Biology, 22*(14), 5114. doi:10.1128/MCB.22.14.5114-5127.2002

52. Zakharova, L., Svetlova, M., & Fomina, A. F. (2007). T cell exosomes induce cholesterol accumulation in human monocytes via phosphatidylserine receptor. *Journal of Cellular Physiology, 212*(1), 174-181. doi:https://doi.org/10.1002/jcp.21013

53. Valadi, H., Ekström, K., Bossios, A., Sjöstrand, M., Lee, J. J., & Lötvall, J. O. (2007). Exosome-mediated transfer of mRNAs and microRNAs is a novel mechanism of genetic exchange between cells. *Nature Cell Biology, 9*(6), 654-659. doi:10.1038/ncb1596

54. Huang, X., Yuan, T., Tschannen, M., Sun, Z., Jacob, H., Du, M., . . . Wang, L. (2013). Characterization of human plasma-derived exosomal RNAs by deep sequencing. *BMC Genomics, 14*(1), 319. doi:10.1186/1471-2164-14-319

55. van Balkom, B. W. M., Eisele, A. S., Pegtel, D. M., Bervoets, S., & Verhaar, M. C. (2015). Quantitative and qualitative analysis of small RNAs in human endothelial cells and

exosomes provides insights into localized RNA processing, degradation and sorting. *Journal of Extracellular Vesicles, 4*(1), 26760. doi:10.3402/jev.v4.26760

56. Skog, J., Würdinger, T., van Rijn, S., Meijer, D. H., Gainche, L., Curry, W. T., . . . Breakefield, X. O. (2008). Glioblastoma microvesicles transport RNA and proteins that promote tumour growth and provide diagnostic biomarkers. *Nature Cell Biology, 10*(12), 1470-1476. doi:10.1038/ncb1800

57. Lai, C. P., Kim, E. Y., Badr, C. E., Weissleder, R., Mempel, T. R., Tannous, B. A., & Breakefield, X. O. (2015). Visualization and tracking of tumour extracellular vesicle delivery and RNA translation using multiplexed reporters. *Nature Communications, 6*(1), 7029. doi:10.1038/ncomms8029

58. Ridder, K., Keller, S., Dams, M., Rupp, A.-K., Schlaudraff, J., Del Turco, D., . . . Momma, S. (2014). Extracellular Vesicle-Mediated Transfer of Genetic Information between the Hematopoietic System and the Brain in Response to Inflammation. *PLOS Biology, 12*(6), e1001874. doi:10.1371/journal.pbio.1001874

59. Maugeri, M., Nawaz, M., Papadimitriou, A., Angerfors, A., Camponeschi, A., Na, M., . . . Valadi, H. (2019). Linkage between endosomal escape of LNP-mRNA and loading into EVs for transport to other cells. *Nature Communications, 10*(1), 4333. doi:10.1038/s41467-019-12275-6

60. Usman, W. M., Pham, T. C., Kwok, Y. Y., Vu, L. T., Ma, V., Peng, B., . . . Le, M. T. N. (2018). Efficient RNA drug delivery using red blood cell extracellular vesicles. *Nature Communications, 9*(1), 2359. doi:10.1038/s41467-018-04791-8

61. Kogure, T., Yan, I. K., Lin, W.-L., & Patel, T. (2013). Extracellular Vesicle-Mediated Transfer of a Novel Long Noncoding RNA TUC339: A Mechanism of Intercellular Signaling in Human Hepatocellular Cancer. *Genes & cancer, 4*(7-8), 261-272. doi:10.1177/1947601913499020

62. Conigliaro, A., Costa, V., Lo Dico, A., Saieva, L., Buccheri, S., Dieli, F., . . . Alessandro, R. (2015). CD90+ liver cancer cells modulate endothelial cell phenotype through the release of exosomes containing H19 lncRNA. *Molecular Cancer, 14*(1), 155. doi:10.1186/s12943-015-0426-x

63. Qu, L., Ding, J., Chen, C., Wu, Z.-J., Liu, B., Gao, Y., . . . Wang, L.-H. (2016). Exosome-Transmitted lncARSR Promotes Sunitinib Resistance in Renal Cancer by Acting as a Competing Endogenous RNA. *Cancer Cell, 29*(5), 653-668. doi:https://doi.org/10.1016/j.ccell.2016.03.004

64. Liu, T., Zhang, X., Gao, S., Jing, F., Yang, Y., Du, L., . . . Wang, C. (2016). Exosomal long noncoding RNA CRNDE-h as a novel serum-based biomarker for diagnosis and prognosis of colorectal cancer. *Oncotarget; Vol 7, No 51*.

65. Dai, X., Chen, C., Yang, Q., Xue, J., Chen, X., Sun, B., . . . Liu, Q. (2018). Exosomal circRNA_100284 from arsenite-transformed cells, via microRNA-217 regulation of EZH2, is involved in the malignant transformation of human hepatic cells by accelerating the cell cycle and promoting cell proliferation. *Cell Death & Disease, 9*(5), 454. doi:10.1038/s41419-018-0485-1

66. Li, Y., Zheng, Q., Bao, C., Li, S., Guo, W., Zhao, J., . . . Huang, S. (2015). Circular RNA is enriched and stable in exosomes: a promising biomarker for cancer diagnosis. *Cell research, 25*(8), 981-984. doi:10.1038/cr.2015.82

67. Ambros, V. (2001). microRNAs: tiny regulators with great potential. *Cell, 107*(7), 823-826. doi:10.1016/S0092-8674(01)00616-X

68. Lee, R. C., Feinbaum, R. L., & Ambros, V. (1993). The C. elegans heterochronic gene lin-4 encodes small RNAs with antisense complementarity to lin-14. *Cell, 75*(5), 843-854. doi:10.1016/0092-8674(93)90529-Y

69. Lewis, B. P., Burge, C. B., & Bartel, D. P. (2005). Conserved Seed Pairing, Often Flanked by Adenosines, Indicates that Thousands of Human Genes are MicroRNA Targets. *Cell, 120*(1), 15-20. doi:https://doi.org/10.1016/j.cell.2004.12.035

70. Bartel, D. P. (2009). MicroRNAs: target recognition and regulatory functions. *Cell, 136*(2), 215-233. doi:10.1016/j.cell.2009.01.002

71. Maragkakis, M., Alexiou, P., Papadopoulos, G. L., Reczko, M., Dalamagas, T., Giannopoulos, G., . . . Hatzigeorgiou, A. G. (2009). Accurate microRNA target prediction correlates with protein repression levels. *BMC Bioinformatics, 10*(1), 295. doi:10.1186/1471-2105-10-295

72. Chong, J. J. H., Yang, X., Don, C. W., Minami, E., Liu, Y.-W., Weyers, J. J., . . . Murry, C. E. (2014). Human embryonic-stem-cell-derived cardiomyocytes regenerate non-human primate hearts. *Nature, 510*(7504), 273-277. doi:10.1038/nature13233

73. Morel, L., Regan, M., Higashimori, H., Ng, S. K., Esau, C., Vidensky, S., . . . Yang, Y. (2013). Neuronal Exosomal miRNA-dependent Translational Regulation of Astroglial Glutamate Transporter GLT1*. *Journal of Biological Chemistry, 288*(10), 7105-7116. doi:https://doi.org/10.1074/jbc.M112.410944

74. Zhang, L., Zhang, S., Yao, J., Lowery, F. J., Zhang, Q., Huang, W.-C., . . . Yu, D. (2015). Microenvironment-induced PTEN loss by exosomal microRNA primes brain metastasis outgrowth. *Nature, 527*(7576), 100-104. doi:10.1038/nature15376

75. Alexander, M., Hu, R., Runtsch, M. C., Kagele, D. A., Mosbruger, T. L., Tolmachova, T., . . . O'Connell, R. M. (2015). Exosome-delivered microRNAs modulate the inflammatory response to endotoxin. *Nature Communications, 6*(1), 7321. doi:10.1038/ncomms8321

76. Kosaka, N., Iguchi, H., Yoshioka, Y., Takeshita, F., Matsuki, Y., & Ochiya, T. (2010). Secretory mechanisms and intercellular transfer of microRNAs in living cells. *The Journal of biological chemistry, 285*(23), 17442-17452. doi:10.1074/jbc.M110.107821

77. McKenzie, A. J., Hoshino, D., Hong, N. H., Cha, D. J., Franklin, J. L., Coffey, R. J., . . . Weaver, A. M. (2016). KRAS-MEK Signaling Controls Ago2 Sorting into Exosomes. *Cell Reports, 15*(5), 978-987. doi:https://doi.org/10.1016/j.celrep.2016.03.085

78. Shurtleff, M. J., Temoche-Diaz, M. M., Karfilis, K. V., Ri, S., & Schekman, R. (2016). Y-box protein 1 is required to sort microRNAs into exosomes in cells and in a cell-free reaction. *eLife, 5*, e19276. doi:10.7554/eLife.19276

79. Temoche-Diaz, M. M., Shurtleff, M. J., Nottingham, R. M., Yao, J., Fadadu, R. P., Lambowitz, A. M., & Schekman, R. (2019). Distinct mechanisms of microRNA sorting into cancer cell-derived extracellular vesicle subtypes. *eLife, 8*, e47544. doi:10.7554/eLife.47544

80. Ghamloush, F., Ghayad, S. E., Rammal, G., Fahs, A., Ayoub, A. J., Merabi, Z., . . . Saab, R. (2019). The PAX3-FOXO1 oncogene alters exosome miRNA content and leads to paracrine effects mediated by exosomal miR-486. *Scientific Reports, 9*(1), 14242. doi:10.1038/s41598-019-50592-4

81. Shen, M., Dong, C., Ruan, X., Yan, W., Cao, M., Pizzo, D., . . . Wang, S. E. (2019). Chemotherapy-Induced Extracellular Vesicle miRNAs Promote Breast Cancer Stemness by Targeting <em>ONECUT2</em&gt. *Cancer Research, 79*(14), 3608. doi:10.1158/0008-5472.CAN-18-4055

82. Abels, E. R., Maas, S. L. N., Nieland, L., Wei, Z., Cheah, P. S., Tai, E., . . . Breakefield, X. O. (2019). Glioblastoma-Associated Microglia Reprogramming Is Mediated by Functional Transfer of Extracellular miR-21. *Cell Reports, 28*(12), 3105-3119.e3107. doi:https://doi.org/10.1016/j.celrep.2019.08.036

83. Wang, L., Jia, Q., Xinnong, C., Xie, Y., Yang, Y., Zhang, A., . . . Zhang, J. (2019). Role of cardiac progenitor cell-derived exosome-mediated microRNA-210 in cardiovascular disease. *Journal of cellular and molecular medicine, 23*(11), 7124-7131. doi:https://doi.org/10.1111/jcmm.14562

84. Feng, Y., Huang, W., Wani, M., Yu, X., & Ashraf, M. (2014). Ischemic preconditioning potentiates the protective effect of stem cells through secretion of exosomes by targeting Mecp2 via miR-22. *PloS one, 9*(2), e88685-e88685. doi:10.1371/journal.pone.0088685

85. Shao, L., Zhang, Y., Lan, B., Wang, J., Zhang, Z., Zhang, L., . . . Li, Y. (2017). MiRNA-Sequence Indicates That Mesenchymal Stem Cells and Exosomes Have Similar Mechanism to Enhance Cardiac Repair. *BioMed Research International, 2017*, 4150705. doi:10.1155/2017/4150705

86. Nakamura, Y., Miyaki, S., Ishitobi, H., Matsuyama, S., Nakasa, T., Kamei, N., . . . Ochi, M. (2015). Mesenchymal-stem-cell-derived exosomes accelerate skeletal muscle regeneration. *FEBS Letters, 589*(11), 1257-1265. doi:https://doi.org/10.1016/j.febslet.2015.03.031

87. Xin, H., Li, Y., Buller, B., Katakowski, M., Zhang, Y., Wang, X., . . . Chopp, M. (2012). Exosome-mediated transfer of miR-133b from multipotent mesenchymal stromal cells to neural cells contributes to neurite outgrowth. *Stem cells (Dayton, Ohio), 30*(7), 1556-1564. doi:10.1002/stem.1129

88. Lou, G., Song, X., Yang, F., Wu, S., Wang, J., Chen, Z., & Liu, Y. (2015). Exosomes derived from miR-122-modified adipose tissue-derived MSCs increase chemosensitivity of hepatocellular carcinoma. *Journal of Hematology & Oncology, 8*(1), 122. doi:10.1186/s13045-015-0220-7

89. Qu, Y., Zhang, Q., Cai, X., Li, F., Ma, Z., Xu, M., & Lu, L. (2017). Exosomes derived from miR-181-5p-modified adipose-derived mesenchymal stem cells prevent liver fibrosis via autophagy activation. *Journal of cellular and molecular medicine, 21*(10), 2491-2502. doi:10.1111/jcmm.13170

90. Chen, S., Tang, Y., Liu, Y., Zhang, P., Lv, L., Zhang, X., . . . Zhou, Y. (2019). Exosomes derived from miR-375-overexpressing human adipose mesenchymal stem cells promote bone regeneration. *Cell Proliferation, 52*(5), e12669. doi:https://doi.org/10.1111/cpr.12669

91. Ma, Y., Li, C., Huang, Y., Wang, Y., Xia, X., & Zheng, J. C. (2019). Exosomes released from neural progenitor cells and induced neural progenitor cells regulate neurogenesis through miR-21a. *Cell Communication and Signaling, 17*(1), 96. doi:10.1186/s12964-019-0418-3

92. Ying, W., Riopel, M., Bandyopadhyay, G., Dong, Y., Birmingham, A., Seo, J. B., . . . Olefsky, J. M. (2017). Adipose Tissue Macrophage-Derived Exosomal miRNAs Can Modulate In Vivo and In Vitro Insulin Sensitivity. *Cell, 171*(2), 372-384.e312. doi:https://doi.org/10.1016/j.cell.2017.08.035

93. Thomou, T., Mori, M. A., Dreyfuss, J. M., Konishi, M., Sakaguchi, M., Wolfrum, C., . . . Kahn, C. R. (2017). Adipose-derived circulating miRNAs regulate gene expression in other tissues. *Nature, 542*(7642), 450-455. doi:10.1038/nature21365

94. Villarroya-Beltri, C., Gutiérrez-Vázquez, C., Sánchez-Cabo, F., Pérez-Hernández, D., Vázquez, J., Martin-Cofreces, N., . . . Sánchez-Madrid, F. (2013). Sumoylated hnRNPA2B1 controls the sorting of miRNAs into exosomes through binding to specific motifs. *Nature Communications, 4*, 2980. doi:10.1038/ncomms3980

95. Santangelo, L., Giurato, G., Cicchini, C., Montaldo, C., Mancone, C., Tarallo, R., . . . Tripodi, M. (2016). The RNA-Binding Protein SYNCRIP Is a Component of the Hepatocyte Exosomal Machinery Controlling MicroRNA Sorting. *Cell Reports, 17*(3), 799-808. doi:10.1016/j.celrep.2016.09.031

96. Koppers-Lalic, D., Hackenberg, M., Bijnsdorp, Irene V., van Eijndhoven, Monique A. J., Sadek, P., Sie, D., . . . Pegtel, D. M. (2014). Nontemplated Nucleotide Additions Distinguish the Small RNA Composition in Cells from Exosomes. *Cell Reports, 8*(6), 1649-1658. doi:https://doi.org/10.1016/j.celrep.2014.08.027

97. Sung, B. H., Ketova, T., Hoshino, D., Zijlstra, A., & Weaver, A. M. (2015). Directional cell movement through tissues is controlled by exosome secretion. *Nature Communications, 6*(1), 7164. doi:10.1038/ncomms8164

98. Ludwig, N., & Whiteside, T. L. (2018). Potential roles of tumor-derived exosomes in angiogenesis. *Expert opinion on therapeutic targets, 22*(5), 409-417. doi:10.1080/14728222.2018.1464141

99. Hoshino, A., Costa-Silva, B., Shen, T.-L., Rodrigues, G., Hashimoto, A., Tesic Mark, M., . . . Lyden, D. (2015). Tumour exosome integrins determine organotropic metastasis. *Nature, 527*(7578), 329-335. doi:10.1038/nature15756

100.Chen, X., Ying, X., Wang, X., Wu, X., Zhu, Q., & Wang, X. (2017). Exosomes derived from hypoxic epithelial ovarian cancer deliver microRNA-940 to induce macrophage M2 polarization. *Oncol Rep, 38*(1), 522-528. doi:10.3892/or.2017.5697

101.Gutkin, A., Uziel, O., Beery, E., Nordenberg, J., Pinchasi, M., Goldvaser, H., . . . Lahav, M. (2016). Tumor cells derived exosomes contain hTERT mRNA and transform nonmalignant fibroblasts into telomerase positive cells. *Oncotarget; Vol 7, No 37*.

102.Zhao, H., Yang, L., Baddour, J., Achreja, A., Bernard, V., Moss, T., . . . Nagrath, D. (2016). Tumor microenvironment derived exosomes pleiotropically modulate cancer cell metabolism. *eLife, 5*, e10250. doi:10.7554/eLife.10250

103.Zhu, L., Kalimuthu, S., Gangadaran, P., Oh, J. M., Lee, H. W., Baek, S. H., . . . Ahn, B.-C. (2017). Exosomes Derived From Natural Killer Cells Exert Therapeutic Effect in Melanoma. *Theranostics, 7*(10), 2732-2745. doi:10.7150/thno.18752

104.Rajendran, L., Honsho, M., Zahn, T. R., Keller, P., Geiger, K. D., Verkade, P., & Simons, K. (2006). Alzheimer's disease beta-amyloid peptides are released in association with exosomes. *Proceedings of the National Academy of Sciences of the United States of America, 103*(30), 11172-11177. doi:10.1073/pnas.0603838103

105.Saman, S., Kim, W., Raya, M., Visnick, Y., Miro, S., Saman, S., . . . Hall, G. F. (2012). Exosome-associated tau is secreted in tauopathy models and is selectively phosphorylated in cerebrospinal fluid in early Alzheimer disease. *The Journal of biological chemistry, 287*(6), 3842-3849. doi:10.1074/jbc.M111.277061

106.Emmanouilidou, E., Melachroinou, K., Roumeliotis, T., Garbis, S. D., Ntzouni, M., Margaritis, L. H., . . . Vekrellis, K. (2010). Cell-produced alpha-synuclein is secreted in a calcium-dependent manner by exosomes and impacts neuronal survival. *The Journal of*

neuroscience : the official journal of the Society for Neuroscience, 30(20), 6838-6851. doi:10.1523/JNEUROSCI.5699-09.2010

107.Fevrier, B., Vilette, D., Archer, F., Loew, D., Faigle, W., Vidal, M., . . . Raposo, G. (2004). Cells release prions in association with exosomes. *Proceedings of the National Academy of Sciences of the United States of America, 101*(26), 9683. doi:10.1073/pnas.0308413101

108.Laflamme, M. A., & Murry, C. E. (2011). Heart regeneration. *Nature, 473*(7347), 326-335. doi:10.1038/nature10147

109.Madonna, R., Van Laake, L. W., Davidson, S. M., Engel, F. B., Hausenloy, D. J., Lecour, S., . . . Sluijter, J. P. G. (2016). Position Paper of the European Society of Cardiology Working Group Cellular Biology of the Heart: cell-based therapies for myocardial repair and regeneration in ischemic heart disease and heart failure. *European Heart Journal, 37*(23), 1789-1798. doi:10.1093/eurheartj/ehw113

110.Shiba, Y., Gomibuchi, T., Seto, T., Wada, Y., Ichimura, H., Tanaka, Y., . . . Ikeda, U. (2016). Allogeneic transplantation of iPS cell-derived cardiomyocytes regenerates primate hearts. *Nature, 538*(7625), 388-391. doi:10.1038/nature19815

111.Jung, J.-H., Fu, X., & Yang, P. C. (2017). Exosomes Generated From iPSC-Derivatives. *Circulation Research, 120*(2), 407-417. doi:10.1161/CIRCRESAHA.116.309307

112.Orlic, D., Kajstura, J., Chimenti, S., Jakoniuk, I., Anderson, S. M., Li, B., . . . Anversa, P. (2001). Bone marrow cells regenerate infarcted myocardium. *Nature, 410*(6829), 701-705. doi:10.1038/35070587

113.Nguyen, P. K., Rhee, J.-W., & Wu, J. C. (2016). Adult Stem Cell Therapy and Heart Failure, 2000 to 2016: A Systematic Review. *JAMA cardiology, 1*(7), 831-841. doi:10.1001/jamacardio.2016.2225

114.Behfar, A., Crespo-Diaz, R., Terzic, A., & Gersh, B. J. (2014). Cell therapy for cardiac repair—lessons from clinical trials. *Nature Reviews Cardiology, 11*(4), 232-246. doi:10.1038/nrcardio.2014.9

115.Murry, C. E., Soonpaa, M. H., Reinecke, H., Nakajima, H., Nakajima, H. O., Rubart, M., . . . Field, L. J. (2004). Haematopoietic stem cells do not transdifferentiate into cardiac myocytes in myocardial infarcts. *Nature, 428*(6983), 664-668. doi:10.1038/nature02446

116.Balsam, L. B., Wagers, A. J., Christensen, J. L., Kofidis, T., Weissman, I. L., & Robbins, R. C. (2004). Haematopoietic stem cells adopt mature haematopoietic fates in ischaemic myocardium. *Nature, 428*(6983), 668-673. doi:10.1038/nature02460

117.He, J.-Q., Vu, D. M., Hunt, G., Chugh, A., Bhatnagar, A., & Bolli, R. (2011). Human cardiac stem cells isolated from atrial appendages stably express c-kit. *PloS one, 6*(11), e27719-e27719. doi:10.1371/journal.pone.0027719

118.van Berlo, J. H., Kanisicak, O., Maillet, M., Vagnozzi, R. J., Karch, J., Lin, S.-C. J., . . . Molkentin, J. D. (2014). c-kit+ cells minimally contribute cardiomyocytes to the heart. *Nature, 509*(7500), 337-341. doi:10.1038/nature13309

119.Kishore, R., & Khan, M. (2016). More Than Tiny Sacks. *Circulation Research, 118*(2), 330.

120.Zomer, H. D., Vidane, A. S., Gonçalves, N. N., & Ambrósio, C. E. (2015). Mesenchymal and induced pluripotent stem cells: general insights and clinical perspectives. *Stem Cells and Cloning : Advances and Applications, 8*, 125-134. doi:10.2147/SCCAA.S88036

121.Dominici, M., Le Blanc, K., Mueller, I., Slaper-Cortenbach, I., Marini, F. C., Krause, D. S., . . . Horwitz, E. M. (2006). Minimal criteria for defining multipotent mesenchymal stromal cells. The International Society for Cellular Therapy position statement. *Cytotherapy, 8*(4), 315-317. doi:https://doi.org/10.1080/14653240600855905

122.Vu, Q., Xie, K., Eckert, M., Zhao, W., & Cramer, S. C. (2014). Meta-analysis of preclinical studies of mesenchymal stromal cells for ischemic stroke. *Neurology, 82*(14), 1277.

123.Heldman, A. W., DiFede, D. L., Fishman, J. E., & et al. (2014). Transendocardial mesenchymal stem cells and mononuclear bone marrow cells for ischemic cardiomyopathy: The tac-hft randomized trial. *JAMA, 311*(1), 62-73. doi:10.1001/jama.2013.282909

124.Hare, J. M., Traverse, J. H., Henry, T. D., Dib, N., Strumpf, R. K., Schulman, S. P., . . . Sherman, W. (2009). A Randomized, Double-Blind, Placebo-Controlled, Dose-Escalation Study of Intravenous Adult Human Mesenchymal Stem Cells (Prochymal) After Acute Myocardial Infarction. *Journal of the American College of Cardiology, 54*(24), 2277-2286. doi:https://doi.org/10.1016/j.jacc.2009.06.055

125.Hare, J. M., Fishman, J. E., Gerstenblith, G., & et al. (2012). Comparison of allogeneic vs autologous bone marrow–derived mesenchymal stem cells delivered by transendocardial injection in patients with ischemic cardiomyopathy: The poseidon randomized trial. *JAMA, 308*(22), 2369-2379. doi:10.1001/jama.2012.25321

126.Amado, L. C., Saliaris, A. P., Schuleri, K. H., St. John, M., Xie, J.-S., Cattaneo, S., . . . Hare, J. M. (2005). Cardiac repair with intramyocardial injection of allogeneic mesenchymal stem cells after myocardial infarction. *Proceedings of the National Academy of Sciences of the United States of America, 102*(32), 11474. doi:10.1073/pnas.0504388102

127.Chen, S.-l., Fang, W.-w., Ye, F., Liu, Y.-H., Qian, J., Shan, S.-j., . . . Sun, J.-p. (2004). Effect on left ventricular function of intracoronary transplantation of autologous bone marrow mesenchymal stem cell in patients with acute myocardial infarction. *The American journal of cardiology, 94*(1), 92-95. doi:https://doi.org/10.1016/j.amjcard.2004.03.034

128.Williams Adam, R., Trachtenberg, B., Velazquez Darcy, L., McNiece, I., Altman, P., Rouy, D., . . . Hare Joshua, M. (2011). Intramyocardial Stem Cell Injection in Patients With Ischemic Cardiomyopathy. *Circulation Research, 108*(7), 792-796. doi:10.1161/CIRCRESAHA.111.242610

129.Toma, C., Pittenger, M. F., Cahill, K. S., Byrne, B. J., & Kessler, P. D. (2002). Human Mesenchymal Stem Cells Differentiate to a Cardiomyocyte Phenotype in the Adult Murine Heart. *Circulation, 105*(1), 93-98. doi:10.1161/hc0102.101442

130.Prockop, D. J. (2009). Repair of tissues by adult stem/progenitor cells (MSCs): controversies, myths, and changing paradigms. *Molecular therapy : the journal of the American Society of Gene Therapy, 17*(6), 939-946. doi:10.1038/mt.2009.62

131.Gnecchi, M., He, H., Liang, O. D., Melo, L. G., Morello, F., Mu, H., . . . Dzau, V. J. (2005). Paracrine action accounts for marked protection of ischemic heart by Akt-modified mesenchymal stem cells. *Nature Medicine, 11*, 367. doi:10.1038/nm0405-367

132.Mirotsou, M., Zhang, Z., Deb, A., Zhang, L., Gnecchi, M., Noiseux, N., . . . Dzau, V. (2007). Secreted frizzled related protein 2 (Sfrp2) is the key Akt-mesenchymal stem cell-released paracrine factor mediating myocardial survival and repair. *Proceedings of the National Academy of Sciences, 104*(5), 1643. doi:10.1073/pnas.0610024104

133.Lai, R. C., Chen, T. S., & Lim, S. K. (2011). Mesenchymal stem cell exosome: a novel stem cell-based therapy for cardiovascular disease. *Regenerative Medicine, 6*(4), 481-492. doi:10.2217/rme.11.35

134.Arslan, F., Lai, R. C., Smeets, M. B., Akeroyd, L., Choo, A., Aguor, E. N. E., . . . de Kleijn, D. P. (2013). Mesenchymal stem cell-derived exosomes increase ATP levels, decrease oxidative stress and activate PI3K/Akt pathway to enhance myocardial viability and prevent adverse remodeling after myocardial ischemia/reperfusion injury. *Stem Cell Research, 10*(3), 301-312. doi:https://doi.org/10.1016/j.scr.2013.01.002

135.Eefting, F., Rensing, B., Wigman, J., Pannekoek, W. J., Liu, W. M., Cramer, M. J., . . . Doevendans, P. A. (2004). Role of apoptosis in reperfusion injury. *Cardiovascular research, 61*(3), 414-426. doi:10.1016/j.cardiores.2003.12.023

136.Wang, K., Jiang, Z., Webster, K. A., Chen, J., Hu, H., Zhou, Y., . . . Wang, J. a. (2017). Enhanced Cardioprotection by Human Endometrium Mesenchymal Stem Cells Driven by Exosomal MicroRNA-21. *STEM CELLS Translational Medicine, 6*(1), 209-222. doi:https://doi.org/10.5966/sctm.2015-0386

137.Shi, B., Wang, Y., Zhao, R., Long, X., Deng, W., & Wang, Z. (2018). Bone marrow mesenchymal stem cell-derived exosomal miR-21 protects C-kit+ cardiac stem cells from oxidative injury through the PTEN/PI3K/Akt axis. *PloS one, 13*(2), e0191616-e0191616. doi:10.1371/journal.pone.0191616

138.Wang, Y., Zhao, R., Liu, D., Deng, W., Xu, G., Liu, W., . . . Shi, B. (2018). Exosomes Derived from miR-214-Enriched Bone Marrow-Derived Mesenchymal Stem Cells Regulate Oxidative Damage in Cardiac Stem Cells by Targeting CaMKII. *Oxidative Medicine and Cellular Longevity, 2018*, 4971261. doi:10.1155/2018/4971261

139.Zhu, J., Lu, K., Zhang, N., Zhao, Y., Ma, Q., Shen, J., . . . Yu, H. (2018). Myocardial reparative functions of exosomes from mesenchymal stem cells are enhanced by hypoxia treatment of the cells via transferring microRNA-210 in an nSMase2-dependent way. *Artificial Cells, Nanomedicine, and Biotechnology, 46*(8), 1659-1670. doi:10.1080/21691401.2017.1388249

140.Zhu, L.-P., Tian, T., Wang, J.-Y., He, J.-N., Chen, T., Pan, M., . . . Bai, Y.-P. (2018). Hypoxia-elicited mesenchymal stem cell-derived exosomes facilitates cardiac repair through miR-125b-mediated prevention of cell death in myocardial infarction. *Theranostics, 8*(22), 6163-6177. doi:10.7150/thno.28021

141.Sun, L., Zhu, W., Zhao, P., Zhang, J., Lu, Y., Zhu, Y., . . . Zhang, F. (2020). Down-Regulated Exosomal MicroRNA-221 – 3p Derived From Senescent Mesenchymal Stem Cells Impairs Heart Repair. *Frontiers in Cell and Developmental Biology, 8*, 263.

142.Chen, H., Xia, W., & Hou, M. (2020). LncRNA-NEAT1 from the competing endogenous RNA network promotes cardioprotective efficacy of mesenchymal stem cell-derived exosomes induced by macrophage migration inhibitory factor via the miR-142-3p/FOXO1 signaling pathway. *Stem Cell Research & Therapy, 11*(1), 31-31. doi:10.1186/s13287-020-1556-7

143.Sharma, S., Liu, J., Wei, J., Yuan, H., Zhang, T., & Bishopric, N. H. (2012). Repression of miR-142 by p300 and MAPK is required for survival signalling via gp130 during adaptive hypertrophy. *EMBO Molecular Medicine, 4*(7), 617-632. doi:10.1002/emmm.201200234

144.Frangogiannis, N. G. (2014). The inflammatory response in myocardial injury, repair, and remodelling. *Nature reviews. Cardiology, 11*(5), 255-265. doi:10.1038/nrcardio.2014.28

145.Teng, X., Chen, L., Chen, W., Yang, J., Yang, Z., & Shen, Z. (2015). Mesenchymal Stem Cell-Derived Exosomes Improve the Microenvironment of Infarcted Myocardium Contributing to Angiogenesis and Anti-Inflammation. *Cellular Physiology and Biochemistry, 37*(6), 2415-2424. doi:10.1159/000438594

146.Budoni, M., Fierabracci, A., Luciano, R., Petrini, S., Di Ciommo, V., & Muraca, M. (2013). The Immunosuppressive Effect of Mesenchymal Stromal Cells on B Lymphocytes is Mediated by Membrane Vesicles. *Cell Transplantation, 22*(2), 369-379. doi:10.3727/096368911X582769b

147.Zhao, J., Li, X., Hu, J., Chen, F., Qiao, S., Sun, X., . . . Xu, B. (2019). Mesenchymal stromal cell-derived exosomes attenuate myocardial ischaemia-reperfusion injury through miR-182-regulated macrophage polarization. *Cardiovascular research, 115*(7), 1205-1216. doi:10.1093/cvr/cvz040

148.Domenis, R., Cifù, A., Quaglia, S., Pistis, C., Moretti, M., Vicario, A., . . . Curcio, F. (2018). Pro inflammatory stimuli enhance the immunosuppressive functions of adipose mesenchymal stem cells-derived exosomes. *Scientific Reports, 8*(1), 13325-13325. doi:10.1038/s41598-018-31707-9

149.Mokarizadeh, A., Delirezh, N., Morshedi, A., Mosayebi, G., Farshid, A.-A., & Mardani, K. (2012). Microvesicles derived from mesenchymal stem cells: Potent organelles for induction of tolerogenic signaling. *Immunology Letters, 147*(1), 47-54. doi:https://doi.org/10.1016/j.imlet.2012.06.001

150.Gianchecchi, E., Delfino, D. V., & Fierabracci, A. (2013). Recent insights into the role of the PD-1/PD-L1 pathway in immunological tolerance and autoimmunity. *Autoimmunity Reviews, 12*(11), 1091-1100. doi:https://doi.org/10.1016/j.autrev.2013.05.003

151.Anginot, A., Espeli, M., Chasson, L., Mancini, S. J. C., & Schiff, C. (2013). Galectin 1 modulates plasma cell homeostasis and regulates the humoral immune response. *Journal of immunology (Baltimore, Md. : 1950), 190*(11), 5526-5533. doi:10.4049/jimmunol.1201885

152.Worthington, J. J., Fenton, T. M., Czajkowska, B. I., Klementowicz, J. E., & Travis, M. A. (2012). Regulation of TGFβ in the immune system: An emerging role for integrins and dendritic cells. *Immunobiology, 217*(12), 1259-1265. doi:https://doi.org/10.1016/j.imbio.2012.06.009

153.Cochain, C., Channon, K. M., & Silvestre, J.-S. (2013). Angiogenesis in the infarcted myocardium. *Antioxidants & redox signaling, 18*(9), 1100-1113. doi:10.1089/ars.2012.4849

154.Xu, H., Wang, Z., Liu, L., Zhang, B., & Li, B. (2020). Exosomes derived from adipose tissue, bone marrow, and umbilical cord blood for cardioprotection after myocardial infarction. *Journal of Cellular Biochemistry, 121*(3), 2089-2102. doi:https://doi.org/10.1002/jcb.27399

155.Vrijsen, K. R., Maring, J. A., Chamuleau, S. A. J., Verhage, V., Mol, E. A., Deddens, J. C., . . . Sluijter, J. P. G. (2016). Exosomes from Cardiomyocyte Progenitor Cells and Mesenchymal Stem Cells Stimulate Angiogenesis Via EMMPRIN. *Advanced Healthcare Materials, 5*(19), 2555-2565. doi:https://doi.org/10.1002/adhm.201600308

156.Collino, F., Pomatto, M., Bruno, S., Lindoso, R. S., Tapparo, M., Sicheng, W., . . . Camussi, G. (2017). Exosome and Microvesicle-Enriched Fractions Isolated from Mesenchymal Stem Cells by Gradient Separation Showed Different Molecular Signatures and Functions on Renal Tubular Epithelial Cells. *Stem cell reviews and reports, 13*(2), 226-243. doi:10.1007/s12015-016-9713-1

157.Kim, H.-S., Choi, D.-Y., Yun, S. J., Choi, S.-M., Kang, J. W., Jung, J. W., . . . Kim, D.-W. (2012). Proteomic Analysis of Microvesicles Derived from Human Mesenchymal Stem Cells. *Journal of Proteome Research, 11*(2), 839-849. doi:10.1021/pr200682z

158.Anderson, J. D., Johansson, H. J., Graham, C. S., Vesterlund, M., Pham, M. T., Bramlett, C. S., . . . Nolta, J. A. (2016). Comprehensive Proteomic Analysis of Mesenchymal Stem Cell Exosomes Reveals Modulation of Angiogenesis via Nuclear Factor-KappaB Signaling. *Stem cells (Dayton, Ohio), 34*(3), 601-613. doi:10.1002/stem.2298

159.Mayourian, J., Ceholski, D. K., Gorski, P. A., Mathiyalagan, P., Murphy, J. F., Salazar, S. I., . . . Costa, K. D. (2018). Exosomal microRNA-21-5p Mediates Mesenchymal Stem Cell Paracrine

Effects on Human Cardiac Tissue Contractility. *Circulation Research, 122*(7), 933-944. doi:10.1161/CIRCRESAHA.118.312420

160.Ferguson, S. W., Wang, J., Lee, C. J., Liu, M., Neelamegham, S., Canty, J. M., & Nguyen, J. (2018). The microRNA regulatory landscape of MSC-derived exosomes: a systems view. *Scientific Reports, 8*(1), 1419-1419. doi:10.1038/s41598-018-19581-x

161.Squillaro, T., Peluso, G., & Galderisi, U. (2016). Clinical Trials with Mesenchymal Stem Cells: An Update. *Cell Transplantation, 25*(5), 829-848. doi:10.3727/096368915X689622

162.Kordelas, L., Rebmann, V., Ludwig, A. K., Radtke, S., Ruesing, J., Doeppner, T. R., . . . Giebel, B. (2014). MSC-derived exosomes: a novel tool to treat therapy-refractory graft-versus-host disease. *Leukemia, 28*(4), 970-973. doi:10.1038/leu.2014.41

163.Nassar, W., El-Ansary, M., Sabry, D., Mostafa, M. A., Fayad, T., Kotb, E., . . . Adel, H. (2016). Umbilical cord mesenchymal stem cells derived extracellular vesicles can safely ameliorate the progression of chronic kidney diseases. *Biomaterials Research, 20*(1), 21. doi:10.1186/s40824-016-0068-0

164.Hausenloy, D. J., & Yellon, D. M. (2013). Myocardial ischemia-reperfusion injury: a neglected therapeutic target. *The Journal of Clinical Investigation, 123*(1), 92-100. doi:10.1172/JCI62874

165.Squadrito, Mario L., Baer, C., Burdet, F., Maderna, C., Gilfillan, Gregor D., Lyle, R., . . . De Palma, M. (2014). Endogenous RNAs Modulate MicroRNA Sorting to Exosomes and Transfer to Acceptor Cells. *Cell Reports, 8*(5), 1432-1446. doi:https://doi.org/10.1016/j.celrep.2014.07.035

166.Skog, J., Würdinger, T., van Rijn, S., Meijer, D. H., Gainche, L., Curry Jr, W. T., . . . Breakefield, X. O. (2008). Glioblastoma microvesicles transport RNA and proteins that promote tumour growth and provide diagnostic biomarkers. *Nature Cell Biology, 10*, 1470. doi:10.1038/ncb1800
https://www.nature.com/articles/ncb1800#supplementary-information

167.Guduric-Fuchs, J., O'Connor, A., Camp, B., O'Neill, C. L., Medina, R. J., & Simpson, D. A. (2012). Selective extracellular vesicle-mediated export of an overlapping set of microRNAs from multiple cell types. *BMC Genomics, 13*(1), 357. doi:10.1186/1471-2164-13-357

168.Roccaro, A. M., Sacco, A., Maiso, P., Azab, A. K., Tai, Y.-T., Reagan, M., . . . Ghobrial, I. M. (2013). BM mesenchymal stromal cell–derived exosomes facilitate multiple myeloma progression. *The Journal of Clinical Investigation, 123*(4), 1542-1555. doi:10.1172/JCI66517

169.Ferguson, S. W., & Nguyen, J. (2016). Exosomes as therapeutics: The implications of molecular composition and exosomal heterogeneity. *Journal of Controlled Release, 228*, 179-190. doi:doi:10.1016/j.jconrel.2016.02.037

170.Bolukbasi, M. F., Mizrak, A., Ozdener, G. B., Madlener, S., Ströbel, T., Erkan, E. P., . . . Saydam, O. (2012). miR-1289 and "Zipcode"-like Sequence Enrich mRNAs in Microvesicles. *Molecular therapy. Nucleic acids, 1*(2), e10. doi:10.1038/mtna.2011.2

171.Zhang, Z., Yang, J., Yan, W., Li, Y., Shen, Z., & Asahara, T. (2016). Pretreatment of Cardiac Stem Cells With Exosomes Derived From Mesenchymal Stem Cells Enhances Myocardial Repair. *Journal of the American Heart Association: Cardiovascular and Cerebrovascular Disease, 5*(1), e002856. doi:10.1161/JAHA.115.002856

172.Katsuda, T., & Ochiya, T. (2015). Molecular signatures of mesenchymal stem cell-derived extracellular vesicle-mediated tissue repair. *Stem Cell Research & Therapy, 6*(1), 212. doi:10.1186/s13287-015-0214-y

173.Council, N. R. (2011). *Guide for the Care and Use of Laboratory Animals: Eighth Edition*. Washington, DC: The National Academies Press.

174.Ren, X., Wang, Y., & Jones, W. K. (2004). TNF-α is required for late ischemic preconditioning but not for remote preconditioning of trauma1 1Funded by National Institutes of Health Grant HL63034-01 (W.K.J.). *Journal of Surgical Research, 121*(1), 120-129. doi:https://doi.org/10.1016/j.jss.2004.03.010

175.Fishbein, M. C., Meerbaum, S., Rit, J., Lando, U., Kanmatsuse, K., Mercier, J. C., . . . Ganz, W. (1981). Early phase acute myocardial infarct size quantification: Validation of the triphenyl tetrazolium chloride tissue enzyme staining technique. *American Heart Journal, 101*(5), 593-600. doi:https://doi.org/10.1016/0002-8703(81)90226-X

176.Huang, D. W., Sherman, B. T., & Lempicki, R. A. (2009). Systematic and integrative analysis of large gene lists using DAVID bioinformatics resources. *Nature Protocols, 4*(1), 44-57. doi:10.1038/nprot.2008.211

177.Agarwal, V., Bell, G. W., Nam, J.-W., & Bartel, D. P. (2015). Predicting effective microRNA target sites in mammalian mRNAs. *eLife, 4*, e05005. doi:10.7554/eLife.05005

178.Betel, D., Wilson, M., Gabow, A., Marks, D. S., & Sander, C. (2008). The microRNA.org resource: targets and expression. *Nucleic Acids Research, 36*(Database issue), D149-D153. doi:10.1093/nar/gkm995

179.Bailey, T. L., Boden, M., Buske, F. A., Frith, M., Grant, C. E., Clementi, L., . . . Noble, W. S. (2009). MEME Suite: tools for motif discovery and searching. *Nucleic Acids Research, 37*(suppl_2), W202-W208. doi:10.1093/nar/gkp335

180.Kim, C. K., Asimes, A., Zhang, M., Son, B. T., Kirk, J. A., & Pak, T. R. (2020). Differential Stability of miR-9-5p and miR-9-3p in the Brain Is Determined by Their Unique Cis- and Trans-Acting Elements. *eneuro, 7*(3), ENEURO.0094-0020.2020. doi:10.1523/ENEURO.0094-20.2020

181.Jung, M. K., & Mun, J. Y. (2018). Sample Preparation and Imaging of Exosomes by Transmission Electron Microscopy. *Journal of visualized experiments : JoVE*(131), 56482. doi:10.3791/56482

182.Zietzer, A., Hosen, M. R., Wang, H., Goody, P. R., Sylvester, M., Latz, E., . . . Jansen, F. (2020). The RNA-binding protein hnRNPU regulates the sorting of microRNA-30c-5p into large extracellular vesicles. *Journal of Extracellular Vesicles, 9*(1), 1786967. doi:10.1080/20013078.2020.1786967

183.Cong, L., Ran, F. A., Cox, D., Lin, S., Barretto, R., Habib, N., . . . Zhang, F. (2013). Multiplex Genome Engineering Using CRISPR/Cas Systems. *Science, 339*(6121), 819. doi:10.1126/science.1231143

184.Livak, K. J., & Schmittgen, T. D. (2001). Analysis of Relative Gene Expression Data Using Real-Time Quantitative PCR and the 2−ΔΔCT Method. *Methods, 25*(4), 402-408. doi:https://doi.org/10.1006/meth.2001.1262

185.Montgomery, R. L., Yu, G., Latimer, P. A., Stack, C., Robinson, K., Dalby, C. M., . . . van Rooij, E. (2014). MicroRNA mimicry blocks pulmonary fibrosis. *EMBO molecular medicine, 6*(10), 1347-1356. doi:10.15252/emmm.201303604

186.van Rooij, E., Sutherland, L. B., Thatcher, J. E., DiMaio, J. M., Naseem, R. H., Marshall, W. S., . . . Olson, E. N. (2008). Dysregulation of microRNAs after myocardial infarction reveals a role of miR-29 in cardiac fibrosis. *Proceedings of the National Academy of Sciences of the United States of America, 105*(35), 13027-13032. doi:10.1073/pnas.0805038105

187.Théry, C., Amigorena, S., Raposo, G., & Clayton, A. (2006). Isolation and Characterization of Exosomes from Cell Culture Supernatants and Biological Fluids. *Current Protocols in Cell Biology, 30*(1), 3.22.21-23.22.29. doi:10.1002/0471143030.cb0322s30

188.Bailey, T. L., Johnson, J., Grant, C. E., & Noble, W. S. (2015). The MEME Suite. *Nucleic Acids Research, 43*(Web Server issue), W39-W49. doi:10.1093/nar/gkv416

189.Abdul Halim, N. S. S., Fakiruddin, K. S., Ali, S. A., & Yahaya, B. H. (2014). A comparative study of non-viral gene delivery techniques to human adipose-derived mesenchymal stem cell. *International journal of molecular sciences, 15*(9), 15044-15060. doi:10.3390/ijms150915044

190.Baglio, S. R., Rooijers, K., Koppers-Lalic, D., Verweij, F. J., Pérez Lanzón, M., Zini, N., . . . Pegtel, D. M. (2015). Human bone marrow- and adipose-mesenchymal stem cells secrete exosomes enriched in distinctive miRNA and tRNA species. *Stem cell research & therapy, 6*(1), 127. doi:10.1186/s13287-015-0116-z

191.Witkos, T. M., Koscianska, E., & Krzyzosiak, W. J. (2011). Practical Aspects of microRNA Target Prediction. *Current molecular medicine, 11*(2), 93-109. doi:10.2174/156652411794859250

192.Betel, D., Wilson, M., Gabow, A., Marks, D. S., & Sander, C. (2008). The microRNA.org resource: targets and expression. *Nucleic Acids Research, 36*(suppl_1), D149-D153. doi:10.1093/nar/gkm995

193.Nikitin, A., Egorov, S., Daraselia, N., & Mazo, I. (2003). Pathway studio—the analysis and navigation of molecular networks. *Bioinformatics, 19*(16), 2155-2157. doi:10.1093/bioinformatics/btg290

194.Small, E. M., O'Rourke, J. R., Moresi, V., Sutherland, L. B., McAnally, J., Gerard, R. D., . . . Olson, E. N. (2010). Regulation of PI3-kinase/Akt signaling by muscle-enriched microRNA-486. *Proceedings of the National Academy of Sciences, 107*(9), 4218.

195.Alexander, M. S., Casar, J. C., Motohashi, N., Vieira, N. M., Eisenberg, I., Marshall, J. L., . . . Kunkel, L. M. (2014). MicroRNA-486–dependent modulation of DOCK3/PTEN/AKT signaling pathways improves muscular dystrophy–associated symptoms. *The Journal of Clinical Investigation, 124*(6), 2651-2667. doi:10.1172/JCI73579

196.Tranter, M., Helsley, R. N., Paulding, W. R., McGuinness, M., Brokamp, C., Haar, L., . . . Jones, W. K. (2011). Coordinated post-transcriptional regulation of Hsp70.3 gene expression by microRNA and alternative polyadenylation. *The Journal of biological chemistry, 286*(34), 29828-29837. doi:10.1074/jbc.M111.221796

197.Lankat-Buttgereit, B., & Göke, R. (2009). The tumour suppressor Pdcd4: recent advances in the elucidation of function and regulation. *Biology of the Cell, 101*(6), 309-317. doi:10.1042/BC20080191

198.White, K., Dempsie, Y., Caruso, P., Wallace, E., McDonald Robert, A., Stevens, H., . . . Baker Andrew, H. (2014). Endothelial Apoptosis in Pulmonary Hypertension Is Controlled by a microRNA/Programmed Cell Death 4/Caspase-3 Axis. *Hypertension, 64*(1), 185-194. doi:10.1161/HYPERTENSIONAHA.113.03037

199.Ruan, Q., Wang, T., Kameswaran, V., Wei, Q., Johnson, D. S., Matschinsky, F., . . . Chen, Y. H. (2011). The microRNA-21–PDCD4 axis prevents type 1 diabetes by blocking pancreatic β cell death. *Proceedings of the National Academy of Sciences, 108*(29), 12030. doi:10.1073/pnas.1101450108

200.Wang, J., Tian, X., Han, R., Zhang, X., Wang, X., Shen, H., . . . Jiang, F. (2013). Downregulation of miR-486-5p contributes to tumor progression and metastasis by targeting protumorigenic ARHGAP5 in lung cancer. *Oncogene, 33*, 1181. doi:10.1038/onc.2013.42 https://www.nature.com/articles/onc201342#supplementary-information

201.Yang, Y., Ji, C., Guo, S., Su, X., Zhao, X., Zhang, S., . . . Chen, H. (2017). The miR-486-5p plays a causative role in prostate cancer through negative regulation of multiple tumor suppressor pathways. *Oncotarget, 8*(42), 72835-72846. doi:10.18632/oncotarget.20427

202.Xu, J. Y., Chen, G. H., & Yang, Y. J. (2017). Exosomes: A Rising Star in Falling Hearts. *Front Physiol, 8*, 494. doi:10.3389/fphys.2017.00494

203.Yu, B., Kim, H. W., Gong, M., Wang, J., Millard, R. W., Wang, Y., . . . Xu, M. (2015). Exosomes secreted from GATA-4 overexpressing mesenchymal stem cells serve as a reservoir of anti-apoptotic microRNAs for cardioprotection. *International Journal of Cardiology, 182*, 349-360. doi:https://doi.org/10.1016/j.ijcard.2014.12.043

204.Wu, B., Su, S., Patil, D. P., Liu, H., Gan, J., Jaffrey, S. R., & Ma, J. (2018). Molecular basis for the specific and multivariant recognitions of RNA substrates by human hnRNP A2/B1. *Nature Communications, 9*(1), 420. doi:10.1038/s41467-017-02770-z

205.Munro, T. P., Magee, R. J., Kidd, G. J., Carson, J. H., Barbarese, E., Smith, L. M., & Smith, R. (1999). Mutational Analysis of a Heterogeneous Nuclear Ribonucleoprotein A2 Response Element for RNA Trafficking. *Journal of Biological Chemistry, 274*(48), 34389-34395.

206.Hoek, K. S., Kidd, G. J., Carson, J. H., & Smith, R. (1998). hnRNP A2 Selectively Binds the Cytoplasmic Transport Sequence of Myelin Basic Protein mRNA. *Biochemistry, 37*(19), 7021-7029. doi:10.1021/bi9800247

207.Alarcón, C. R., Goodarzi, H., Lee, H., Liu, X., Tavazoie, S., & Tavazoie, S. F. (2015). HNRNPA2B1 Is a Mediator of m(6)A-Dependent Nuclear RNA Processing Events. *Cell, 162*(6), 1299-1308. doi:10.1016/j.cell.2015.08.011

208.Lee, H., Li, C., Zhang, Y., Zhang, D., Otterbein, L. E., & Jin, Y. (2019). Caveolin-1 selectively regulates microRNA sorting into microvesicles after noxious stimuli. *Journal of Experimental Medicine, 216*(9), 2202-2220. doi:10.1084/jem.20182313

209.Lei, Y., Guo, W., Chen, B., Chen, L., Gong, J., & Li, W. (2018). Tumor-released lncRNA H19 promotes gefitinib resistance via packaging into exosomes in non-small cell lung cancer. *Oncol Rep, 40*(6), 3438-3446. doi:10.3892/or.2018.6762

210.Chen, C., Luo, Y., He, W., Zhao, Y., Kong, Y., Liu, H., . . . Lin, T. (2020). Exosomal long noncoding RNA LNMAT2 promotes lymphatic metastasis in bladder cancer. *The Journal of Clinical Investigation, 130*(1), 404-421. doi:10.1172/JCI130892

211.Keerthikumar, S., Chisanga, D., Ariyaratne, D., Al Saffar, H., Anand, S., Zhao, K., . . . Mathivanan, S. (2016). ExoCarta: A Web-Based Compendium of Exosomal Cargo. *Journal of molecular biology, 428*(4), 688-692. doi:10.1016/j.jmb.2015.09.019

212.Ohshima, K., Inoue, K., Fujiwara, A., Hatakeyama, K., Kanto, K., Watanabe, Y., . . . Mochizuki, T. (2010). Let-7 MicroRNA Family Is Selectively Secreted into the Extracellular Environment via Exosomes in a Metastatic Gastric Cancer Cell Line. *PloS one, 5*(10), e13247. doi:10.1371/journal.pone.0013247

213.Nolte-'t Hoen, E. N. M., Buermans, H. P. J., Waasdorp, M., Stoorvogel, W., Wauben, M. H. M., & 't Hoen, P. A. C. (2012). Deep sequencing of RNA from immune cell-derived vesicles

uncovers the selective incorporation of small non-coding RNA biotypes with potential regulatory functions. *Nucleic Acids Research, 40*(18), 9272-9285. doi:10.1093/nar/gks658

214.Qiao, S., Olson, J. M., Paterson, M., Yan, Y., Zaja, I., Liu, Y., . . . Ge, Z.-D. (2015). MicroRNA-21 Mediates Isoflurane-induced Cardioprotection against Ischemia-Reperfusion Injury via Akt/Nitric Oxide Synthase/Mitochondrial Permeability Transition Pore Pathway. *Anesthesiology, 123*(4), 786-798. doi:10.1097/ALN.0000000000000807

215.Cheng, Y., Zhu, P., Yang, J., Liu, X., Dong, S., Wang, X., . . . Zhang, C. (2010). Ischaemic preconditioning-regulated miR-21 protects heart against ischaemia/reperfusion injury via anti-apoptosis through its target PDCD4. *Cardiovascular research, 87*(3), 431-439. doi:10.1093/cvr/cvq082

216.Tu, Y., Wan, L., Fan, Y., Wang, K., Bu, L., Huang, T., . . . Shen, B. (2013). Ischemic Postconditioning-Mediated miRNA-21 Protects against Cardiac ischemia/reperfusion Injury via PTEN/Akt Pathway. *PloS one, 8*(10), e75872. doi:10.1371/journal.pone.0075872

217.Varga, Z. V., Zvara, Á., Faragó, N., Kocsis, G. F., Pipicz, M., Gáspár, R., . . . Ferdinandy, P. (2014). MicroRNAs associated with ischemia-reperfusion injury and cardioprotection by ischemic pre- and postconditioning: protectomiRs. *American Journal of Physiology-Heart and Circulatory Physiology, 307*(2), H216-H227. doi:10.1152/ajpheart.00812.2013

218.Wang, S., Aurora, A. B., Johnson, B. A., Qi, X., McAnally, J., Hill, J. A., . . . Olson, E. N. (2008). The endothelial-specific microRNA miR-126 governs vascular integrity and angiogenesis. *Developmental cell, 15*(2), 261-271. doi:10.1016/j.devcel.2008.07.002

219.Liang, W., Guo, J., Li, J., Bai, C., & Dong, Y. (2016). Downregulation of miR-122 attenuates hypoxia/reoxygenation (H/R)-induced myocardial cell apoptosis by upregulating GATA-4. *Biochemical and Biophysical Research Communications, 478*(3), 1416-1422. doi:https://doi.org/10.1016/j.bbrc.2016.08.139

220.Hu, Y., Du, G., Li, G., Peng, X., Zhang, Z., & Zhai, Y. (2019). The miR-122 inhibition alleviates lipid accumulation and inflammation in NAFLD cell model. *Archives of Physiology and Biochemistry*, 1-5. doi:10.1080/13813455.2019.1640744

221.Song, J.-J., Yang, M., Liu, Y., Song, J.-W., Wang, J., Chi, H.-J., . . . Zhong, J.-C. (2020). MicroRNA-122 aggravates angiotensin II-mediated apoptosis and autophagy imbalance in rat aortic adventitial fibroblasts via the modulation of SIRT6-elabela-ACE2 signaling. *European journal of pharmacology, 883*, 173374-173374. doi:10.1016/j.ejphar.2020.173374

222.Song, G., Zhu, L., Ruan, Z., Wang, R., & Shen, Y. (2019). MicroRNA-122 promotes cardiomyocyte hypertrophy via targeting FoxO3. *Biochemical and Biophysical Research Communications, 519*(4), 682-688. doi:https://doi.org/10.1016/j.bbrc.2019.09.035

223.Guo, D., Ma, J., Li, T., & Yan, L. (2018). Up-regulation of miR-122 protects against neuronal cell death in ischemic stroke through the heat shock protein 70-dependent NF-κB

pathway by targeting FOXO3. *Experimental Cell Research, 369*(1), 34-42. doi:https://doi.org/10.1016/j.yexcr.2018.04.027

224.Zhang, X., Wang, X., Zhu, H., Zhu, C., Wang, Y., Pu, W. T., . . . Fan, G.-C. (2010). Synergistic effects of the GATA-4-mediated miR-144/451 cluster in protection against simulated ischemia/reperfusion-induced cardiomyocyte death. *Journal of Molecular and Cellular Cardiology, 49*(5), 841-850. doi:10.1016/j.yjmcc.2010.08.007

225.Wang, X., Zhu, H., Zhang, X., Liu, Y., Chen, J., Medvedovic, M., . . . Fan, G.-C. (2012). Loss of the miR-144/451 cluster impairs ischaemic preconditioning-mediated cardioprotection by targeting Rac-1. *Cardiovascular research, 94*(2), 379-390. doi:10.1093/cvr/cvs096

226.Cao, J., Da, Y., Li, H., Peng, Y., & Hu, X. (2020). Upregulation of microRNA-451 attenuates myocardial I/R injury by suppressing HMGB1. *PloS one, 15*(7), e0235614. doi:10.1371/journal.pone.0235614

227.Song, L., Su, M., Wang, S., Zou, Y., Wang, X., Wang, Y., . . . Wang, J. (2014). MiR-451 is decreased in hypertrophic cardiomyopathy and regulates autophagy by targeting TSC1. *Journal of cellular and molecular medicine, 18*(11), 2266-2274. doi:10.1111/jcmm.12380

228.Devaux, Y., Vausort, M., McCann, G. P., Zangrando, J., Kelly, D., Razvi, N., . . . Squire, I. B. (2013). MicroRNA-150. *Circulation: Cardiovascular Genetics, 6*(3), 290-298. doi:10.1161/CIRCGENETICS.113.000077

229.Tang, Y., Wang, Y., Park, K.-M., Hu, Q., Teoh, J.-P., Broskova, Z., . . . Kim, I.-M. (2015). MicroRNA-150 protects the mouse heart from ischaemic injury by regulating cell death. *Cardiovascular research, 106*(3), 387-397. doi:10.1093/cvr/cvv121

230.Liu, Z., Ye, P., Wang, S., Wu, J., Sun, Y., Zhang, A., . . . Xia, J. (2015). MicroRNA-150 Protects the Heart From Injury by Inhibiting Monocyte Accumulation in a Mouse Model of Acute Myocardial Infarction. *Circulation: Cardiovascular Genetics, 8*(1), 11-20. doi:10.1161/CIRCGENETICS.114.000598

231.Li, X., Kong, M., Jiang, D., Qian, J., Duan, Q., & Dong, A. (2013). MicroRNA-150 aggravates H2O2-induced cardiac myocyte injury by down-regulating c-myb gene. *Acta Biochimica et Biophysica Sinica, 45*(9), 734-741. doi:10.1093/abbs/gmt067

232.Zhang, X., Zhang, C., Wang, N., Li, Y., Zhang, D., & Li, Q. (2018). MicroRNA-486 Alleviates Hypoxia-Induced Damage in H9c2 Cells by Targeting NDRG2 to Inactivate JNK/C-Jun and NF-κB Signaling Pathways. *Cellular Physiology and Biochemistry, 48*(6), 2483-2492. doi:10.1159/000492686

233.Sun, X.-H., Wang, X., Zhang, Y., & Hui, J. (2019). Exosomes of bone-marrow stromal cells inhibit cardiomyocyte apoptosis under ischemic and hypoxic conditions via miR-486-5p targeting the PTEN/PI3K/AKT signaling pathway. *Thrombosis Research, 177*, 23-32. doi:10.1016/j.thromres.2019.02.002

234.Sun, Y., Su, Q., Li, L., Wang, X., Lu, Y., & Liang, J. (2017). MiR-486 regulates cardiomyocyte apoptosis by p53-mediated BCL-2 associated mitochondrial apoptotic pathway. *BMC Cardiovascular Disorders, 17*(1), 119. doi:10.1186/s12872-017-0549-7

235.Vazquez, F., Ramaswamy, S., Nakamura, N., & Sellers, W. R. (2000). Phosphorylation of the PTEN Tail Regulates Protein Stability and Function. *Molecular and Cellular Biology, 20*(14), 5010. doi:10.1128/MCB.20.14.5010-5018.2000

236.Schmid, T., Jansen, A. P., Baker, A. R., Hegamyer, G., Hagan, J. P., & Colburn, N. H. (2008). Translation Inhibitor Pdcd4 Is Targeted for Degradation during Tumor Promotion. *Cancer Research*. doi:10.1158/0008-5472.CAN-07-1719

237.Palamarchuk, A., Efanov, A., Maximov, V., Aqeilan, R. I., Croce, C. M., & Pekarsky, Y. (2005). Akt Phosphorylates and Regulates Pdcd4 Tumor Suppressor Protein. *Cancer Research, 65*(24), 11282. doi:10.1158/0008-5472.CAN-05-3469

238.Göke, R., Barth, P., Schmidt, A., Samans, B., & Lankat-Buttgereit, B. (2004). Programmed cell death protein 4 suppresses CDK1/cdc2 via induction of p21Waf1/Cip1. *American Journal of Physiology-Cell Physiology, 287*(6), C1541-C1546. doi:10.1152/ajpcell.00025.2004

239.Hwang, H. W., & Mendell, J. T. (2006). MicroRNAs in cell proliferation, cell death, and tumorigenesis. *British Journal of Cancer, 94*(6), 776-780. doi:10.1038/sj.bjc.6603023

240.Suzuki, C., Garces, R. G., Edmonds, K. A., Hiller, S., Hyberts, S. G., Marintchev, A., & Wagner, G. (2008). PDCD4 inhibits translation initiation by binding to eIF4A using both its MA3 domains. *Proceedings of the National Academy of Sciences of the United States of America, 105*(9), 3274-3279. doi:10.1073/pnas.0712235105

241.Kang, M.-J., Ahn, H.-S., Lee, J.-Y., Matsuhashi, S., & Park, W.-Y. (2002). Up-regulation of PDCD4 in senescent human diploid fibroblasts. *Biochemical and Biophysical Research Communications, 293*(1), 617-621. doi:https://doi.org/10.1016/S0006-291X(02)00264-4

242.Su, Q., Li, L., Zhou, Y., Wang, J., Liu, Y., & Ma, G. (2014). Induction of Myocardial PDCD4 in Coronary Microembolization-Related Cardiac Dysfunction: Evidence from a Large-Animal Study. *Cellular Physiology and Biochemistry, 34*(2), 533-542. doi:10.1159/000363020

243.Gao, Y., Li, H., Zhou, Y., Lv, H., & Chen, Y. (2019). PDCD4 expression in coronary atherosclerosis rat models and its mechanism. *Experimental and therapeutic medicine, 17*(4), 3150-3154. doi:10.3892/etm.2019.7296

244.Zhang, J., Zhang, M., Yang, Z., Huang, S., Wu, X., Cao, L., . . . Gao, F. (2020). PDCD4 deficiency ameliorates left ventricular remodeling and insulin resistance in a rat model of type 2 diabetic cardiomyopathy. *BMJ Open Diabetes Research & Care, 8*(1), e001081. doi:10.1136/bmjdrc-2019-001081

245.Su, Q., Su, Q., Li, L., Liu, Y., Zhou, Y., Wang, J., & Sun, Y. (2014). Effect of Intensive Atorvastatin Therapy on Periprocedural PDCD4 Expression in CD4+ T Lymphocytes of

Patients with Unstable Angina Undergoing Percutaneous Coronary Intervention. *Cardiology, 127*(3), 169-175. doi:10.1159/000356434

246.Wang, J., Jia, Z., Zhang, C., Sun, M., Wang, W., Chen, P., . . . Zhou, C. (2014). miR-499 protects cardiomyocytes from H 2O 2-induced apoptosis via its effects on Pdcd4 and Pacs2. *RNA biology, 11*(4), 339-350. doi:10.4161/rna.28300

247.Li, Y., Lu, J., Bao, X., Wang, X., Wu, J., Li, X., & Hong, W. (2016). MiR-499-5p protects cardiomyocytes against ischaemic injury via anti-apoptosis by targeting PDCD4. *Oncotarget, 7*(24), 35607-35617. doi:10.18632/oncotarget.9597

248.Yaoita, H., Ogawa, K., Maehara, K., & Maruyama, Y. (2000). Apoptosis in relevant clinical situations: contribution of apoptosis in myocardial infarction. *Cardiovascular research, 45*(3), 630-641. doi:10.1016/S0008-6363(99)00349-1

249.Leidal, A. M., Huang, H. H., Marsh, T., Solvik, T., Zhang, D., Ye, J., . . . Debnath, J. (2020). The LC3-conjugation machinery specifies the loading of RNA-binding proteins into extracellular vesicles. *Nature Cell Biology, 22*(2), 187-199. doi:10.1038/s41556-019-0450-y

250.Sverdlov, E. D. (2012). Amedeo Avogadro's cry: What is 1 μg of exosomes? *BioEssays, 34*(10), 873-875. doi:https://doi.org/10.1002/bies.201200045

251.Webber, J., & Clayton, A. (2013). How pure are your vesicles? *Journal of Extracellular Vesicles, 2*, 10.3402/jev.v3402i3400.19861. doi:10.3402/jev.v2i0.19861

252.Chevillet, J. R., Kang, Q., Ruf, I. K., Briggs, H. A., Vojtech, L. N., Hughes, S. M., . . . Tewari, M. (2014). Quantitative and stoichiometric analysis of the microRNA content of exosomes. *Proceedings of the National Academy of Sciences of the United States of America, 111*(41), 14888-14893. doi:10.1073/pnas.1408301111

253.He, D., Wang, H., Ho, S.-L., Chan, H.-N., Hai, L., He, X., . . . Li, H.-W. (2019). Total internal reflection-based single-vesicle in situ quantitative and stoichiometric analysis of tumor-derived exosomal microRNAs for diagnosis and treatment monitoring. *Theranostics, 9*(15), 4494-4507. doi:10.7150/thno.33683

254.Gurha, P., Abreu-Goodger, C., Wang, T., Ramirez, M. O., Drumond, A. L., van Dongen, S., . . . Rodriguez, A. (2012). Targeted deletion of microRNA-22 promotes stress-induced cardiac dilation and contractile dysfunction. *Circulation, 125*(22), 2751-2761. doi:10.1161/CIRCULATIONAHA.111.044354

255.Wang, J., Huang, W., Xu, R., Nie, Y., Cao, X., Meng, J., . . . Zheng, Z. (2012). MicroRNA-24 regulates cardiac fibrosis after myocardial infarction. *Journal of cellular and molecular medicine, 16*(9), 2150-2160. doi:10.1111/j.1582-4934.2012.01523.x

256.Cambier, L., de Couto, G., Ibrahim, A., Echavez, A. K., Valle, J., Liu, W., . . . Marbán, E. (2017). Y RNA fragment in extracellular vesicles confers cardioprotection via modulation of

IL-10 expression and secretion. *EMBO Molecular Medicine, 9*(3), 337-352. doi:10.15252/emmm.201606924

257.Cambier, L., Giani, J. F., Liu, W., Ijichi, T., Echavez, A. K., Valle, J., & Marbán, E. (2018). Angiotensin II-Induced End-Organ Damage in Mice Is Attenuated by Human Exosomes and by an Exosomal Y RNA Fragment. *Hypertension (Dallas, Tex. : 1979), 72*(2), 370-380. doi:10.1161/HYPERTENSIONAHA.118.11239

258.Huang, Y. (2020). Exosomal lncRNAs from mesenchymal stem cells as the novel modulators to cardiovascular disease. *Stem Cell Research & Therapy, 11*(1), 315. doi:10.1186/s13287-020-01812-6

259.Gerstberger, S., Hafner, M., & Tuschl, T. (2014). A census of human RNA-binding proteins. *Nature Reviews Genetics, 15*(12), 829-845. doi:10.1038/nrg3813

VITA

Anh Phan attended University of Medicine and Pharmacy at Ho Chi Minh City, Vietnam for his undergraduate degree in pharmacy. After graduation, he worked for two years as a pharmacist in the department of Pharmacy at the Hospital of Blood Transfusion and Hematology at Ho Chi Minh City.

He was accepted in 2014 to Loyola University Chicago's Integrated Program in Biomedical Sciences and joined the Department of Molecular Pharmacology and Neuroscience shortly after. He completed his doctoral work in the laboratory of Dr. W. Keith Jones to study the cardioprotective role of microRNAs in the extracellular vesicles secreted by mesenchymal stem cells. He will continue this work during his postdoctoral fellowship at Icahn School of Medicine at Mount Sinai in the laboratory of Dr. Susmita Sahoo.